Lehrstuhl für Bioverfahrenstechnik
RWTH-Aachen
Prof. Dr.-Ing. Jochen Büchs

A New Method to Quantify the CO₂ Sensitivity of Micro-organisms in Shaken Bioreactors and Scale up to Stirred Tank Fermentors

Von der Fakultät für Mathematik, Informatik und Naturwissenschaften
der Rheinisch-Westfälischen Technischen Hochschule Aachen
zur Erlangung des akademischen Grades eines Doktors
der Naturwissenschaften genehmigte Dissertation

vorgelegt von

Master of Science in Chemical Engineering

Ghassem Amoabediny

aus

Tehran Iran

Berichter:

Universitätsprofessor Dr.-Ing. Jochen Büchs
Universitätsprofessor Dr.-Ing. Winfried Hartmeier

Tag der mündlichen Prüfung: **06 October 2006**

Diese Dissertation ist auf den Internetseiten der Hochschulbibliothek online verfügbar

Dedicated to my devoted wife,
and my daughters; Zeinab and Fatemeh

This research work was carried out at Department of Biochemical Engineering of RWTH-Aachen Technical University, Germany, under the supervision of Prof. Dr. Eng. Jochen Büchs between March 2002 and October. 2006.

Examiners:

University Professor Dr.-Ing. Jochen Büchs

University Professor Dr.-Ing. Winfried Hartmeier

University Professor Dr.rer.nat. Ulrich Klinner

Chairman:

University Professor Dr.rer.nat.Lothar Elling

Date of oral examination: **06 October 2006**

Diese Dissertation ist auf den Internetseiten der Hochschulbibliothek online verfügbar.

Acknowledgment

This work was done during my PhD research at the Department of Biochemical Engineering of RWTH-Aachen Technical University, Germany, from April 2002 to August 2006.

My sincerest gratitude and greatest thanks to my supervisor Prof. Dr. Eng. Jochen Büchs the head of the Department of Biochemical Engineering, for his guidance and advices during this work and his correction of this thesis. His enthusiasm sustained my research project in spite of many disappointments and difficulties. Discussion with him always added greatly to my knowledge.

I would like to acknowledge my great indebtedness to the University of Tehran for their sponsorship and financial supports.

I would like to thank Prof. Dr. Eng Winferied Hartmeier the head of the Department of Biotechnology and Prof. Dr Ulrich Klinner the head of the Department of Microbiology at the RWTH-Aachen Technical University for agreeing as examiner and Prof. Dr. Lothar Elling.the head of the Department of the biomaterial as chairman of my exam.

To all my colleagues Christoph Stöckmann, Keyur Raval, Alfredo Ramos-Plasencia, Ali Akgün, Arnd Knoll, Frank Kensy, Stefan Taubert, Archana Trivedi, Cyril Peter, Andreas Daub, Yasaman Dayani, Werner Eberhard, Juri Seletzky, Gregor Steinhorn and to all students Stefan Barch, Anika Kremer, Carstan Bäumchen, Kashani for their help and interesting discussion "Danke für eure Freundshaft und Hilfe". Furthermore, I would like to express thanks to Amizon Azizan as co-corrector of this thesis.

I am thankful to all my friends in Iran and Germany-Aachen specially Dr. Rahmandost, Reza Sajadi, Saber Mirzaie, Amir Kiarashi, and Hadi Tabesh, for their help.

And, my father Hasssan and my mother Javaher and my parents in low, Mostafa and Razieh as well as my grand brother Ali deserve my sincere gratitude for their encouragement throughout my life and my study.

Finally, I am extremely thankful to my dear wife Zahra Vatandoost for her patience, understanding encouragement and help all over my life and my study, "Thanks for everything"

However, it is all thanks to God for his leadership towards reality through my whole life and for his unlimited favors.

Ghassem Amoabediny

October 2006

Table of Contents: Page

of Micro-organisms in small scale Bioreactors

Chapter 8: A New Scale-Up Method from Shake Flask to Stirred Tank   **98**

  Fermentor Based on the Effect of CO_2 Ventilation

Abstract

Small scale shaken bioreactors (e.g. shake flasks) traditionally equipped with different types of sterile closures are very useful tools in biotechnology. The gas transfer coefficient of the sterile closures (k_{plug}) plays an important role in aeration of shaken bioreactors. The value of k_{plug} depends on the average diffusion coefficient of oxygen (D_{eO2}) and different lengths or/and diameters of the neck of flask. Therefore, in this study, a series of pipes with different lengths or/and diameters filled with cotton for a special shake flask, so-called ventilation flask, were employed. The gas transfer through the sterile closure of the ventilation flasks was characterized. Constant values of CO_2 and O_2 diffusion coefficient were found in all of the ventilation flasks. Considering these values and the neck geometry, a variety of k_{plug} in ventilation flasks were obtained. Since, decreasing k_{plug} causes a reduction of O_2 concentration and an accumulation of CO_2 in the gas phase of the shaken bioreactors, a realistic understanding and estimation of gas transfer in shaken bioreactors is advantageous to avoid oxygen limitation or carbon dioxide inhibition of a microbial culture. In this study, an unsteady state gas transfer model for shake flasks was developed and experimentally investigated for a wide range of gas transfer coefficients (k_{plug}). The introduced approach is based on the model of Henzler and Schedel [23], which describes the spatially-resolved gas partial pressures inside the sterile closure, affected by the local gas diffusion coefficients and convective Stefan flow. For further easy processing, the resulting total mass transfer coefficient (k_{plug}) is described as a function of the mass flow through the sterile plug (OTR_{plug}) by an empirical equation. This equation is introduced into a simulation model which calculates the gas partial pressures in the head space of the flask. Additionally, the gas transfer rates through the sterile closure and gas-liquid interface inside the flask are provided. Simulations indicate that neglecting the oxygen in the head space volume of the flask at initial conditions (simple steady state assumption) may lead to an underestimation of the oxygen transfer into the liquid phase. The extension of error depends on the conditions. A good agreement between the introduced unsteady state model and experimental results for the sulfite and biological system confirmed the validity and usefulness of the proposed unsteady state approach.

Moreover, a novel and easy method for quantification of CO_2-sensitivity of microorganisms in ventilation flask was investigated, using the properties of ventilation flasks. The differences between the values of accumulated CO_2 and concentration of oxygen in a culture system in ventilation flasks confirmed the validity of method. The effect of aeration on the removal of

CO_2 from the fermentation broth has been documented. Additionally, based on the data of the oxygen transfer rate (OTR), obtained by a Respiratory Activity Monitoring System (RAMOS) under a variety of specific aeration rates, the purposed new method was developed as an online monitoring method for CO_2 sensitivity of microorganisms in shaken bioreactors.

A maximum accumulated CO_2 concentration of 12% was derived in both above methods, provided that the cultivation system is carried out under optimal conditions (e.g. the same filling volume (15m1), appropriate media and buffer capacity to control the pH, the suitable OTR (0.05 mol/l/h), operating under non oxygen limitation and RQ≈1). The proper operation condition could be predicted using the unsteady state model.

Applying these mentioned method, a significant effect of accumulated CO_2 on the biomass concentration, growth rate and lysine product in the fermentation of *C. glutamicum* DM 1730 was found. Furthermore, the experimental results on *Arxula adeninivorans* LS3 and *Hansenula polymorpha* (WT ATCC 34438 and RB11-FMD-GFP) indicated that the CO_2 had no effect on these microorganisms. *Pseudomonas fluorescens* DSM 50090 on yeast extract + glucose and *Corynebacterium glutamicum* ATCC WT13032 on L-lactate were found to be especially sensitive to CO_2, which agree with literature. Some of the important advantages of the new methods are simplicity, lower cost and time consumption, easy of handling and producing similar results as large scale fermentation.

Besides, a new aeration strategy from the ventilation flasks to an aerated fermentation system (e.g. measuring flask and stirred tank fermentor) was developed, based on the same concentration of gas compounds (O_2 and CO_2) in the headspace of these vessels. By applying this method, the concentrations of CO_2 and O_2 in the gas phase obtained from measuring (aerated) flasks and stirred tank bioreactors were comparable to those obtained from ventilation flasks.

Finally in this study a new scale up method from shake flasks to stirred tank bioreactors, concerning the aeration strategy, was investigated based on the effect of CO_2 ventilation. Even for different sets of aerations, similar trends were found for the values of the biomass concentration, L-lysine formation, maximum OTR and specific growth rate for fermentation of *C .glutamicum* DM1730 as a model organism, in the both scales. Thus, the possibility of scaling up from ventilation flasks to stirred tank bioreactors based on CO_2 ventilation criterion was demonstrated.

Glossary of Abbreviations and Symbols:

A	cross sectional area of the flask neck (m^2)
a, b and c	fitting parameters of Eq. (21) (-)
ATCC	American Type Culture Collection
CER	carbon dioxide evaluation rate (mol/l/h)
C_f	Calibration factor for OTR analyzer (bar/volt)
Chap.	Chapter (-)
CO_2	carbon dioxide (-)
C_{O2}	concentration of oxygen consumption during fermentation (mol/l)
$CO_{2, g}$	carbon dioxide concentration in gas phase ()
C_{Na2SO3}	sodium sulfite concentration (mol/l)
CTR	carbon dioxide transfer rate (mol/l/h)
D	diameter of the sterile closure (m)
D_{CO2}	diffusion coefficient of carbon dioxide (m^2/h)
D_{eO2}	effective diffusion coefficient of oxygen (m^2/h)
D_i	diffusion coefficient of in a gas mixture (m^2/h)
D_{ij}	binary diffusion coefficients of O_2, CO_2, H_2 and H_2O in a gas mixture (m^2/s)
do	shaking diameter in the shaker (cm)
DSM/DM	German Collection of Micro-organism
Eq./Eqs.	Equation(s) (-)
ER	Water Evaporation Rate (g/h)
f	proportional factor of Eq. 4.12 (-)
f1-f9	number of employed ventilation flasks (-)
Figure	Figure (-)
gr	gram (-)
gr/l	gram per liter
h	height co-ordinate of the sterile closure (m)
H	height of the sterile closure (m)
H_{eCO2}	Henry's constant for carbon dioxide (mol/l/atm)
K_1	equilibrium constant rate for the reaction of Eq. 6.1 (1/sec)
k_1	first order reaction constant (L/mol/h)
K_2	equilibrium constant rate for the reaction of Eq. 6.1 (1/sec)
K_{acid}	constant value of carbonic acid dissociation in Eq. 6.2 (mol/m^3)
$k_L.a$	volumetric gas–liquid mass transfer coefficient (1/h)

k_{O2}	Michaelis Menten kinetic for oxygen (mol/l)
k_{plug}	overall gas transfer coefficient in sterile closure (mol/sec)
$k_{plug, CO2}$	carbon dioxide transfer coefficient in sterile closure (mol/sec)
$k_{plug, O2}$	oxygen transfer coefficient in sterile closure (mol/sec)
k_s	Michaelis Menten kinetic for substrate (gr/l)
L_{O2}	solubility of oxygen (mol/L/bar)
M	molarity (-)
max	maximum (-)
mg	milligram (-)
ml	milliliter (-)
n	shaking frequency (1/min)
O_2	oxygen (-)
$O_{2,L}$	oxygen in liquid phase (-)
OD	optical density (600nm)
OTR	oxygen transfer rate (mol/L/h)
OTR^α	oxygen transfer rate in stationary condition at rising phase (mol/L/h)
$OTR_{g\text{-}L}$	oxygen transfer rate from gas to liquid phase (mol/L/h)
OTR_{plug}	oxygen transfer rate through the sterile closure (mol/L/h)
$OTR_{st.st}$	oxygen transfer rate in steady state condition (mol/L/h)
OUR	oxygen uptake rate (mol/L/h)
p	total pressure (bar)
$p°_{O2}$	initial partial pressure of oxygen (bar)
p_{abs}	absolute pressure (bar)
P_{abs}	absolute pressure (bar)
pH	power of acidity (-)
p_i	partial pressure of the component "i" (bar)
pO_2	oxygen partial pressure in headspace of the flask (bar)
PO_2^α	partial pressure of O_2 in stationary condition at rising phase (bar)
$pO_{2,L}$	oxygen partial pressure in liquid phase (bar)
$pO_{2,out}$	oxygen partial pressure in the surrounding environment (bar)
p_{sat}	saturation partial pressure of water inside of flasks
qi	area-based volume flow of the component "i" ($m^3/s/m^2$)
q_{O2}	area-based volume flow of oxygen ($m^3/s/m^2$)
q_{in}	specific aeration plug flow rate (vvm)

R	gas coefficient (L·bar/mol/°K)
RAMOS	Respiratory Activity Monitoring System (-)
ref.	reference
rf	measuring flask (-)
rpm	rotation per minute (1/min)
RQ	respiratory quotient (-)
S	substrate (gr/l)
sec	second (-)
Sec.	Section (-)
T	temperature (°C)
t	time (h)
$T_{ave.}$	average temperature (°C)
U	voltage signal of O_2 sensor (volt)
U^{α}	voltage signal of O_2 sensor in stationary condition at rising phase (volt)
U^m	voltage signal of O_2 sensor in stationary condition at measuring phase (volt)
$U°$	initial voltage of O_2 sensor (volt)
U_{CO2}	voltage signal of CO_2 sensor (volt)
vf	ventilation flask(-)
V_g	gas volume of the headspace of the flask (m^3)
V_L	filling volume (mL)
V_{mo}	molar gas volume (L/mol)
V_{Na2SO3}	sodium sulfite stoichiometric coefficient (-)
v_{O2}	oxygen stoichiometric coefficient (-)
vvm	volume per volume per minute (-)
v/v	volume per volume (-)
w	velocity (m/s)
WT	wild type strain (-)
X	dry cell weight (gr/l)
Xo	initial dry cell weight (gr/l)
$Y_{x/O2}$	biomass yield coefficient on oxygen consumption (gr/mol)
$Y_{x/s}$	biomass yield coefficient on substrate (gr/gr)
ζ_{cotton}	bulk density of cotton (gr/cm^3)
μ	specific growth rate (1/h)
$\mu_{max.}$	maximum specific growth rate (1/h)

n_{O2} mole of oxygen in headspace gas volume of flask (mol)

$n_{O2\ g\text{-}L}$ transfer rate of oxygen from gas to liquid (mol/h)

$n_{O2,O2}$ transfer rate of oxygen through the sterile closure (mol/h)

RH_{inside} relative humidity inside of flask ()

$RH_{outside}$ relative humidity outside of flask ()

, g   index for gas phase (-)

, L   index for liquid phase (-)

,in   index for input and inside (-)

,out   index for output and outside (-)

$[CO_{2,L}]$ dissolved carbon dioxide concentration (mol/l)

$[CO_3^{2-}]$ carbonates concentration (mol/l)

$[HCO_3^{-}]$ bicarbonate concentration (mol/l)

°C   degree of centigrade

List of Tables

List of Figures

$p_{sat.}$=0.03969 bar [61], filling volume V_L=15 ml, density of cotton plug ζ_{cotton}=0.15 g/cm^3.

Figure 4.5: Model results for the oxygen transfer rate trough the sterile closure (OTR$_{plug}$) and from the gas in the headspace to the liquid phase (OTR$_{g-L}$) over time in ventilation flask f1 and f9 (Table 4.1). The collapse of OTR$_{g-L}$ to zero (vertical dashed lines) indicate the exhaustion of the 0.5 M sulfite solution, T=25 °C, 300 rpm, d$_o$=5 cm, V_L=15 ml. Eqs. 4.1, 4.5, 4.12, 4.17, 4.19 and Eqs. 4.2, 4.12, and 4.15 for unsteady state and steady state calculation were used, respectively.

Figure 4.6: Simulation results of head space partial pressure of oxygen (p$_{O2}$) and the time of exhaustion of sulfite and end of the oxidation reaction under unsteady state gas transfer condition in the ventilation flasks f1-f9 with different k$_{plug}$ as a function of OTR$_{plug}$ (Table 4.1); sulfite system (0.5M), T=25 °C, n=300 rpm, d$_o$=5 cm, V_L=15 ml, ζ_{cotton}=0.15 g/cm^3.

Figure 4.7: Comparison of measured and calculated change of partial pressure of oxygen (pO$_2$) in the head space of ventilation flasks with different sterile closures (f1, f4, f7 and f9). Sulfite system (0.5 M), T=25 °C, n=300 rpm, d$_o$=5 cm, V_L=15 ml, ζ_{cotton}=0.15 g/cm^3.

Figure 4.8: Comparison of measured and calculated time of the oxidation reaction of a sulfite solution (0.5M) until complete exhaustion. The unsteady state values for the ventilation flasks f1-f9 (●) were calculated by Eqs. 4.1, 4.5, 4.12, 4.17 and 4.19 and steady state values by Eq. 4.2, 4.12 and 4.15, using D$_{eO2}$=0.153 cm^2/s (Table 3.1), T=25 °C, d$_o$=5 cm, 4 ml<V_L<25 ml, 100 rpm<n<400 rpm.

Figure 4.9: Model results for OTR$_{plug}$, OTR$_{g-L}$ and pO$_2$ in the ventilation flasks f1 and f9. The input parameters were selected for a fermentation of *C. glutamicum* DM1730 on 10 g/l glucose (n=400 rpm, V_L=10 ml, T=30 °C, d$_o$=5 cm, Y$_{x/s}$=0.48, Y$_{x/o2}$=53 g/mol, RQ=1, Xo=0.5 gr/l, f=0.23 calculated by Eq. 4.13, K$_S$=0.0045 gr/l, K$_{O2}$=10^{-6} mol/l, μ_{max}=0.32 h^{-1}).

Figure 4.10: Comparison between unsteady state model and experimental results for the partial pressure of oxygen in the headspace of the ventilation flasks f1, f4, f7, f9 obtained for the fermentation of *C. glutamicum* DM1730 on 10 g/l glucose and 21 g/l MOPS (n=400 rpm, T=30°C, d$_o$=5 cm, Y$_{x/s}$=0.48, Y$_{x/o2}$=53 g/mol, RQ=1 [5]).

Figure 5.1: Development of the aeration system of the RAMOS devices [3] employed in this study.

Figure 5.2: Simulation results of q$_{in}$ for the aerated flasks of the RAMOS device resulting in the same headspace concentration as in ventilation flask f1, using the unsteady state model and Eq. 5.4 for fermentation of *C. glutamicum* DM1730 (n=350 rpm, d$_o$=5 cm, V_L=15 ml, 15 gr/l glucose, Y$_{x/s}$=0.48, Y$_{x/O2}$=53 g/mol, T=30°C, μ_{max}=0.32 1/h, K$_S$=0.0045 gr/l, K$_{O2}$=0.0000008 mol/l [5, 68]).

Figure 5.3: Simulation results of q$_{in}$ for the aerated flasks of the RAMOS device resulting in the same headspace concentration as in ventilation flask f9, using the unsteady state model and Eq. 5.4 for fermentation of *C. glutamicum* DM 1730 (n=350 rpm,

d_o=5 cm, V_L=15 ml, 15 gr/l glucose, $Y_{x/s}$=0.48, $Y_{x/O2}$=53 g/mol, T=30 °C, μ_{max}=0.32 1/h, K_S=0.0045 gr/l, K_{O2}=10^{-6} mol/l [5, 68]).

Preface

The research presented in this thesis was conducted at the Department of Biochemical Engineering, RWTH Aachen University, Germany. This study is based on the following Chapter:

Chapter 1: In this chapter, general literature is reviewed, and the motivations of this research work are also briefly presented.

Chapter 2: Common materials and methods used in the different experiments are separately explained, and also a specially designed shake flask, so called ventilation flask, is introduced.

Chapter 3: The gas transfer through the sterile closure of ventilation flask is characterized in this chapter.

Chapter 4: An unsteady sate model for gas transfer in the shaken bioreactors, based on a variety of mass transfer resistances of the sterile closure and the gas liquid interface, is experimentally investigated.

Chapter 5: This chapter covers a new aeration strategy from the ventilation flasks to the aerated fermentation system (e.g. measuring (aerated) flask and stirred tank fermentor), using the unsteady state model.

Chapter 6: A novel and easy method for the quantification of CO_2 sensitivity of micro-organism in shaken bioreactors is described.

Chapter 7: In this chapter, an online monitoring method to quantify the CO_2 sensitivity of micro-organisms is developed utilizing a Respiration Activity Monitoring System (RAMOS).

Chapter 8: In the final chapter a new scale up method from a ventilation flask to a stirred tank bioreactors based on the effect of CO_2 ventilation is illustrated.

A summary of this work and possible future investigation are given.

Also, the references are provided in the alphabetical manner.

Finally, the declaration and curriculum vita of the author are attached at the end of this thesis.

Chapter 1

Literature Review
and
Motivation

1.1   Literature review

Shake flask as a small scale bioreactor is a very common and useful tool in bioprocess industries, because of its simplicity, low cost and convenient handling [11]. Shake flasks are traditionally equipped with different types of gas permeable closures to prevent contamination [57 and 66].

Aerobic micro-organisms will be oxygen limited if the oxygen transfer rate is smaller than the oxygen uptake rate in shaken bioreactors [18, 23, 49, 57, 66 and 79]. To avoid oxygen limitation in the shake flasks, it is essential to have a good understanding and estimation of the gas transfer conditions. Therefore, it is necessary to evaluate the oxygen transfer rate through the sterile closure (OTR_{plug}) and gas liquid oxygen transfer rate (OTR_{g-L}) in the shaken bioreactors [57 and 76]. OTR_{g-L} and OTR_{plug} are related to the values of the gas transfer coefficients through the sterile closure (k_{plug}) and volumetric gas transfer coefficients gas-liquid (k_La), respectively. A number of studies have been carried out to describe the parameters k_La and k_{plug} by different experimental methods and/ or empirical models [23, 24, 25, 76 and 79]. Sulfite oxidation has been used as a chemical model for the evaluation of the k_La value [24, 44, 46 and 49]. The parameter k_{plug} has been assessed in literature using the effective oxygen diffusion coefficient ($D_{e,O2}$) in addition to the geometry of the sterile closure [23, 26 and 66]. It can be obtained theoretically by the Henzler model [23] or some experimental methods [21, 25 and 57]. Moreover, several methods for the determination of $D_{e,O2}$ have been reported [23, 49, 57and 66]. According to these reports, a proportional dependency of $D_{e,O2}$ on bulk density of the applied closure has been demonstrated.

Using a sterile closure leads to a reduction of O_2 and An accumulation of CO2 in the gas phase of the headspace of the shake flask in an aerobic cultivation system [25, 66 and 80]. This carbon dioxide accumulation, produced by the metabolism of the micro-organisms, may be a fundamental inhibition or stimulant for the cell growth and productivity [2, 19, 25-27, 50 and 51]. This CO_2 can particularly play a significant role in industrial micro-organisms for the fermentation of some important bio-products (e.g. amino acids, antibiotics and etc.) [60]. Many authors have indicated the inhibitory effects of CO_2 on bacteria [19 and 54], yeasts [34] and fungal micro-organisms [12, 26 and 50] in a cultivation process. The most important mentioned effects comprise altering growth [12, 19, 34 and 41] and product formation [12 41, and 54].

Many papers have emphasized that the sterile closures play an important role in the aeration of the shaken bioreactors [18, 29 and 66]. In addition, the effect of aeration on the removal of the

volatile compounds (e.g. organic acids, NH_3, alcohols, hormones, CO_2, etc.), so called ventilation, from the fermentation broth has been demonstrated [15, 59 and 75]. It has been reported that the reduction of aeration in an aerobic fermentor led to an incense of the autogenously produced CO_2 by micro-organisms [43]. The CO_2 inhibition can be the most important parameter in the industrial scale fermentors, since the dissolved CO_2 concentration is increased by increasing the hydrostatic pressure near to the bottom of the vessels [26, 38]. Controlling aeration, especially in scale up from shake flask to fermentor, in order to provide sufficient oxygen for aerobic cultures is highly demandable [8, 74 and 75]. The suitability of scale up methods are usually confirmed by experimental results, which show that, there is no difference between fermentation results in various types of small and large scales carried out under the same oxygen transfer rate [21]. In spite of this condition, the effect CO_2 ventilation may become as an important parameter to a discrepancy between the results of both scales [15, 59 and 75]. Therefore, it is introduced that the ventilation of a bioreactor can be an additional scale up criterion [75]. Besides, the failure of scale up from shake flask with sterile closure to a stirred tank bioreactor and the possibility of it from an aerated flask to stirred tank bioreactor have been reported. This could be due to the effect of CO_2 ventilation [37].

1.2   Motivation

The influence of CO_2 on the cultivation system has rarely been studied, compared to O_2 [30 and 31]. Considering the importance of the CO_2 effects on productivity and growth rate of the industrial micro-organisms, several quantitative methods in the batch, fed-batch and continuous fermentors, for the evaluation of these effects have been established [2, 19, 25-27, 50 and 51]. Although, these mentioned methods have brought valuable results, the operating cost, time consumption and reproducibility for experimental results are the limiting factors. And even though the CO_2 sensitivity of micro-organisms has been addressed using of these methods, until now no report has been available on the quantification of the CO_2 sensitivity of micro-organisms in the small scale shaken bioreactors e.g. shake flask.

In this study, a novel, easy and economical method for the quantification of CO_2 sensitivity of micro-organisms in shaken flask bioreactors will be established and developed into an online monitoring system. This method is based on the values of the mass transfer coefficient of a sterile closure of shake flasks.

Finally, a new aeration strategy from a ventilation flask to an aerated fermentation system (e.g. measuring flask and stirred tank fermentor) will be developed for making possibility to scale up from shake flask to stirred tank fermentor based on the effect of CO_2 ventilation.

Besides, a new unsteady state model will be prepared for advanced understanding of the gas transfer in the specially designed shake flasks, so called ventilation flasks, since the current steady state model was not capable for achieving our goals.

Chapter 2

Materials and Methods

2.1   Description of equipment

2.1.1   Ventilation flask

The gas transfer coefficient of the sterile closure (k_{plug}) plays an important role in aeration, for the reduction of the oxygen supply and the an accumulation of CO_2 in the gas phase of the headspace of the shaken bioreactors [23, 49 and 66]. The value of k_{plug} depends on the effective diffusion coefficient of oxygen (D_{eO2}) and different dimensions (length or/and diameter) of the neck of the flask [23, 29 and 66]. Therefore, in this study a series of pipes with different lengths or/and diameters designed for the 250 ml Erlenmeyer flasks (German standard, DIN 12380), so called ventilation flasks, were employed (Figure 2.1.B).
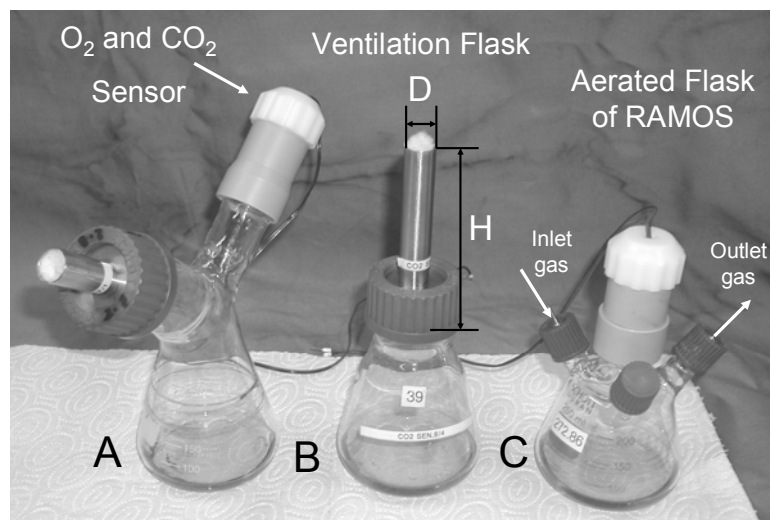
Figure 2.1: Different kinds of shake flasks; A: ventilation flask equipped with oxygen or carbon dioxide sensor, B: ventilation flask C: aerated flask of the RAMOS device

The dimensions of the sterile closures used in the ventilation flasks are given in Table 2.1. The necks of these flasks were filled with cotton wool with a constant density of 0.15 g/cm^3. This ensures the same value of effective diffusion coefficient of oxygen (D_{eO2}) for this sterile closure in the ventilation flasks [57, 23, 29 and 66]. In chapter 3, details of the characteristics of the gas transfer through the sterile closures in the ventilation flask will be described.

A series of ventilation flasks were used for the investigation of a new method to quantify the CO_2 sensitivity of micro-organisms in shaken bioreactors (Chapter 6). These flasks were also utilized in a new aeration strategy for scale up from shake flask to aerated system such as aerated flask and stirred tank fermentor (Chapters 5 and 8). The Figure 2.2 illustrates a series of these flasks with different neck geometries.

Table 2.1: The dimensions of the sterile closures of ventilation flasks.

Ventilation flask	D_{pipe} (cm)	H_{pipe} (cm)
f1	2.80	2.12
f2	2.80	4.20
f3	2.00	3.60
f4	2.00	4.72
f5	1.50	3.90
f6	1.50	4.85
f7	1.50	7.00
f8	1.50	11.00
f9	0.7	3.10
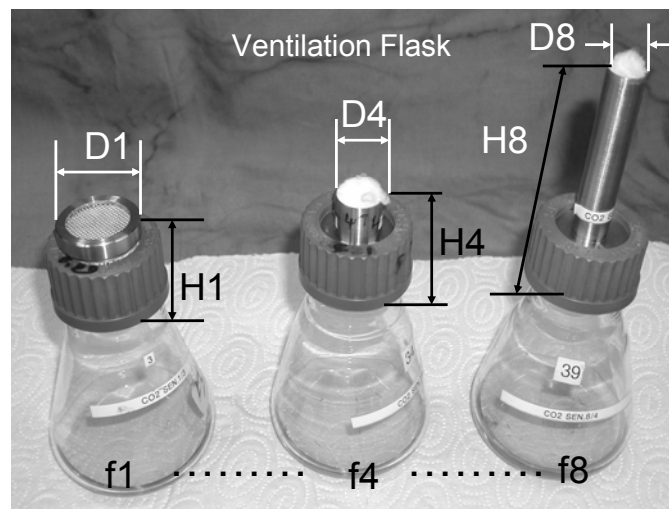
Figure 2.2: Ventilation flasks with a variety of gas transfer resistances of the sterile closure, employed in this study (the dimensions of the neck of ventilation flasks are given in Table 2.1)

2.1.2 Respiration Activity Monitoring System (RAMOS) and measuring (aerated) flask

The Respiration Activity Monitoring System (RAMOS) for the on-line measurement of OTR, CTR and RQ in shake flasks was described by Anderlei et al. [3 and 4]. This device has been

successfully applied for the determination of optimal operating conditions and detection of limitations in shaken bioreactors, and also obtaining important information for scale up to a stirred tank fermentor in several previous projects [72 and 24]. The flasks of this device, so called measuring (aerated) flask, are specially designed having one opening at the top of the oxygen sensor and three openings for air inlet, air outlet and inoculation (Figure 2.1.C). In chapter 7 an online monitoring method for CO_2 sensitivity of micro-organisms will be investigated by developing an aeration system for RAMOS. The details of these aeration systems will be discussed in chapter 5.

2.1.3   Laboratory scale fermentor

In this study of a new scale up method from ventilation flask to stirred tank fermentors, a foil fermentor (Visual Safety- Fermentor (VSF), Bioengineering AG, Wald, CH) was used. The operation condition and some important information experimental parameters are given in Table 2.3 and Chapter 8.

2.1.4   Oxygen and carbon dioxide sensors

For detecting the partial pressure of oxygen and the concentration of CO_2 in the gas phase of the headspace of a flask, an oxygen sensor (Maxtec MAX-250 C, Maxtec Inc., Salt Lake City, Utah, USA) and IR- CO_2 sensor (GS10, sensor devices GmbH Germany) were inserted in to the wall of ventilation shake flask and response curves are monitored by a recorder (Figure 2.1.A). A calibration between the signal output of the sensors and pO_2 and concentration of CO_2 could be obtained by Eqs. 2.1 and 2.2:

$$p_{O_2} = \frac{(U - 0.23) \cdot p_{O_2}^0}{U^0 - 0.23} \qquad\qquad (2.1)$$

$$\%CO_2 = (U_{CO2} - 4.1112)/4.2305 \qquad\qquad (2.2)$$

Where U and U_{CO2} are the signals of oxygen and CO_2 sensors during the process and U^o and $p^o{}_{O2}$ are the initial signals and partial pressure, respectively.

2.2   General experimental conditions in ventilation, RAMOS and laboratory scale fermentor

The values of experimental parameter in ventilation flasks, measuring flasks (RAMOS) and lab scale fermentors are given in Table 2.2. In this study an orbital shaker (d_o=5 cm) (Lab-Shaker, Kuehner, Basel, Switzerland) for agitating the ventilation and aerated flasks was used. A suitable shaking frequency and a filling volume (VL) in ventilation and aerated flasks were

selected to ensure a sufficient oxygen transfer capacity for avoidance of oxygen limitation [44]. This is possible using a suitable model for gas transfer in ventilation flasks (Chapter 4). The experiments were performed under a range of filling volume between 4 and 25 ml in shake flasks and 1800 ml in fermentors. The aeration in measuring flask was adjusted between 3 and 0.8 vvm; however, the aeration in the fermentor was 1.5, 0.39 and 0.1 vvm. Regarding to the experiments, the shaking frequency (n) in shake flasks was between 200 and 400 rpm. The agitation for the fermentor was selected between 300 and 1000 rpm according to the dissolved oxygen concentration.

Table 2.2: The values of experimental parameters for ventilation flasks, measuring flasks (RAMOS) and laboratory scale fermentor

Parameter	Ventilation flasks*	Aerated flasks**	Fermentor***	unit
Filling volume (V_L)	Variable between 4 and 25	Variable between 4 and 25	1800	ml
Shaking frequency, stirred speed (n)	Variable between 200 and 400	Variable between 200 and 400	300→600 600→900 900→1200	rpm
Temperature	25, 30	25, 30	30	°C
Shaking diameter (d)	5	5	-	cm
Specific aeration rate (q_{in})	(Chap. 5)	Variable between 3 and 0.08 vvm in one flow system (Chapter 5)	1.5, 0.39, 0.1	vvm

*   Applied for water evaporation method, sulfite and a cultivation system
**   Applied for sulfite and a cultivation system in RAMOS
***   Applied for a scale up method based on the effect of CO_2 ventilation

2.3   Analytical methods

During the fermentation, samples were taken from the ventilation flasks and fermentor. However, samples from measuring flask were only taken at the end of the fermentation. The analysis of the fermentation system was performed by the determination of the pH values, optical density (OD=600 nm), cell dry weight (biomass), concentrations of carbon source (glycerol, L-lactic acid and D-glucose) and L-lysine production.

2.3.1   pH measurement

The pH meter (CG804, Schott, Germany) and pH electrode (Electrolyte 9811, InLab®422, Mettler Toledo) for off-line and on-line measurements, respectively, were calibrated before each experiment.

2.3.2   Determination of cell dry weight (biomass) concentration

For the determination of biomass concentration empty 15 ml Falcon Tubes were dried in an oven at 100 °C for 48 h, placed in the desiccators for 0.5 h and then weighted by a precision balance. For each condition at least about 12 ml sample were taken. For each sample, a weighted Falcon Tube was filled with 10ml of culture medium and centrifuged for 10 min at 4°C and 4000 rpm (ROTINA 32 R, Hettich, Germany). The supernatant was decanted and used for the analysis of the medium components. The humid pellet in the bottom of the Falcon Tube was dried for 48 h in the oven at 100 °C and, afterwards, placed in the desiccators for 0.5 h and weighted for the determination of the cell dry weight.

The biomass of *Arxula* and *H. polymorpha* was determined as cell dry weight (biomass) by a filtration method. In this method 8 ml culture broth was filtered through dried and pre-weighed cellulose acetate filters, with pore size 0.2 μm (11107-47-N, Sartorius, Germany). The filter residue was re-suspended once in 9 g/l NaCl, filtrated again and dried in the oven at 105 °C until the mass remained constant.

2.3.3   Cell density determination (Optical Density)

In addition to the biomass measurement, the optical density (OD) was determined at a wavelength of 600 nm on a two-channel photometer (UVIKON 922, Kontron Instruments, Germany). For each sample, two measurements were accomplished and the arithmetic mean of the determined values was calculated. The remaining sample volume was used for external control of the pH value.

2.3.4   Carbon sources and by-products concentration

The amount of glucose, L-lactic acid and ethanol concentration in the supernatant of the samples were analyzed by High Performance Liquid Chromatography (HPLC) (Dionex Pumpenserie P 580 with Chromelon Software, Dionex Corp., USA).

2.3.5   L-lysine concentration

For quantitative determination of lysine, the supernatant of samples were analyzed by the high-performance liquid chromatography system (LC 1090, Hewlett- Packard, Avondale, California) [34].

2.4   Applied models and software

The following models and software were applied. The input values for our suggested models are summarized in the Table 2.3. The details of these models will be described in the related Chapters.

a- Henzler and Schedel model [23] for description of gas transfer through the sterile closures in ventilation flasks (Chapter 3). The mathematical models, was transferred into the Model Maker software (version 3, 1997 Cherwell Scientific publishing Ltd).

Table 2.3: Input value for simulation models applied in this study, p=1.01325 [bar], V_{mo}=22.14 [l/mol], R=0.0831878 [L·bar/mol/°K] (T=25 °C) [61]

Parameter	Value	Henzler model	New unsteady state model		RAMOS	unit
			Sulfite	Biological		
Solubility (L_{O2})	[67]	+++	+++	+++	+++	mol/L/ bar
Temperature (T)	20-30	+++	+++	+++	+++	°C
Neck geometry (D, and H)	Table 2.1	+++	+++	+++	---	cm
k_{plug}	Chapter 3	---	+++	+++	---	cm
V_L	Table 2.2	+++	+++	+++	---	ml
Shaking frequency (n)	Table 2.2	---	+++	+++	---	rpm
Carbon source	5-50	---	---	+++	---	g/l
U (voltage of O_2 sensor)	Chapter 7	---	---	---	+++	mV
Water evaporation rate (ER)	Chapter 3	+++	---	---	---	g/l
Related humidity	Chapter 3	+++	---	---	----	-

b- Model of unsteady state gas transfer in the ventilation flask based on k_{plug} (Chaps. 4 and 5). In order to simulate the effect of k_{plug} and other operation conditions, the mathematical equations were transferred into the Model Maker software (version 3, 1997 Cherwell Scientific publishing Ltd.).

c- Lab-view program for RAMOS device (Chaprer 7)

2.5   Micro-organisms and medium preparation

In this study, the yeast strains *Arxula adeninivorans* WT LS3 and *Hansenula polymorpha* (WT ATCC34438 and RB11-FMD-GFP), bacterial strains of *Corynebacterium glutamicum* (ATCC WT13032 and DSM1730) and *Pseudomonas fluorescens* DSM50090 were used as model organisms.

The cultivation of these micro-organisms was performed on agar, complex and minimal mediums. The agar plates were made in order to store the micro-organism in the fridge. In this study the composition of the complex medium were the same as the agar plate medium except the agar-agar component. For the main cultures of the fermentation in ventilation, measuring flasks and fermentor, the mineral mediums were used which contained a carbon source, appropriate for micro-organisms.

All fermentations were accomplished with inoculation from the agar plate to a complex medium as pre-culture one, and from complex medium to a mineral medium as pre-culture two, and finally from pre-culture two to the mineral medium as main culture. The medium of the main culture was distributed among the single flasks (ventilation and aerated shake flasks) or fermentor. The details of components and preparation methods of these media for each cultivation system are separately described as follows.

2.5.1   Cultivation of *Arxula adeninivorans* (WT LS3) and *Hansenula polymorpha* (WT ATCC 34438 and RB11-FMD-GFP)

The chemical components and the method of preparation of both YPD and YNB agar and complex medium are given in Tables 2.4 for *Arxula adeninivorans* and *Hansenula polymorpha*, respectively [78 and 40]. The pH of the YPD medium, an agar plate and complex liquid medium, was adjusted to '6' using 5 M NaOH.

The components of YNB, ammonium sulfate, and glycerol were dissolved with 800ml distilled water and then its pH was adjusted to '6' by 0.5 M NaOH. The phosphate buffer

solution of 200 ml was prepared according to Table 2.5. The pH of the phosphate solution was adjusted to '6' and added to YNB solution.

Table 2.4: YPD and YNB complex medium for cultivation of *Arxula adeninivorans* and *Hansenula polymorpha*.

YPD for *Arxula adeninivorans*	Amount (g/l)	YNB for *Hansenula polymorpha*	Amount (g/l)
Glucose monohydrate ($C_6H_{12}O_6$•H2O)	22	YNB	1.4
Gelatin, (peptone) (Roth 07357562)	20	Ammonium Sulfate	5
Yeast extract (Roth 25465689)	10	Glycerin ($C_3H_8O_3$)	10
		Phosphate buffer	Table 2.5
Agar-Agar* (Roth 01251539)	18	Agar-Agar * (Roth 01251539)	20
Final pH	6.4	Final pH	6.4

*Agar was used for agar plate culture.

Table 2.5: The solution of phosphate buffer for YNB medium of *H. polymorpha*

Phosphate puffer solution	Concentration [g/l]	% Volume of components from stock solution for obtaining a value of pH=6	Amount of component after titration [g/l]
Na_2HPO_4	70,98	12,3	8,73
NaH_2PO_4 • H_2O	69,00	87,7	60,51

The parameters of the cultivations in our vessels are presented in Table 2.6.

The main culture of these micro-organisms was prepared using a Syn6 minimal medium (Table 2.7). For preparation of Syn6 medium, first the basic solution (pH was adjusted to '6.4' by adding 0.5 M NaOH), $CaCl_2$, micro elements, vitamin and trace elements, were separately prepared and sterilized. Finally, after the cooling $CaCl_2$, micro elements, vitamins and trace elements with following volumes and concentrations were added as noted in Table 2.7.

Table 2.6: The parameters for cultivation of *Arxula adeninivorans* and *Hansenula polymorpha*

Parameters	*Arxula adeninivorans*	*Hansenula polymorpha*	
Type strain	WT-LS3	WT ATCC 34438	RB11-FMD-GFP
C-source (g/l)	Glucose 20	Glycerin 10	Glucose 20
Minimal medium	Syn6 Table2.7	--------	Syn6 Table2.7
Buffer solution	MES (0.14 M)	Table 2.5	MES (0.14 M)
Initial pH	6.4	6	6.4
T (°C)	30	30	
Filling volume (VL, ml)	between 4 and 15	between 4 and 15	10, 15
Agar medium	YPD Table 2.4	YNB Table 2.4	YNB Table 2.4
Complex medium	YPD Table 2.4	YNB Table 2.4	YNB Table 2.4
n (rpm)	350	200, 350	350
aeration rate in RAMOS (vvm)	between 2.25 and 0.22	between 2.25 and 0.22	1.5, 0.39, 0.19, 0.1
Inoculation (Xo)	3-10 % of total filling volume		

2.5.2   Cultivation of *Corynebacterium glutamicum* (ATCC WT13032 and DSM1730)

The fermentation of the strains of *Corynebacterium glutamicum* (ATCC 13032WT and DM1730) on D-glucose and L-lactate were performed in the ventilation and measuring flasks under a variety of accumulated CO_2. *C. glutamicum* DM1730 as a L-lysine product the strain was also used for investigation of a new scale up method from a ventilation flask to a stirred tank fermentor, based on the effect of CO_2 ventilation (Chapter 8). The operation conditions for cultivation of these micro-organisms in these vessels are given in Table 2.8.

The chemical components and the methods for preparation of the medium for cultivation of *C. glutamicum* are described in Tables 2.9 and 2.10. The agar and complex medium has been introduced by Buechs [7] and minimal medium by Seletzky et al. [68]. Stored micro organisms on agar plates from a fridge were used for a maximum of 10 days. Two pre-cultures were carried out in experiments. The first one was performed using the complex medium in the RAMOS device, and then inoculated from this pre-culture to a minimal medium (5 % of the total volume) as second pre-culture.

Table 2.7: Composition and preparation of mineral Syn6-MES 0.14 M medium with glucose as carbon source for the cultivation of *Arxula adeninivorans* and *Hansenula polymorpha* [16].

Stock solution	Components		Preparation	Volume
Basic solution with C- and N-source	Glucose monohydrate ($C_6H_{12}O_6 \cdot H2O$)	22 g	to be solved in 990 ml distilled water and adjusted pH to 6.4 with 5M NaOH and then autoclaved and filled up to 1000ml	1000 ml
	KH_2PO_4	1 g		
	$(NH_4)_2SO_4$	7.66 g		
	KCl	3.3 g		
	$MgSO_4 \cdot 7\ H_2O$	3.0 g		
	NaCl	0.3 g		
	MES ($C_6H_{13}NO_4SH_2O$)	27.3 g		
Calcium chloride	$CaCl_2 \cdot 2H_2O$	15 g	to be solved in 100 ml distilled water and autoclaved	6.67 ml
Micro-element	$(NH_4)_2Fe(SO_4)_2 \cdot 6\ H2O$	1000 mg	to be solved in 100 ml distilled water and sterilized by filter	6.67 ml
	$CuSO_4 \cdot 5\ H_2O$	80 mg		
	$ZnSO_4 \cdot 7\ H_2O$	300 mg		
	$MnSO_4 \cdot H_2O$	400 mg		
	EDTA (Titriplex III)	1000 mg		
Vitamin	D-Biotin	6 mg in 10 ml 50 % (v/v) 2-Propanol	to be mixed for 100 ml and sterilized by filter and used to be kept in refrigerator for max. one week	6.67 ml
	Thiamin chloride-hydrochloride	2000 mg in 90 ml		
Traces – element	$NiSO_4 \cdot 6\ H_2O$	10 mg	to be solved in 50 ml distilled water and sterilized by filter	3.33 ml
	$CoCl_2 \cdot 6\ H_2O$	10 mg		
	Boric Acid	10 mg		
	KI	10 mg		
	$Na_2MoO_4 \cdot 2\ H_2O$	10 mg		

Table 2.8: Operation condition for cultivation of *Corynebacterium glutamicum*

Parameters	*Corynebacterium glutamicum*	
Type strain	ATCC 13032 WT	DM 1730*
C-source (g/l)	L-lactate (10)	D-glucose (15)
Minimal medium	Table 2.10	
Buffer solution (g/l)	MOPS (21)	
Initial pH	between 6 and 7	between 7and 7.5
T (°C)	30	
Inoculation (Xo)	3-10% of total filling volume	3-7% of total filling volume
Filling volume (ml)	between 4 and 15	
Agar medium	Table 2.9	
Complex medium	Table 2.9	
Shaking frequency	350, 400 rpm	
aeration in RAMOS (vvm)	Variable between 1.54 and 0.1	Variable between 1.3 and 0.2

*This strain was kindly provided by Dr. Eggeling, IBT-1, Research Centre Jülich, Germany

The media were buffered using MOPS buffer solution. The stock solutions were prepared separately. All components were dissolved together in distilled water except biotin and 3,4-dihydroxybenzoic acid (protocatechuate).

The pH value of the resulting solution of trace elements was adjusted to pH equal 1 with concentrated H_2SO_4 in order to obtain a better solubility of the involved components. The vitamins and 3, 4-dihydroxybenzoic acid solutions have to be freshly prepared because of their instability. They can not be stored in a refrigerator until one week. Biotin was dissolved with 50 % (v/v) 2-propanol and protocatechuate in a 100 g/l NaOH solution.

For the preparation of the mineral medium, the carbon source and salts solutions were autoclaved, cooled, and mixed together. The trace elements, calcium chloride, biotin and protocatechuate solutions were added to this solution through a sterile filter and syringe. The pH of the final solution was adjusted between 7 and 7.5.

Table 2.9: Composition of agar plates and complex medium for *C. glutamicum* [7]

Substances	Concentration (g/l)	Preparation (1000 ml)
Glucose	20	Prepared separately and autoclaved (100 ml) and then mixed with other stock solution
Yeast extract (Roth 25465689)	10	890 ml is prepared and adjusted to a pH between 7-7.5 and filled up to 900 ml and mixed with glucose solution.
$MgSO_4 \cdot 7H_2O$	0.25	
NaCl	2,5	
Peptone Roth 07357562	10	
MOPS	21	
Agar-Agar	15	For agar plate
pH adjusted between 7 and 7.5 with 5 M NaOH		

2.5.3   Cultivation of *Pseudomonas fluorescens* (DSM50090)

Pseudomonas fluorescens as a model organism sensitive to CO_2 [19] was selected. The agar and minimal media composition and operation condition are given in Tables 2.11, 2.12 and 2.13, respectively.

Table 2.10: Composition and preparation method of the mineral medium with glucose and acid lactic as carbon sources for the cultivation of bacterial strains of *C. glutamicum* in the ventilation and aerated flasks and lab scale fomenters [68]

Stock solution	Component	Amount (g/L)	Preparation for stock solution	Mixing (ml)
C –source	Glucose monohydrate for DM 1730 strain	15	to be solved in 50 ml distilled water and then autoclaved	50ml
	Lactic acid for WT 13032 strain	10	to be solved in 50 ml distilled water solution and adjust pH to 7 with 97 % sulfuric acid (H_2SO_4), before sterilization	
Basic solution	$(NH_4)_2SO_4$	1	to be solved in 890 ml distilled water	890ml
	KH_2PO_4	7.66		
	K_2HPO_4	3.3		
	$MgSO_4 \cdot 7H_2O$	3.0		
MOPS	$C_7H_{15}NO_4S$	21	to be solved in 50 ml distilled water	50ml
Calcium chloride	$CaCL_2 \cdot 2H_2O$	10	1gr is solved in 100ml distilled water autoclaved and 1ml used for medium	1ml
Micro-element	$FeSO_4 \cdot 7H_2O$	10	1/10 of these components are dissolved in 100 ml distilled water and adjusted to pH 1 with 97% sulfuric acid (H_2SO_4) 1 ml of sterile filtered solution was used for the medium	1ml
	$MnSO_4 \cdot H_2O$	10		
	$ZnSO_4 \cdot 7H_2O$	1		
	$CuSO_4$	0.2		
	$NiCl_2 \cdot 6H_2O$	0.02		
Vitamin	D-Biotin $C_{10}H_{16}N_2O_3S$	0.2	0.02gr. is solved in 50 % (v/v) 2-propanol and filled up to 100 ml with distilled water and sterilized by filter and 1 ml used for medium. To be kept in fridge for max. one week	1ml
3,4-dihydroxybenzoic acid	$C_7H_6O_4$	30	3 gr. is dissolved in 10 % NaOH (100 g/l) and filled up to 100 ml, kept in fridge and 1ml used for medium	1ml
Total volume	pH adjusted between 7 and 7.5 with 97% sulfuric acid (H_2SO_4) or NaOH 5M, and filling up to 1000 ml with sterilized distilled water			1000ml

Table 2.11: Composition of agar and minimal medium for *P. fluorescens*

Minimal medium		Agar medium	
substances	Concentration (g/l)	substances	Concentration (g/l)
Glucose	5	peptone	5
Yeast extract	2	Meat extract	3
$MgSO_4 \cdot 7H_2O$	0.25	Agar-agar	15
$(NH_4)_2SO_4$	6		
MOPS	21		
$CaCl_2 \cdot 2H_2O$	0.02		
Phosphate puffer	Table2.13		
adjusted pH to 7 with 5 M NaOH			

Table 2.12: Operation condition for cultivation of *Pseudomonas fluorescens*

Parameters	*Pseudomonas fluorescens*
Type strain	DSM 50090
C-source	Glucose (5 g/l) + yeast extract (2 g/l)
Minimal medium	Table 2.11
Buffer solution	MOPS (21 g/l)
Initial pH	7
Temperature	30 (°C)
Inoculation (Xo)	%10
Filling volume	10 (ml)
Agar medium	Table 2.11
Shaking frequency	350 (rpm)
Aeration in RAMOS	2.35, 0.22, 0.15 (vvm)

Table 2.13: The solution of phosphate buffer for minimal medium of *P. fluorescens*

Phosphate puffer solution	Amount [g/l]
Na_2HPO_4	3.5
$NaH_2PO_4 \cdot H_2O$	3.5

2.5.4   Buffer capacity and adjusting pH

The media were buffered by MES, phosphate and MOPS buffer solutions. The pH was adjusted to a requested value by 15M NaOH or 30 % and 98 % H_2SO_4.

2.5.5   Sterilization of medium

The sterilization of the media took place via heat sterilization for 20 min with 121 °C, either in autoclaves (Varioklav Dampfsterilisator, H+P Labortechnik GmbH) or in situ in the fermentor. Since the thermal treatment of the medium during sterilization procedure destroys the added vitamins or trace elements, the vitamins and 3, 4-dihydroxybenzoic acid had to be sterilized separately by sterile filter and combined with the other solution under sterile conditions.

2.5.6   Inoculation

An active and optimal inoculation size (usually 3-10 % (v/v)) was generally used to obtain a main culture with a minimized lag phase and to avoid low reproducibility of production fermentations.

Chapter 3

Characterisation of Gas Transfer through the Sterile Closure of a Ventilation Flask

3.1   Introduction

Shake flasks are traditionally equipped with different types of gas permeable closures, made from cotton, cloth, paper, polymeric sponger or membrane to prevent contamination. These closures play an important role in the aeration of the shaken bioreactors. This role can be characterized by mass transfer rates through the sterile closure (OTR_{plug}). The OTR_{plug} depends on the value of the gas transfer coefficients of the sterile closure (k_{plug}) and oxygen driving concentration [23, 57 and 66]. The parameter k_{plug} was assessed in literature using the effective oxygen diffusion coefficient ($D_{e,O2}$), in addition to the geometry of the sterile closure [23, 26 and 66]. It can also be obtained by experimental methods [21, 25 and 57]. Several methods for the determination of $D_{e,O2}$ have been reported [23, 49, 57, 66]. According to these reports, a proportional dependency of $D_{e,O2}$ to bulk density of the applied closure has been demonstrated.

Henzler and Schedel [23] have modeled the diffusive steady state gas transfer through a sterile closure by considering Fick´s multi-component gas diffusion [25, 26, 66, 76], combined with Stefan's convection flow. They demonstrated that the diffusion coefficient for oxygen is dependent on the gas concentration and, therefore, changes with the spatial location inside the sterile closure the operating condition of the shake flask, and the activity of the microbial culture. As a consequence, these authors recommended to use the diffusion coefficient for carbon dioxide, which is independent of gas concentration and, therefore, suitable to characterize the gas mass transfer through a sterile closure.

Mrotzek et al. [57] used an extended version of the Henzler and Schedel model [23]. They introduced an experimental steady state water loss method to characterize the mass transfer through a sterile closure and the concentrations of the gas components in the gas phase of the headspace of a shake flask (pi). It is a great advantage of this method that no special apparatus like an oxygen gas analyzer [25], a polarographic Clark electrode [79] or a non-invasive optical sensor [21] is necessary. In this Chapter, the gas transfer coefficient through the cotton closure (k_{plug}) will be experimentally characterized using the steady state water loss method [57] in the ventilation flasks (Sec. 2.1.1) and the Henzler and Schedel model [23].

3.2   Theory

Henzler and Schedel [23] modeled the steady state gas transfer through the sterile closure in shake flasks considering Fick´s diffusion combined with Stefan's convective flow, which occurs due to non-equimolar gas component transfer (Figure 3.1).
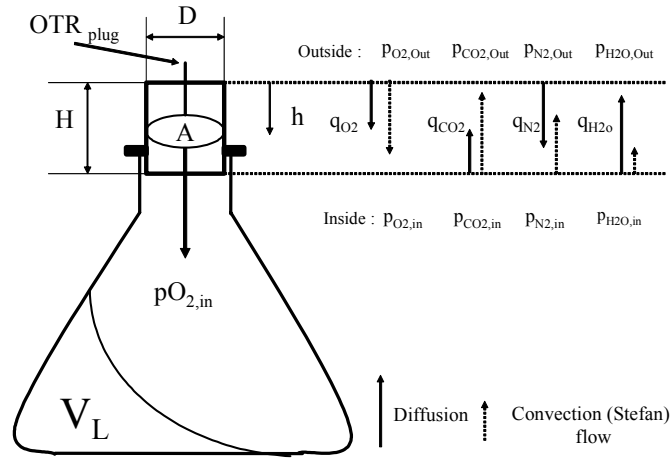
Figure 3.1: Schematic representation of the gas transfer through the sterile closure of a ventilation flask [23]

The effect of diffusion (D_i) and convective flow (w) on the gas transfer in the sterile closures of shake flasks is given by Eq.3.1:

$$q_i = -D_i \frac{\partial (p_i/p)}{\partial h} + w \frac{p_i}{p} \tag{3.1}$$

where D_i is the local effective diffusion coefficient of component "i" (Eq. 3.6) and p_i/p is the mole fraction of component "i" in a multi-component gas mixture (H_2O, O_2, N_2 and CO_2). The parameter h is the heights coordinate of the closure. The velocity (w) of the Stefan's convective flow (while the flow rate of the inert component nitrogen will be zero) is given by Eq. 3.2:

$$w = D_{N_2} \cdot \frac{\partial \left(\frac{p_{N_2}}{p} \right)}{\partial h} \cdot \frac{p}{p_{N_2}} \tag{3.2}$$

A combination of equations 3.1 and 3.2 gives:

$$q_{O_2} = -D_{O_2} \cdot \frac{\partial \left(\frac{p_{O_2}}{p} \right)}{\partial h} + D_{N_2} \cdot \frac{\partial \left(\frac{p_{N_2}}{p} \right)}{\partial h} \cdot \frac{p_{O_2}}{p_{N_2}} \tag{3.3}$$

$$q_{CO_2} = -D_{CO_2} \cdot \frac{\partial \left(\frac{p_{CO_2}}{p} \right)}{\partial h} + D_{N_2} \cdot \frac{\partial \left(\frac{p_{N_2}}{p} \right)}{\partial h} \cdot \frac{p_{CO_2}}{p_{N_2}} \tag{3.4}$$

$$q_{H_2O} = -D_{H_2O} \cdot \frac{\partial \left(\frac{p_{H_2O}}{p} \right)}{\partial h} + D_{N_2} \cdot \frac{\partial \left(\frac{p_{N_2}}{p} \right)}{\partial h} \cdot \frac{p_{H_2O}}{p_{N_2}} \tag{3.5}$$

The diffusion coefficient of compounds in the multi-component mixture (D_i) depends on the composition of the gas mixture [77] and is given by Eq. 3.6:

$$D_i = \frac{p - p_i}{\sum\limits_{j=1}^{n} \frac{p_j}{D_{ij}}} \quad ; i \neq j \tag{3.6}$$

The diffusion coefficient of the compounds O_2, CO_2, N_2 and H_2O are, therefore, given by following equations, respectively:

$$D_{O2} = \frac{p - p_{O2}}{\frac{p_{CO2}}{D_{O2-CO2}} + \frac{p_{N2}}{D_{O2-N2}} + \frac{p_{H2O}}{D_{O2-H2o}}} \tag{3.7}$$

$$D_{CO2} = \frac{p - p_{CO2}}{\frac{p_{O2}}{D_{CO2-O2}} + \frac{p_{N2}}{D_{CO2-N2}} + \frac{p_{H2O}}{D_{CO2-H2o}}} \tag{3.8}$$

$$D_{N2} = \frac{p - p_{N2}}{\frac{p_{O2}}{D_{N2-O2}} + \frac{p_{CO2}}{D_{N2-CO2}} + \frac{p_{H2O}}{D_{N2-H2O}}} \tag{3.9}$$

The kinetic properties of nitrogen and oxygen, which are very similar to each other [61], make the binary diffusion coefficients D_{CO2-O2} and D_{CO2-N2} equal. Furthermore, the partial pressure of nitrogen is 25 times higher than the partial pressure of water vapor. Thus, the partial pressure of water vapor can be neglected in the Eq. 3.8. The total pressure (p) is defined as the sum of the partial pressures:

$$p = \sum p_i = p_{O2} + p_{CO2} + p_{N2} + p_{H2O} \tag{3.10}$$

The consideration of Eqs. 3.8 and 3.10 and above assumptions lead to an equal value of the diffusion coefficient of carbon dioxide (D_{CO2}) with the values of the binary diffusion coefficients D_{CO2-O2} and D_{CO2-N2} in the multi-component gas mixture. It is, therefore, suggested that the diffusion coefficient of carbon dioxide is very useful to characterize the mass transfer through a sterile closure [23]. The diffusion coefficient for oxygen (D_{O2}) is dependent on the local gas concentration inside the sterile closure. The gas concentrations can change by operating conditions and the activity of the microbial culture. Hence, the average (effective) diffusion coefficient of oxygen **(D_{eO2})** should be considered, which can be calculated by Eq. 3.11.

$$D_{eO2} = \dfrac{\displaystyle\int_0^H D_{O2}\, dh}{H} \tag{3.11}$$

Important parameters for characterizing the gas transfer are the diffusion coefficients of the gas compounds in the multi-component mixture (D_i), the concentrations of the gas components in gas phase of the headspace of a shake flask (p_i) and the exact value of the gas transfer coefficient through the sterile closure (k_{plug}). OTR_{plug} can be calculated using pO_2 and k_{plug} with Eq. 3.12.

$$OTR_{plug} = k_{plug,\,O2} \cdot \dfrac{1}{V_L \cdot p_{abs}} \cdot (p_{O2,\,out} - p_{O2}) \tag{3.12}$$

An approximate value of k_{plug} and OTR_{plug} can also be derived from Fick's diffusion law [23 and 66]:

$$OTR_{plug} = \dfrac{D_{eO2} \cdot A}{H \cdot V_{mo}} \cdot \dfrac{1}{p_{abs} \cdot V_L} \cdot (p_{O2,\,out} - p_{O2}) \tag{3.13}$$

where:

$$k_{plug,\,O2} = \dfrac{D_{eO2} \cdot A}{H \cdot V_{mo}} \tag{3.14}$$

It is noted that the value of D_{eO2} depends on the density of the cotton closure and can be obtained by experimental methods [21, 26 and 79]. By the same method the gas transfer coefficient of CO_2 can be obtained:

$$k_{plug,\,CO2} = \dfrac{D_{CO2} \cdot A}{H \cdot V_{mo}} \tag{3.15}$$

where A/H (cross section area / height) is the neck geometric ratio of the flask.

3.3   Materials and methods

3.3.1   Ventilation flasks

In this study the experiments were carried out by using five equal flasks each of nine ventilation flask types f1-f9 (Chapter 2, Figure 2.2). The dimensions of these flasks are given in Table 2.1. The sterile barriers were made from steal pipes with different lengths or/and diameters, filled by cotton. In these experiments the constant cotton density was 0.15 g/cm^3. For this selected cotton density, an average value for the oxygen diffusion coefficient D_{eO2} of 0.153 cm^2/sec can be obtained from literature (Table 3.1).

Table 3.1: Average value of effective diffusion coefficient of oxygen through the sterile closure (D_{eo2}) obtained from literature; the ratio A/H characterizes the plug geometry.

Type of shake flask	Geometric ratio A/H (cm)	Density of cotton (g/cm^3)	D_{eo2} (cm^2/sec)	ref.
500ml narrow neck	1.7	0.17	0.130	[57]
250ml wide neck	3	0.16	0.135	[57]
500ml narrow neck	1.1	0.135	0.167	[23]
500ml narrow neck	1.8	0.135	0.170	[23]
500ml narrow neck	1.3	0.15	0.17	[66]
500ml narrow neck	2.4	0.15	0.153	[76]
Average			0.153	

3.3.2 Steady state water evaporation method to calculate D_{eO2} and D_{CO2} in sterile closures

For the measurement of D_{eO2} and D_{CO2}, a steady state water evaporation method and an extended model were used [57]. At first, the ventilation flasks f1-f9 were filled with 25 ml distilled water and were shaken under standard conditions (a shaken diameter of 5 cm, a shaking frequency of 200 rpm and a constant temperature of 30°C (Table 2.2)). After shaking for about 24 hours, in order to reach steady state conditions, the flasks were weighted and continuously shaken in an appropriate interval for about 260 hours. The flasks were weighted again to determine the rate of water loss during shaking.

3.3.3 The model of Henzler and Schedel

In this study the extended model of Henzler and Schedel [23] was applied. A ModelMaker (Version 3, 11997, Cherwell Scientific Publishing Ltd, UK) program (Eqs. 3.1-9, 3.11 and 3.12) was prepared similar to Mrotzek et al. [57]. The characteristics of gas transfer in the sterile closures were acquired using the data of water evaporation rates and the neck geometry of ventilation flasks. The important input variables of this model comprise the average relative environmental humidity of the shake flask ($RH_{outside.}$), the average temperature ($T_{ave.}$) detected by the sensor (Testo 625, Testo GmbH and Co. Germany), the geometry factor of the shake flask which is the quotient of the cross-sectional area and the height of closure (H/A), and the water evaporation rate (ER). These variables are summarized in the Table 2.3.

3.4 Results and Discussions

3.4.1   Water evaporation rates in the ventilation flasks

The effect of the sterile closure resistance on the mass transfer can be evaluated using the water evaporation rate method [57]. Figure 3.2 shows the mean values of the water evaporation rate in the ventilation flasks f1-f9 and its standard deviation. The deviation clearly demonstrates a significant difference between the results of the ventilation flasks f1-f9.
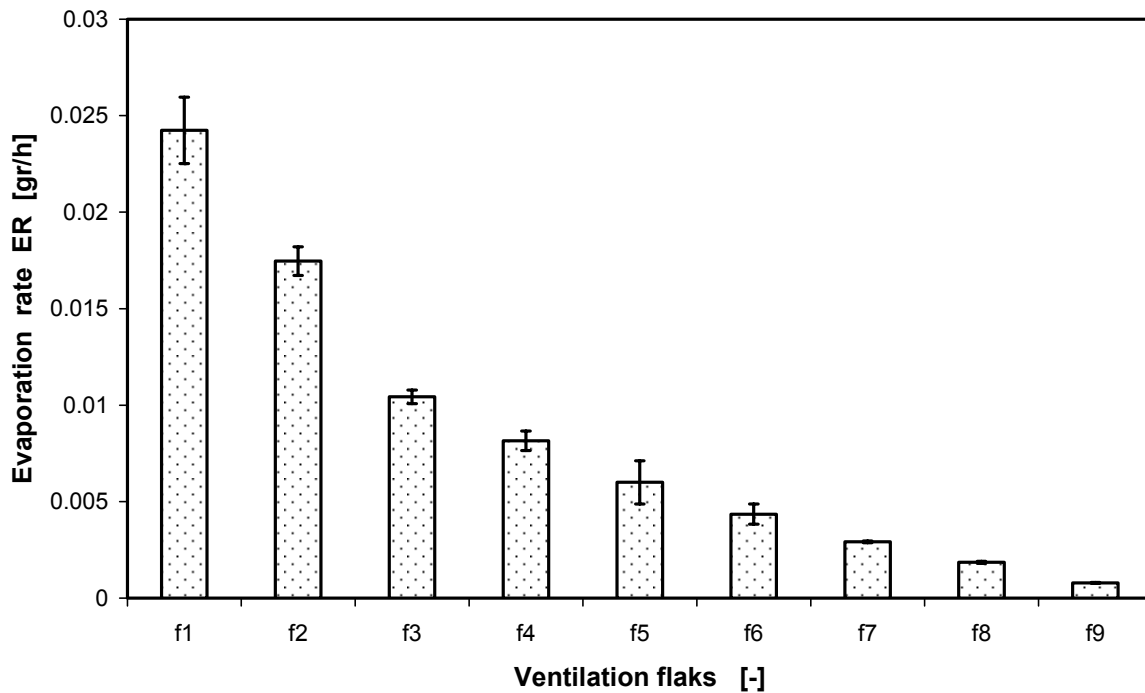
Figure 3.2: The values of water evaporation rate in ventilation flasks f1-f9, obtained using the water evaporation method (V_L=25 ml, T_{ave}=29.85°C, %$RH_{outside}$=23.4, do=5 cm, n=200 rpm, ξ=0.15 g/cm^3, experimental time=210-260 hours)

For instance, the water evaporation rate of the flask f9 was 31 times less than that of the flask f1. The effect of the closure dimensions on the amount of water evaporation in a shake flask has been also reported [18].

3.4.2   Determination of D_{CO2} and D_{eO2} in ventilation flasks

The diffusion coefficient of carbon dioxide (D_{CO2}) and the average diffusion coefficient of oxygen (D_{eO2}) through the sterile closure of the ventilation flasks were acquired using the values of the water evaporation rates (ER) (Sec. 3.4.1) in the extended Model of Henzler and Schedel [23]. Other parameters are mentioned in the legend of the Figure 3.2.

Figure 3.3 illustrates the values of D_{CO2}. No discrepancy between the mean values of D_{CO2} for the sterile closures of the ventilation flasks f2-f9 can be observed. The mean value of D_{CO2} is 0.123 cm^2/sec. The differences between the average carbon dioxide diffusion coefficients of ventilation flasks are lower than 7%. This minor error was due to the manually preparation of the closures. As an important consequence of these results, D_{CO2} has to be regarded independent of the geometry of the ventilation flasks, for a selected constant density of cotton (0.15 g/cm^3) [23 and 57].
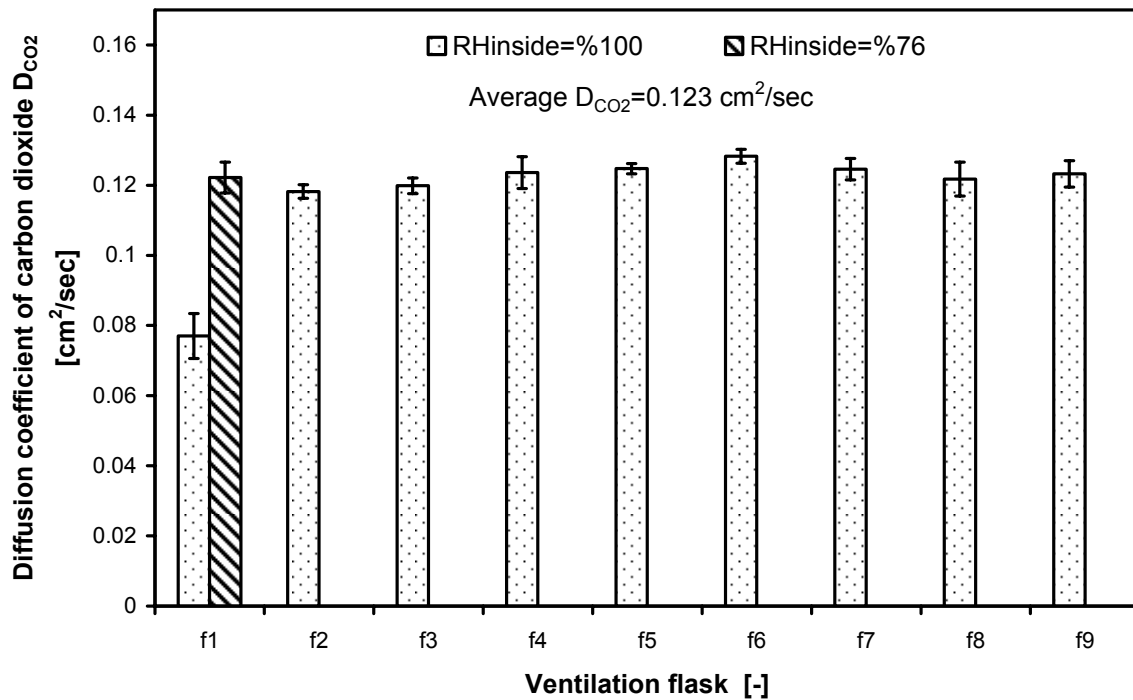
Figure 3.3: The comparison of the diffusion coefficient of carbon dioxide (D_{CO2}) determined by the water loss method and Henzler model in ventilation flasks f1-f9, (V_L=25ml, $T_{ave.}$=29.85, $RH_{outside}$=23.4 %, d_o=5 cm, n=200 rpm, geometry factor (Table 2.1), ER obtained from Figure 3.2)

In Figure 3.3 the value of D_{CO2} for flask f1 is less than that for the others. This can occur as a result of the difference between the relative humidity inside of this flask and the other flasks f2-f9. The relative humidity of the headspace (RH_{inside}), as an important input parameter of Henzler model, was assumed 100%. The correction of this assumption has been verified for normal shake flasks before by measurements [57]. In case of ventilation flask f1 the mass transfer resistance of the sterile closure with relatively wide cross sectional area and short height (Table 2.1) is obviously to decrease that a relative humidity in the headspace of 100% is not reached. Therefore, the average value of 0.123 cm^2/sec from the other flask f2-f9 was used as input value of the model of Henzler and Schedel [23] for flask f1 and the resulting relative humidity in the headspace of flask f1 was calculated. Comparison between the water evaporation rates (Figure 3.2) and those calculated by the Henzler and Schedel model showed

that the inside RH was about 76 % instead of 100 % in the headspace of the ventilation flask f1.

3.4.3   Determination of the O_2 and CO_2 transfer coefficients ($k_{plug,O2}$ and $k_{plug,CO2}$) in the sterile closure of the ventilation flasks

The values of D_{eO2} (with the average of 0.162 cm^2/sec) were calculated by Eq.3.11. The value of D_{eO2} is close to the average value of D_{eO2} obtained from literature (Table 3.1). Considering the values of D_{eO2} and D_{CO2} (Figure 3.3) in Eqs. 3.14 and 3.15, the values of $k_{plug,O2}$ and $k_{plug,CO2}$ can be calculated, respectively.

Figure 3.4 shows the values of D_{eO2} and $k_{plug,O2}$. As depicted in this Figure, there is no difference of the values of D_{eO2} for different flasks. On the other site there were considerable changes in the values of $k_{plug,O2}$ for the ventilation flasks f1-f9. $k_{plug,O2}$ in flask f1 is 23.4 times larger than that in flasks f9.

In a similar way, $k_{plug,CO2}$ could be calculated considering the average value of D_{CO2} in Eq. 3.15, which are illustrated by Figure 3.5.
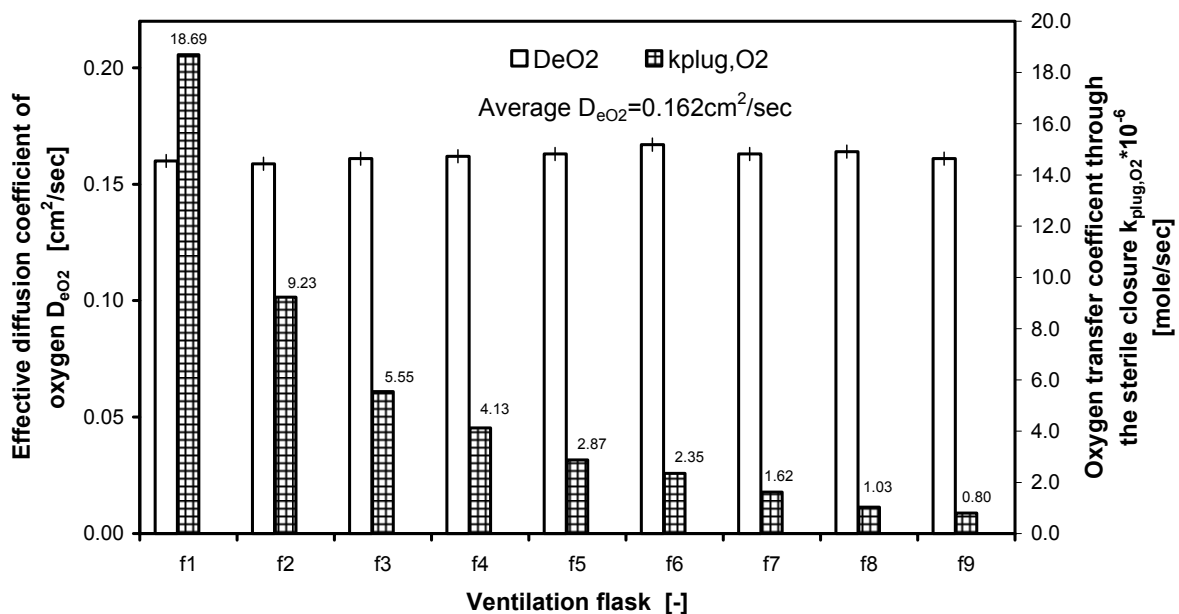
Figure 3.4: Average diffusion coefficient of oxygen (D_{eO2}) calculated using Eq.3.11, and the gas transfer coefficient of $k_{plug,O2}$ calculated by Eq.3.14 in the ventilation flasks f1-f9, (V_L=25 ml, $T_{ave.}$=29.85 °C, $RH_{outside}$=23.4 %, do=5 cm, n=200 rpm)
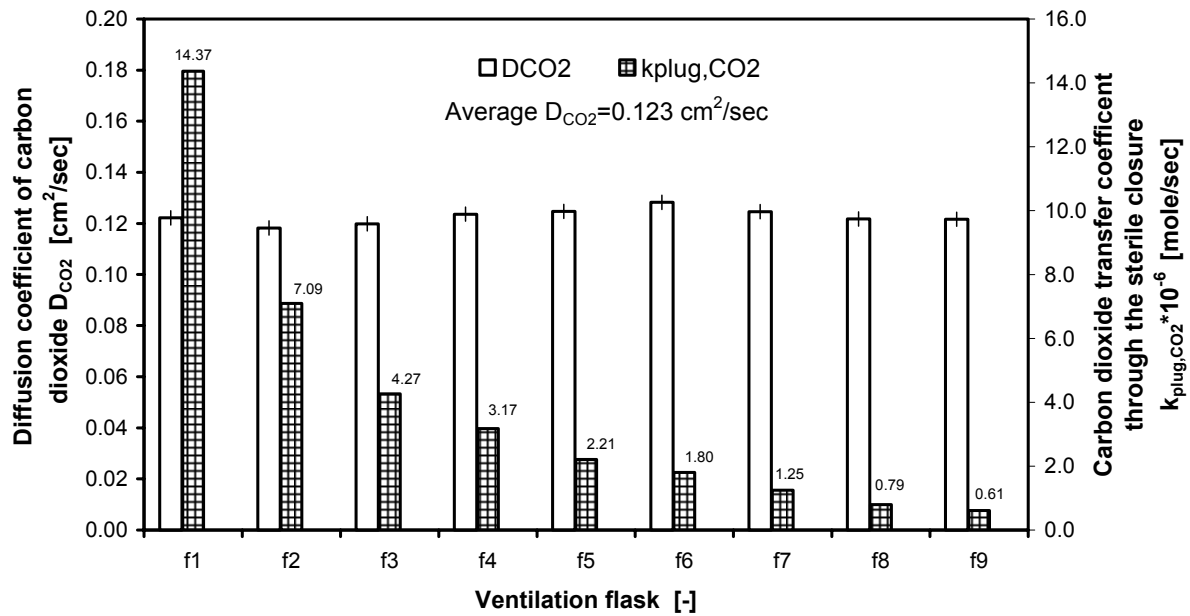
Figure 3.5: Diffusion coefficient of carbon dioxide (D_{CO_2}) determined by the water evaporation method and the Henzler and Schedel model, and the CO2 transfer coefficient k_{plug,CO_2} calculated from Eq.3.15 in ventilation flasks f1-f9, (V_L=25 ml, $T_{ave.}$=29.85 °C, $RH_{outside}$=23.4 %, d_o=5 cm, n=200 rpm, ER obtained from Figure 3.2)

3.5   Conclusion

The gas transfer through the sterile closure of ventilation flasks f1-f9 was characterized using D_{eo_2} and D_{CO_2} which were obtained by the water evaporation method and the model of Henzler and Schedel. These results indicate that D_{CO_2} is independent on the values of the neck geometry (Figure 3.3). There were some considerable differences between the values of k_{plug,O_2} obtained in the ventilation flasks f1-f9 (Figure 3.5).

In Chapter 4 the gas transfer in shake flasks will be modeled using the characteristics of gas transfer through the sterile closure. Furthermore, the differences between the values of k_{plug,CO_2} in the ventilation flasks (Figure 3.4) lead to different An accumulation of CO2 s in the headspace of the ventilation flasks f1-f9 containing a biological systems. This property of the ventilation flasks will be used in Chapter 6 for the investigation of a new method for quantification of CO_2 sensitivity of micro-organisms.

Chapter 4

Modeling and Advance Understanding of Unsteady State Gas Transfer in Shaken Bioreactors

4.1   Introduction

Aerobic micro-organisms will be oxygen limited if the oxygen transfer rate is smaller than the oxygen uptake rate in shaken bioreactors equipped with sterile closures [18, 23, 49, 57, 66 and 79]. To avoid oxygen limitation in the shake flasks, it is essential to have a good understanding and estimation of the gas transfer conditions. Therefore, it is necessary to evaluate the oxygen transfer rate through the sterile closure (OTR_{plug}) and gas liquid oxygen transfer rate (OTR_{g-L}) in the shaken bioreactors (Figure 4.1.A). The determination of the OTR_{g-L} and OTR_{plug} are related to the values of the gas transfer coefficients through the sterile closure (k_{plug}) and volumetric gas transfer coefficients of gas-liquid ($k_L a$). A number of studies have been carried out to describe the parameters $k_L a$ and k_{plug} by different experimental methods and/ or empirical models [23, 24, 25, 76 and 79]. For the evaluation of the $k_L a$ value e.g. the sulfite oxidation was used as a chemical model system and the dependency of $k_L a$ was systematically determined for a large variation of operating conditions [24, 44, 46 and 49]. It has also been known that for surface aerated shake flasks the gas/liquid mass transfer characterized by the sulfite oxidation method can directly be applied for microbial cultures employing a specific proportionality factor [46].

The calculation of parameter k_{plug} has already been explained in Sec. 3.4.3. Henzler and Schedel [23] have modeled the diffusive steady state gas transfer through a sterile closure and an extended version of this model to characterize the mass transfer through a sterile closure, an experimental steady state water loss method, was used as mentioned in Chapter 3.

In the above mentioned methods, steady state conditions are assumed ($OTR_{plug}=OTR_{g-L}$) and the "buffer capacity" of the gas amount in the head space of the flask is neglected. This assumption is not justified any more, if the resistance of the sterile closure becomes as large as the resistance of the gas-liquid interface Eq. 4.15. In this case the oxygen in the head space of the flask originating from the initial conditions at the time of the inoculation has to be taken into account. This oxygen may significantly contribute to the oxygen transfer for biological or chemical reaction in liquid phase, calling for an unsteady state approach (Figure 4.1.A).

The present work is aimed at modeling and understanding of unsteady state gas transfer in shake flask. The derived model is able to predict suitable operating conditions and prevent oxygen limitation and aeration problems in shaken bioreactors. The validity of the derived model was experimentally evaluated with the sulfite oxidation method. The application of this model for a biological system is shown later.
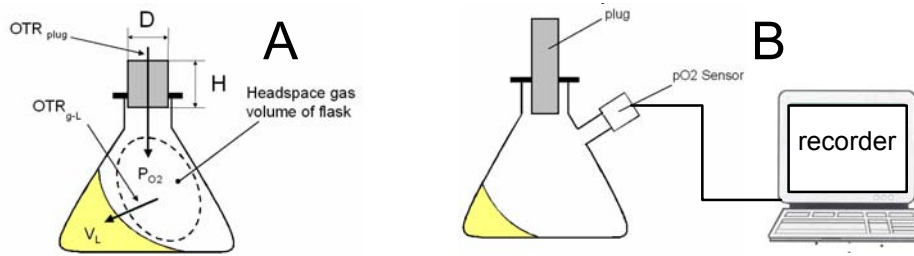
Figure 4.1: Schematic drawings of shake flasks, employed in this study; A-representation of gas transfer in a shake flask; B-apparatus for online measuring of pO_2 at varying gas transfer resistances of the sterile closures.

4.2 Theory

4.2.1 Mathematical background and models

In shaken bioreactors, containing a chemical (sulfite) or biological reaction system, the partial pressure of oxygen is dependent on OTR_{plug} and OTR_{g-L}. A mathematical modeling is useful for better understanding and quantitatively describing the gas transfer phenomena and analyzing the sensitivity of key parameters in shaken bioreactors. Thus, in the following part OTR_{g-L} based on an empirical equation for a sulfite reaction and a biological system is outlined. Then, the characteristics of steady state gas transfer in sterile closures is explained using a simple approximate model and the extended model of Henzler and Schedel [4] as described in Sec.3.2. Finally, the equations for modeling of an unsteady state gas transfer will be given.

4.2.2 Determination of gas transfer trough a sterile closure (OTR_{plug})

As mentioned in Chapter 3, the relation between the oxygen mass transfer through the sterile closure (OTR_{plug}) and the mass transfer coefficient (k_{plug}) is given by the following equations:

$$OTR_{plug} = k_{plug} \cdot \frac{1}{V_L \cdot p_{abs}} \cdot (p_{O2, out} - p_{O2}) \tag{4.1}$$

$$k_{plug} = \frac{D_{eo2} \cdot A}{H \cdot V_{mo}} \tag{4.2}$$

The values of D_{eO2} in the ventilation flasks (Sec. 3.4.2) was calculated using the experimental steady state water loss method [57] and Henzler and Schedel model [23] (Sec. 3.2). Eq. 4.2 is additionally used to approximately evaluate the value of k_{plug} in the applied ventilation flasks [26 and 66]. These values were determined in the section 3.4.3. In this study, a dependency between OTR_{plug} and the exact value of k_{plug} will be obtained using the above model.

4.2.3 Gas-liquid oxygen transfer with sulfite reaction system

The sulfite reaction system is frequently applied to characterize the gas-liquid mass transfer in shaken bioreactors [8, 23, 24, 44 and 46]. Hermann et al. [24] and Maier et al. [46] have recently described details of the gas-liquid mass transfer by the sulfite system. According to the theory of absorption and the assumption of the film model, the order of the sulfite oxidation reaction is classified as zero, one and two for sulfite, catalyst and oxygen, respectively [42 and 63].

When the oxygen concentration in the liquid phase is larger than zero, the gas-liquid oxygen transfer rate (OTR_{g-L}) can be calculated by:

$$OTR_{g-L} = k_L a \cdot L_{O_2} \cdot (p_{O_2} - p_{O_2,L})$$ (4.3)

where L_{O_2} is the solubility of oxygen in the sulfite solution (0.0008 mol/l/bar), which can e.g. be calculated by the method of Schumpe et al. [67].

It was demonstrated that the concentration of catalyst is an important factor for OTR_{g-L} [44, 46 and 63]. Maier et al. [44] have proven a linear dependency between OTR_{g-L} and $pO_{2,L}$ (Eq. 4.4) for a first order reaction at a catalyst concentration of 10^{-7} M:

$$OTR_{g-L} = k_1 \cdot L_{O_2} \cdot p_{O_2L}$$ (4.4)

Where k_1 is the first-order reaction constant of 2.358 h^{-1}, reported by Hermann et al. [24]. By resolving Eq. 4.4 for $pO_{2,L}$ and inserting this into Eq. 4.3 the following equation is obtained:

$$OTR_{g-L} = \frac{k_1 \cdot k_L a \cdot L_{O_2} \cdot pO_2}{(k_1 + k_L a)}$$ (4.5)

4.2.4 Gas-liquid oxygen transfer in a biological system

In order to model the gas transfer in a biological system the partial pressure of oxygen in liquid phase over the time of fermentation could be given as following:

$$\frac{\partial p_{O_2,L}}{\partial t} = -OUR + OTR_{g-L}$$ (4.6)

Where OUR is oxygen uptake rate and is given by:

$$OUR = \frac{1}{Y_{X/O_2}} \cdot \mu.X$$ (4.7)

The increase in cell mass during the fermentation is obtained from Eq. 4.8:

$$\frac{\partial X}{\partial t} = -\mu.X$$ (4.8)

where μ is specific growth rate, which depends on the substrate and the oxygen concentration, and calculates as:

$$\mu = \mu_{max} \cdot \frac{S}{S + K_S} \cdot \frac{O_{2,L}}{O_{2,L} + K_{O_2}}$$ (4.9)

$O_{2,L}$ is the dissolved oxygen. The consumption of substrate is described by:

$$\frac{\partial S}{\partial t} = -\frac{1}{Y_{X/S}} \cdot \mu \cdot X \tag{4.10}$$

In Eqs. 4.7 and 4.10 $Y_{X/S}$ and $Y_{X/O2}$ could be obtained from literature data [5].

4.2.5 Maximum oxygen transfer capacity (OTR_{max}) and gas-liquid transfer coefficient ($k_L a$)

The maximum possible oxygen uptake rate (OUR) of an aerobic culture is restricted by the maximum oxygen transfer capacity (OTR_{max}) [44]. In shake flask cultures, OTR_{max} strongly depends on the surface area of the gas-liquid interface of the rotating liquid and its velocity. The operating conditions (shaking frequency, shaking diameter, flask size and shape and the liquid culture volume) have an effect on these parameters [44], and consequently, on OTR_{max}. The value of OTR_{max} in shake flask can be calculated considering the $k_L a$ and the partial pressure of oxygen in the gas phase (refer to Eq. 4.3 when $pO_{2,L}$ is zero).

$$OTR_{max} = k_L a \cdot L_{O2} \cdot p_{O2} \tag{4.10}$$

The following empirical equation for $k_L a$ is inserted into Eq. 4.5 [44]:

$$k_L a = f \cdot 10^{-4} \cdot V_L^{-0.85} \cdot n^{1.15} \cdot do^{0.38} \tag{4.12}$$

The factor 'f' for a 0.5 M sulfite system equals to 5.51. Eq. 4.12 can also be applied for a biological system and the factor 'f' is experimentally determined by comparing a sulfite system with the studied biological system. Thus, this factor is calculated as following [72]:

$$f = \frac{OTR_{max} \quad \text{(biology)}}{OTR_{max} \quad \text{(sulfite)}} = \frac{k_L a \quad \text{(biology)}}{k_L a \quad \text{(sulfite)}} \tag{4.13}$$

4.2.6 Steady state gas transfer condition in shake flask

Assuming that the same amount of oxygen entering the flask through the plug is directly transferred to the liquid phase, the condition of steady state oxygen transfer ($OTR_{st.st.}$) is given [23, 25 and 79]:

$$OTR_{st.st.} = OTR_{plug} = OTR_{g-L} \tag{4.14}$$

Resolving Eq. 4.1 for pO_2 and introducing this expression into Eq. 4.5 the following equation for the oxygen transfer rate through the sterile closure or gas liquid interface in the steady state condition ($OTR_{st.st}$) is obtained.

$$OTR_{st..st.} = \left(\frac{V_L \cdot p_{abs}}{k_{plug}} + \frac{k_1 + k_L a}{k_1 \cdot k_L a \cdot L_{O2}} \right)^{-1} \cdot pO_{2,\,out} \tag{4.15}$$

Eq. 4.15 clearly shows that if the contribution of the resistance of the sterile closure

($\dfrac{V_L \cdot p_{abs}}{k_{plug}}$) is in the order of the resistance of the gas-liquid interface ($\dfrac{k_1 + k_L a}{k_1 \cdot k_L a \cdot L_{O2.L}}$), the plug

will play an important role for the total gas transfer in shaken bioreactors.

4.2.7   Unsteady state gas transfer condition in shaken bioreactors

In an unsteady state gas transfer model, the mole oxygen balance in the headspace volume of a shake flask (Figure 4.1.A) can be developed as follows:

$$\frac{\partial n_{O2}}{\partial t} = \dot{n}_{O2,\,plug} - \dot{n}_{O2,\,g\text{-}L} \tag{4.16}$$

According to the ideal gas law, the following equation is derived from Eq. 4.16:

$$\frac{\partial p_{O2}}{\partial t} = (OTR_{plug} - OTR_{g-L}) \cdot \frac{R \cdot T \cdot V_L}{V_g} \tag{4.17}$$

4.3   Material and Methods

4.3.1   Ventilation Flasks

A series of the ventilation flasks f1-f9, described in the section 2.1, were employed as described in Secs. 2.2.1 and 3.3.1 (Figure 2.2 and Table 2.1 for characteristic properties).

4.3.2   Apparatus for online measurement of pO_2 in ventilation flasks

For detecting the partial pressure of oxygen in the gas phase of the headspace of the flask, a calibrated oxygen sensor (MAX-250 C, Maxtec Inc., Salt Lake City, Utah, USA) was mounted in a special flask and response curves were monitored by a recorder. Figure 4.1.B shows this apparatus. In section 2.1.4 the measurement of O_2 by oxygen sensor was explained in detail.

4.3.3   Sulfite system

For experimental determination of the oxygen partial pressure in the head space of the flasks (pO_2) and the time for complete oxidation, the ventilation flasks were filled with sulfite solution. This solution consisted of 0.5 M sodium sulfite (98% purity, Roth, Karlsruhe, Germany), 10^{-7} M cobalt sulfate $CoSO_4$, (Fluka, Buchs, Swizerland), 0.012M phosphate buffer (Na_2HPO_4/NaH_2PO_4, Merck, Darmstadt, Germany), 10^{-5} M bromthymol blue (Fluka, Buchs, Swizerland), pH 8 adjusted with 2 M sulfuric acid. The flasks were fixed on an orbital shaker (shaking diameter do=5 cm, Lab-Shaker, Kuehner, Birsfelden, Switzerland). The experiments were carried out at a temperature=25 °C, shaking frequency=300 rpm and a filling volume 5<VL<20 ml.

4.3.4   Optical color change method

For the determination of the overall OTR the sulfite method described by Hermann et al. [24] was used. The exhaustion time of sulfite is required in this method. It was determined by optically monitoring the color change of the sulfite solution [24]. The depletion of sulfite is accompanied by a drop of the pH value from about 8 to about 4, which is followed by the color change of the employed pH indicator bromothymol blue from dark blue at pH 7.3 to yellow at pH 6.2. The color change was recorded by a video camera (DCR-VX700E, Sony, Germany). The overall oxygen transfer (OTR) is proportional to the moles of oxygen consumed by the sulfite oxidation and the duration of the sulfite reaction, yielding:

$$OTR = \frac{C_{Na_2SO_3} \cdot V_{O_2}}{t \cdot V_{Na_2SO_3}} \tag{4.18}$$

4.3.5   Biological system

For the validation of our unsteady state model to simulate the gas transfer in a biological system in the ventilation flasks, a strain of *Corenobacteriu glutamicum* DM 1730 was used as a model organism. The composition and preparation of medium (Tables 2.9 and 10) and the operation conditions (Table 2.8) were explained in Chapter 2.

4.3.6   Applied models

4.3.6.1 Steady state model

For the calculation of the steady state oxygen transfer ($OTR_{st.st.}$) Eqs. 4.2 and 4.15 are applied. The parameter $k_L a$ is obtained from Eq. 4.12

4.3.6.2 Unsteady state model

The unsteady state model is based on the extended model of Henzler and Schedel [23]. A ModelMaker program (Version 3, 11997, Cherwell Scientific Publishing Ltd, UK) was prepared similar to Mrotzek et al. [57]. By this model for the determination of the spatially-resolved concentrations and diffusion coefficients of the gas components in the sterile closures, the partial pressure of oxygen in the headspace of the flask (pO_2) and the exact value of k_{plug} were calculated.

In order to simulate the unsteady state gas transfer in shake flasks at a variety of operation conditions, represented by different resistances of the sterile closure (neck geometry) and kinetics of the chemical reaction or the activity of the microbial culture, a second time-

resolved ModelMaker program was prepared incorporating Eqs. 4.1, 4.5, 4.12 and 4.17. The required parameter k_{plug} is calculated from the model of Henzler and Schedel [23], e.g. Eqs. 3.1-9.

However, with these equations the spatially-resolved gas concentration in the sterile closure is calculated, whereas Eq. 4.17 has to be used to calculate the time-resolved oxygen partial pressure in the headspace. These equations can not be solved simultaneously by the applied ModelMaker software. Therefore, the dependency of k_{plug} on OTR_{plug} had to be calculated beforehand and was correlated by the following simple empirical equation:

$$k_{plug} = \frac{a \cdot OTR_{plug}}{b + OTR_{plug} + \dfrac{OTR_{plug}^2}{c}} \qquad (4.19)$$

This procedure is depicted in Figure 4.2. The model from Henzler and Schedel [23] and Eq. 4.1 resolved for k_{plug}, was employed. Considering Figure 4.2, first random values for OTR_{plug} (theoretically obtained by changing the operation conditions (V_L, n and do)) between zero and 0.04 mol/l/h for a flask with a certain neck geometry is selected.
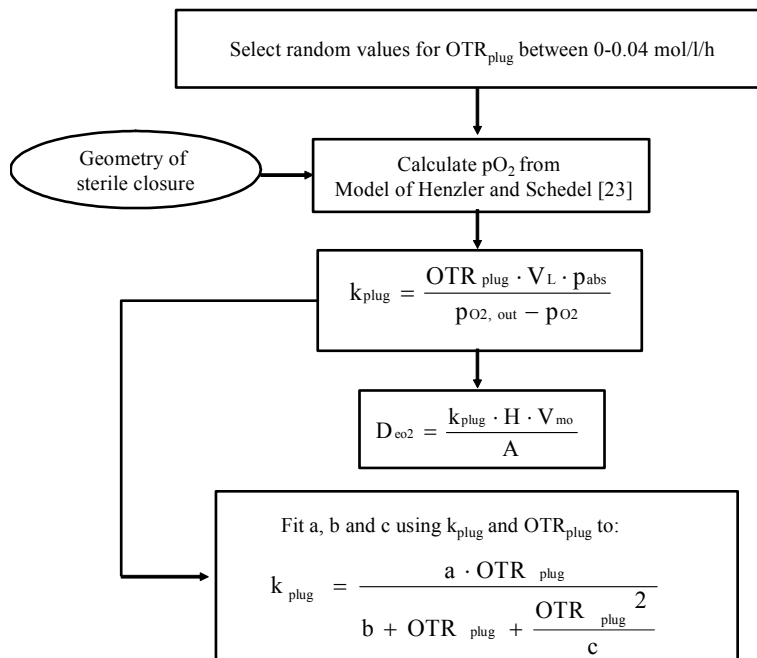
Figure 4.2: Flow sheet for the determination of the dependency of D_{eo2} and k_{plug} on OTR_{plug} by the model of Henzler and Schedel [23] considering the concentration dependency of the diffusive mass transfer and the convective Stefan flow.

Table 4.1: Characteristics of the sterile closures of the different shake (ventilation) flasks employed; values of k_{plug} as a function of OTR_{plug} and k_{plug} as a function of neck geometry (sulfite system (0.5 M), T=25 °C, n=300 rpm, d_o=5 cm, ζ_{cotton}=0.15 g/cm^3, D_{CO2}=0.116 cm^2/s, L_{O2}=0.0008 mol/l/bar)

Number of flask	D_{pipe} (cm)	H_{pipe} (cm)	k_{plug}^* (mol/s) $= \dfrac{a \cdot OTR_{plug}}{b + OTR_{plug} + \dfrac{OTR_{plug}^2}{c}}$		
-	-	-	$a*10^{-6}$	$b*10^{-3}$	c
f1	2.8	2.12	22.4	6.95	19.97
f2	2.8	4.20	11.06	5.36	10.5
f3	2.0	3.60	6.68	4.51	6.5
f4	2.0	4.72	4.98	3.87	2
f5	1.5	3.90	3.54	2.67	1.99
f6	1.5	4.85	2.85	2.22	0.923
f7	1.5	7.00	1.96	1.53	0.68
f8	1.5	11.00	1.25	0.97	0.47
f9	0.7	3.10	0.94	0.49	0.43

*Calculated according to procedure depicted in Figure 4.2

The partial pressure of oxygen in the headspace of the flask (pO_2) and then the exact value of k_{plug} (Eq. 4.1) is calculated. With this k_{plug} the effective diffusion coefficient D_{eO2} is obtained (Eq. 4.2). Finally the values of k_{plug} are correlated to OTR_{plug} by fitting the parameters of a, b and c (Table 4.1) of the selected empirical Eq. 4.19. The coefficient of correlation factor (r^2) was 1. The input parameters for this model and also the experimental conditions are summarized in the legends of each Figures and Tables.

4.4 Results and Discussions

The effect of the sterile closure of a shake flask is rarely considered in evaluating the over-all gas mass transfer. If the sterile closure is taken into account in literature, (in almost all cases) only simple steady state approaches with constant diffusion coefficients have been applied so far. Therefore, the effect of the spatially changing gas concentration inside the sterile closure and the buffer capacity of the gas present in the head space of the flask at the beginning of an experiment is investigated in this work.

4.4.1 Comparison between the resistances of sterile closure and gas-liquid interface in the sulfite system in the ventilation flasks

For the interpretation of the effect of sterile closures on the gas transfer, the resistance of the sterile closure ($\frac{V_L \cdot p_{abs}}{k_{plug}}$) and the resistance of the gas-liquid interface ($\frac{k_1 + k_L a}{k_1 \cdot k_L a \cdot L_{O2.L}}$) were compared [23, 26 and 79]. To calculate these resistances, k_{plug} and $k_L a$ obtained by the Eqs. 4.2 and 4.12 were used respectively. Figure 4.3 illustrates the comparison between these resistances for the 0.5 M sulfite system under a steady state condition. As it shows, the resistances of gas-liquid interface in the all flasks except f9 is larger than those of the sterile closures.

4.4.2 Dependency of D_{eO2} on OTR_{plug} considering the spatially changing concentration in the sterile closure

The procedure depicted in Figure4.2 was used to calculate the dependency of D_{eO2} on OTR_{plug} for the ventilation flasks f1-f9 (Table 4.1). The results are shown in Figure4.4.
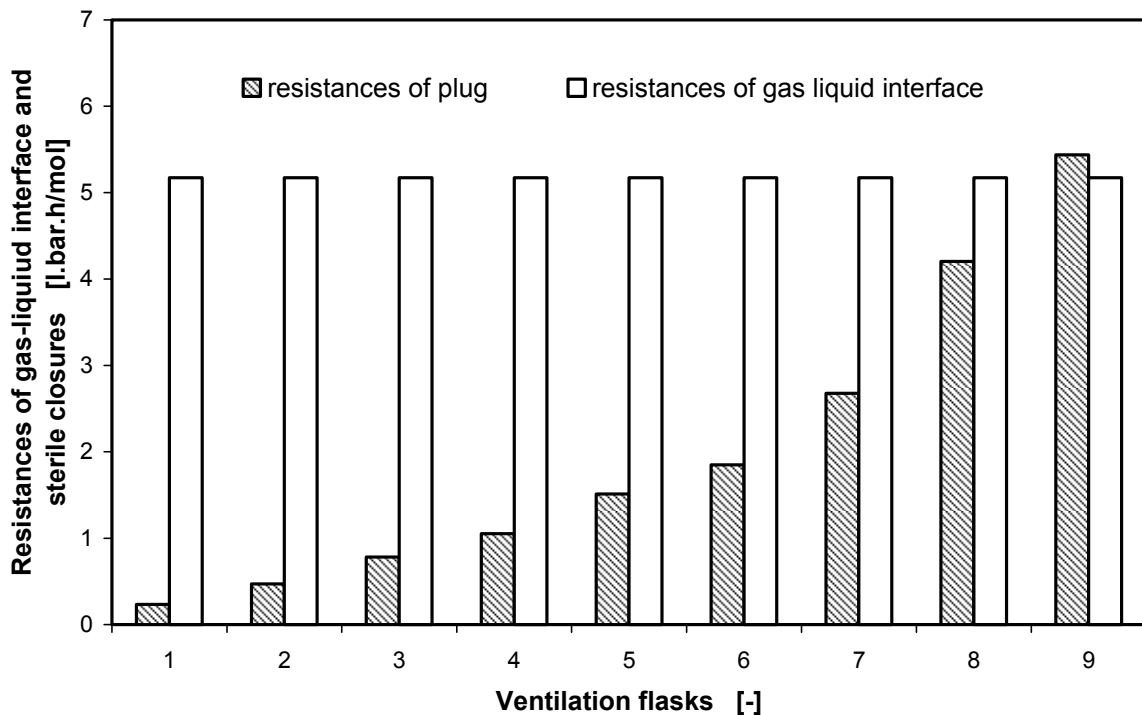
Figure 4.3: Comparison between the resistances of sterile closure and of the gas-liquid interface for the sulfite system (0.5 M); (T=25 °C, n=300 rpm, d_o=5 cm, V_L=15 ml) in the ventilation flasks f1-f9, A steady state gas transfer condition was assumed.

As illustrated by Figure 4.4, a variation of OTR_{plug} leads to a change in the values of the effective diffusion coefficient D_{eO2}. The resulting values are different for the different

geometries (ventilation flasks) and don't fall onto one curve. The calculated effective diffusion coefficients are evenly distributed above and below the literature value, depending on OTR_{plug} and the geometry. It should be noted that the cotton density of the sterile closures used in this work (ζ_{cotton}=0.15 g/cm^3) was roughly in the same order of magnitude as those cited from literature (ζ_{cotton}=0.135 - 0.17 g/cm^3, see the Table 3.1).
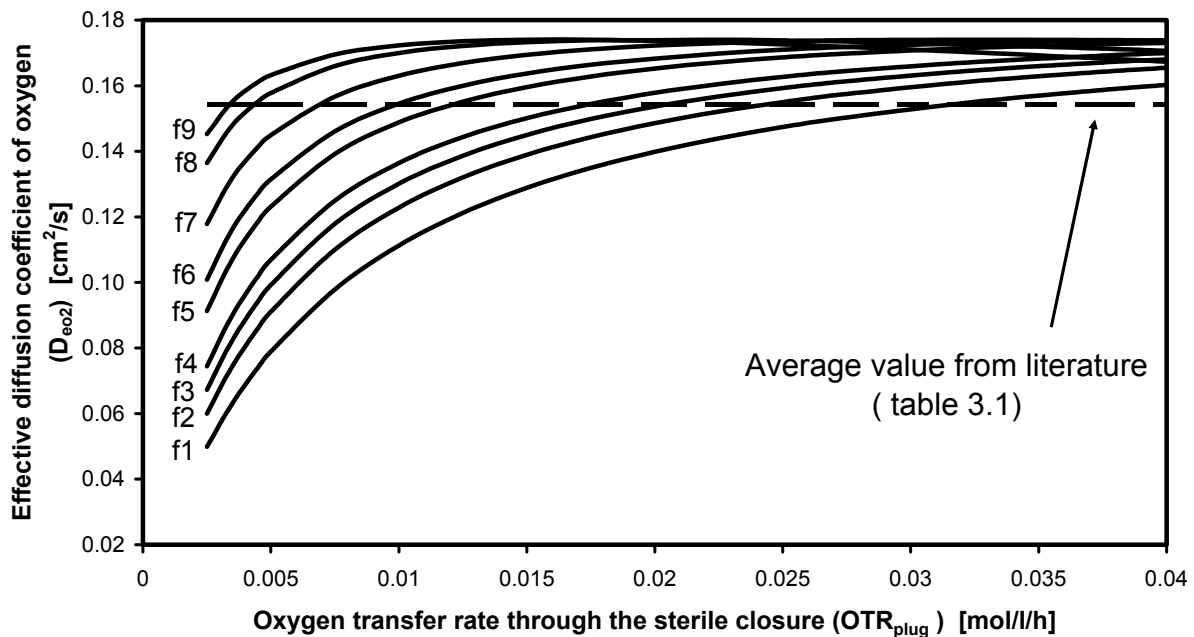
Figure 4.4: Dependency of the effective diffusion coefficient for oxygen (D_{eO2}) on the oxygen transfer rate through the sterile closure (OTR_{plug}) in flask f1-f9 (Table 4.1), calculated by the procedure depicted in Figure 4.2. For comparison the (constant) average diffusion coefficient from literature data (Table 3.1) is shown. Input parameters: sulfite system (0.5M), T=25 °C, n=300 rpm, shaking diameter d_o=5cm, saturated partial pressure of water vapor in the head space of the flasks $p_{sat.}$=0.03969 bar [61], filling volume V_L=15 ml, density of cotton plug ζ_{cotton}=0.15 g/cm^3

4.4.3 Simulation of gas transfer (OTR_{plug}, OTR_{g-L} and pO_2) in shake flasks by unsteady state modeling

It is interesting to investigate whether an unsteady state oxygen mass transfer approach will result in large differences compared to a simple steady state approach. Figure 4.5 shows a simulation of the oxygen transfer through the sterile closure (OTR_{plug}) and from the gas in the headspace of the flask to the liquid (OTR_{g-L}) for ventilation flasks f1 and f9 (Table 4.1) for the oxidation of a 0.5M sulfite solution. Eqs. 4.1, 4.5, 4.12, 4.17and 4.19 were used for calculating the unsteady state oxygen mass transfer. Note that k_{plug} is continuously recalculated from Eq. 4.19 using the parameters a, b and c from Table 4.1 for each time step. As a mentioned before, the steady state mass transfer was calculated by Eqs. 4.2, 4.12 and 4.15.
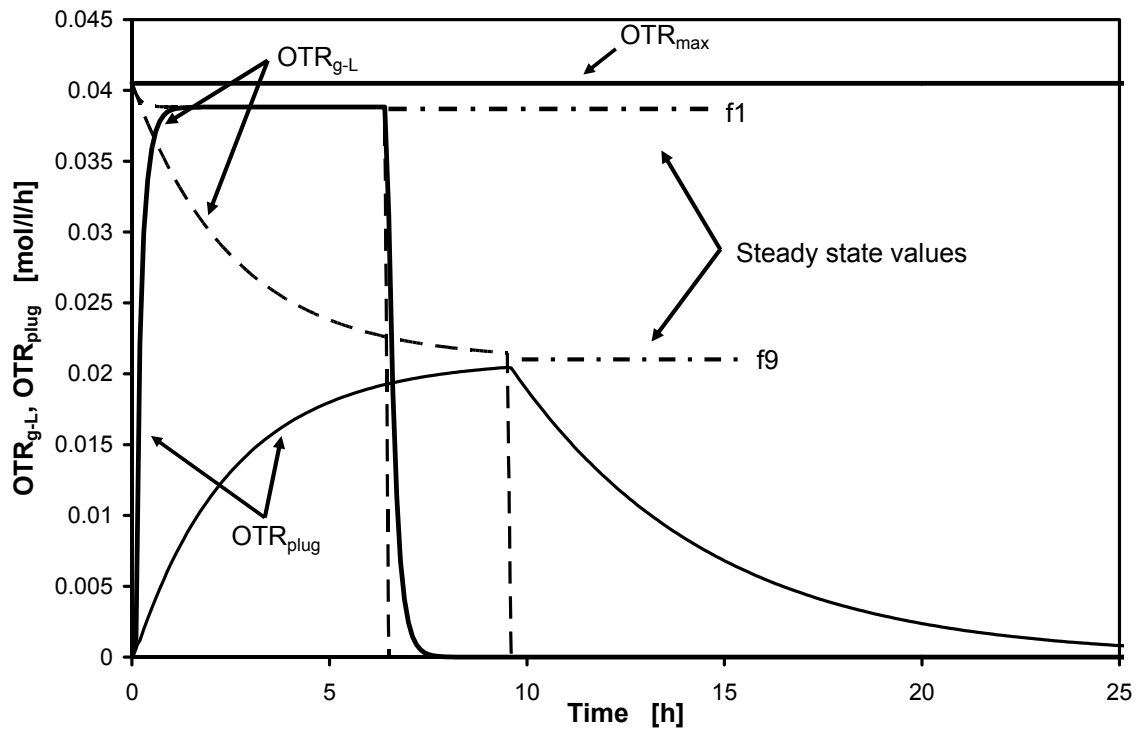
Figure 4.5: Model results for the oxygen transfer rate trough the sterile closure (OTR_{plug}) and from the gas in the headspace to the liquid phase (OTR_{g-L}) over time in ventilation flask f1 and f9 (Table 4.1). The collapse of OTR_{g-L} to zero (vertical dashed lines) indicate the exhaustion of the 0.5 M sulfite solution, T=25 °C, 300 rpm, d_o=5 cm, V_L=15 ml. Eqs. 4.1, 4.5, 4.12, 4.17, 4.19 and Eqs. 4.2, 4.12, and 4.15 for unsteady state and steady state calculation were used, respectively.

It can be seen that the OTR_{g-L} is at a maximum level (0.039mol/L/h) at the very beginning of the experiment. At this initial moment the head space of the flask is filled with air and, therefore, the driving concentration gradient from the head space gas phase to the liquid phase is maximal. On the contrary, OTR_{plug} is zero as no driving concentration gradient is present over the sterile plug at this time. Due to the continuous consumption of oxygen in the liquid and, consequently, removal of oxygen from the head space of the flask, its oxygen partial pressure decreases (see also Figure 4.6) as a result of mass transfer limitation of the sterile closure (see the Figure 4.3). OTR_{g-L} and OTR_{plug} decreases and increases, respectively, and both values approach a common steady state value (horizontal dash-dotted lines in Figure 4.5). In case of ventilation flask f1 (with a low mass transfer resistance of the sterile closure) this steady state value (0.036mol/L/h) is practically reached in a relatively short time of about 2 hours before the total amount of 0.5 M sulfite is exhausted and OTR_{g-L} collapses to zero at about 7 hours. In case of ventilation flask f9 (representing a relatively high mass transfer resistance of the sterile closure, Figure 4.3) the steady state value (0.021mol/L/h) has never been reached before complete exhaustion of the sulfite solution shortly before 10 hours. After the chemical reaction is completed (and OTR_{g-L} is zero) OTR_{plug} requires some time to

decrease to zero. In ventilation flask f9 this takes more time than the reaction itself and is even not completed after 25 hours.

Figure 4.6 shows the unsteady state oxygen partial pressures in the head space (pO_2) for all ventilation flasks f1-f9. The partial pressures of the flasks with 0.5 M sulfite solution is depicted as solid lines with small symbols. The hypothetical partial pressures for a reaction of infinite duration, approaching steady state conditions, are illustrated as dashed lines. At initial conditions all flasks contain air and the oxygen partial pressure is 0.2095 bars. As already explained before, the flasks with relatively low mass transfer resistance of the sterile closure (f1-f4) reach the steady state value more or less during the reaction. The other flasks (f5-f9) approach the steady state value, but the reaction is terminated due to exhaustion of sulfite before the oxygen partial pressure becomes close to the steady state value. The smaller the mass transfer resistance of the sterile closure of the flask the earlier the oxidation reaction is completed. If the hypothetical duration of a sulfite oxidation experiment is calculated based on stoichiometry and steady state assumptions (Eqs. 4.2, 4.12 and 4.15), values of 6.45 and 12.66 hours are obtained for f1 and f9, respectively. Theses times are 1.1 and 25 %, respectively, larger than the times obtained by considering unsteady state conditions (6.38 and 9.5 hours).
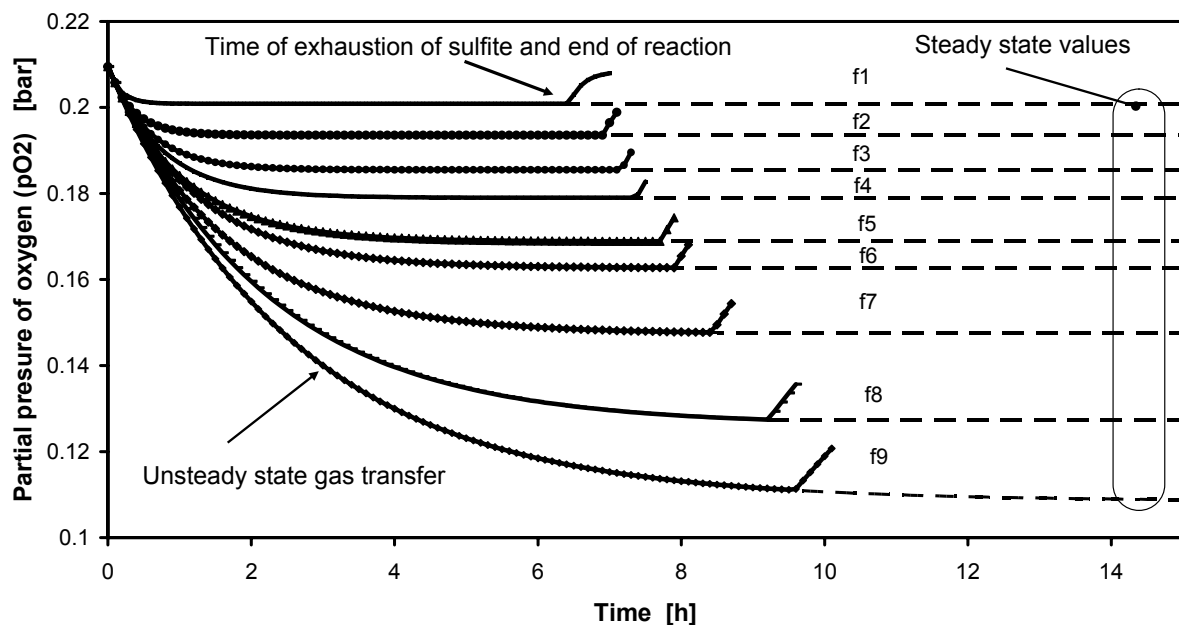
Figure 4.6: Simulation results of head space partial pressure of oxygen (p_{O2}) and the time of exhaustion of sulfite and end of the oxidation reaction under unsteady state gas transfer condition in the ventilation flasks f1-f9 with different k_{plug} as a function of OTR_{plug} (Table 4.1); 0.5 M sulfite solution, T=25 °C, n=300 rpm, d_o=5 cm, V_L=15 ml, ζ_{cotton}=0.15 g/cm^3

This is reasonable because the oxygen "buffer" in the head space, present from the start of the experiment, gives a significant contribution to total oxygen consumption. In total, the oxygen partial pressure in the head space is larger than that of under steady state assumption and consequently the driving concentration gradient for gas-liquid mass transfer is larger. These results in a faster reaction and a shorter time required for complete exhaustion of the sulfite.

These examples clearly demonstrate that a chemical or biological reaction in a shake flask may be strongly influenced by the mass transfer characteristics of the sterile closure. Due to the high "buffer capacity" of the head space, which is typically given in case of shake flasks, the kinetics may be completely different than calculated assuming simple steady state mass transfer conditions.

4.4.4   Validation of unsteady state model

For validation of the new unsteady state approach the model results for the oxygen partial pressure in the head space of a shake flask (pO_2) and the duration required for complete oxidation of 0.5 M sulfite was compared with experimental values.

For on-line monitoring of pO_2 special ventilation flasks (of f1, f4, f7 and f9) and oxygen sensors were used as illustrated in Figure 4.1.B. As can be seen from Figure 4.7, the value for the oxygen partial pressure (pO_2) is 0.2095 bar at the beginning of the experiment. Subsequently pO_2 decreases over time as the chemical reaction proceeds, the flasks with the larger mass transfer resistance of the sterile closure (higher flask numbers) approaching a lower level of partial pressure. At a specific time pO_2 starts to increase due to the exhaustion of the sulfite solution. As has already been discussed for Figure 4.6, the time of sulfite exhaustion occurs at later times for flaks with larger mass transfer resistance. There is a reasonable agreement between the measured and simulated time course of the oxygen partial pressures and the time of sulfite exhaustion. This proves that the general approach is justified and unsteady state gas transfer should not be neglected.

It has to be noted that the agreement between measured and simulated partial pressures is not fully given. This may be due to the fact that an approximation (Eq. 4.19) is used here to mathematically represent the spatially-resolved oxygen concentration in the sterile closure and, therefore, the mass transfer resistance (k_{plug}) as function of the oxygen transfer (OTR_{plug}). Another possible explanation of the slight deviation may be incomplete mixing of the gas phase of the special ventilation flasks (e.g. in the adapter of the sensor) applied for pO_2 measurement.
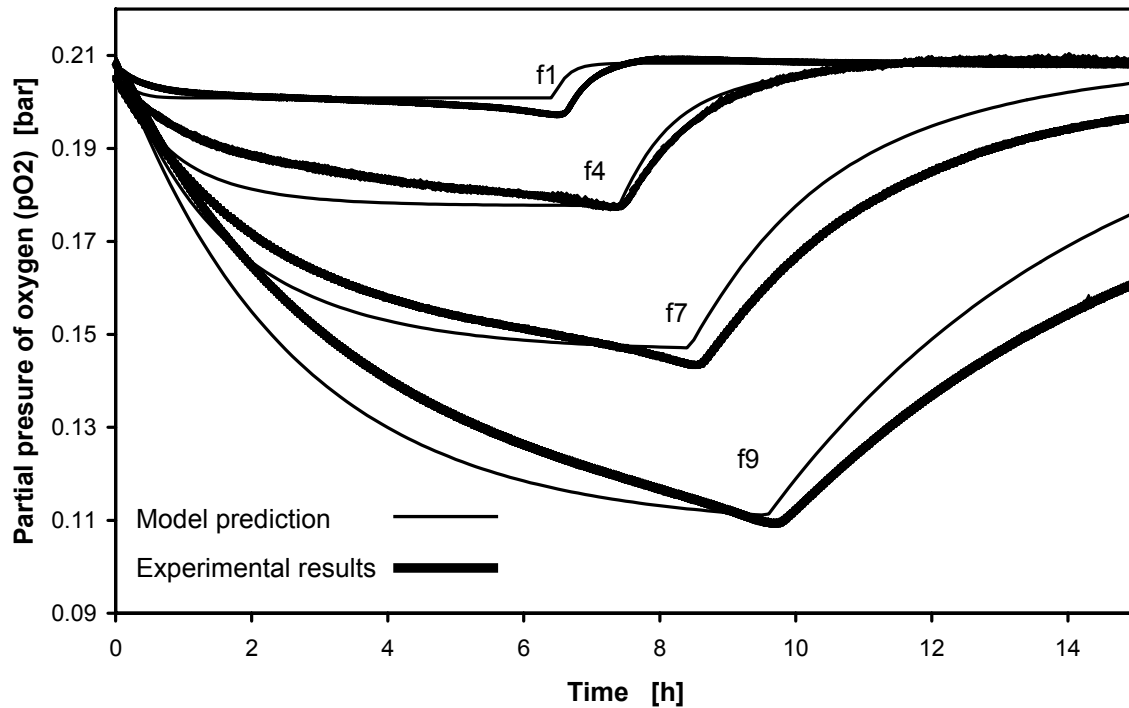
Figure 4.7: Comparison of measured and calculated change of partial pressure of oxygen (pO$_2$) in the head space of ventilation flasks with different sterile closures (f1, f4, f7 and f9). 0.5 M Sulfite solution, T=25 °C, n=300 rpm, d$_o$=5 cm, V$_L$=15 ml ζ_{cotton}=0.15 g/cm^3

For additional validation of the new unsteady state approach the time of the exhaustion of 0.5 M sulfite was recorded for many different operating conditions (ventilation flasks f1-f9 at different filling volumes and shaking frequencies) with the color change method described by Hermann et al. [24]. The experimental results are compared in a parity plot with simulation results for equivalent conditions obtained on the one hand by the steady state and on the other hand by the unsteady state approach. Figure 4.8 shows a systematic error for the data points calculated by the steady state method. The calculated time for the completion of the oxidation reaction is generally being too large.

It is obvious that the deviation between experiment and prediction is maximal for the shake flask with the largest mass transfer resistance of the sterile closure (f9). With decreasing mass transfer resistance (f8-f1) the deviation becomes smaller. On the other hand Figure 4.8 indicates a good agreement (with a regression coefficient (r^2) of 0.96) between the experimental and predicted time of sulfite exhaustion for all ventilation flasks calculated by the unsteady state method. Accordingly, this confirms the validity of the unsteady state model for prediction of the gas transfer in shake flasks.
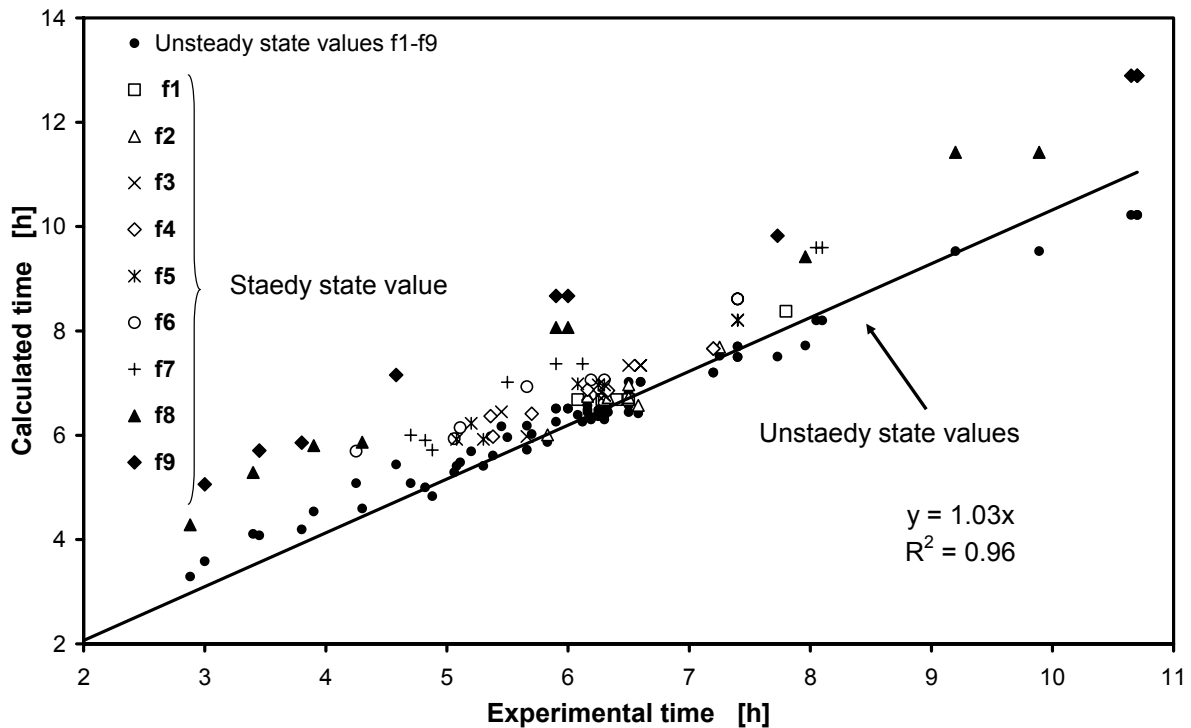
Figure 4.8: Comparison of measured and calculated time of the oxidation reaction of a sulfite solution (0.5M) until complete exhaustion. The unsteady state values for the ventilation flasks f1-f9 (●) were calculated by Eqs. 4.1, 4.5, 4.12, 4.17 and 4.19 and steady state values by Eq. 4.2, 4.12 and 4.15, using $D_{eO2}=0.153$ cm^2/s (Table 3.1), T=25 °C, do=5 cm, 4 ml<V_L<25 ml, 100 rpm<n<400 rpm.

4.4.5 Application of unsteady state model for a biological system

The proposed model was modified for an application to simulate the gas transfer in a biological system in the ventilation flasks. In order to do that, Eqs. 4.6, 4.7, 4.8, 4.9 and 4.10 were implemented in our unsteady state model. The simulation of the gas transfer for the fermentation of *C. glutamicum* DM 1730 on 15 g/L glucose in the ventilation flasks f1 and f9 was obtained using this model. Figure.4.9 shows this simulation results. The values of the applied parameters for this model are given in the legend of Figure 4.9 (Table 2.3). As illustrated in this Figure, the model is able to predict the characteristics of gas transfer in this biological system, e.g. pO$_2$, OTR$_{g-L}$, OTR$_{plug}$. With this model it is also possible to predict suitable operation conditions to avoid oxygen limitation in ventilation flasks. The simulation results for flask f9 confirm strong unsteady state condition, as similar to the sulfite system (Figure 4.5).

For the validation of the unsteady state model for a biological system (Figure 4.9), the fermentation of *C. glutamicum* DM1730 (10 g/l glucose and 10 ml filling volume) in the ventilation flasks f1, f4, f7 and f9 equipped with an oxygen sensor (Figure 4.1.B) was carried out according to Materials and Methods (Sec. 4.3.5).
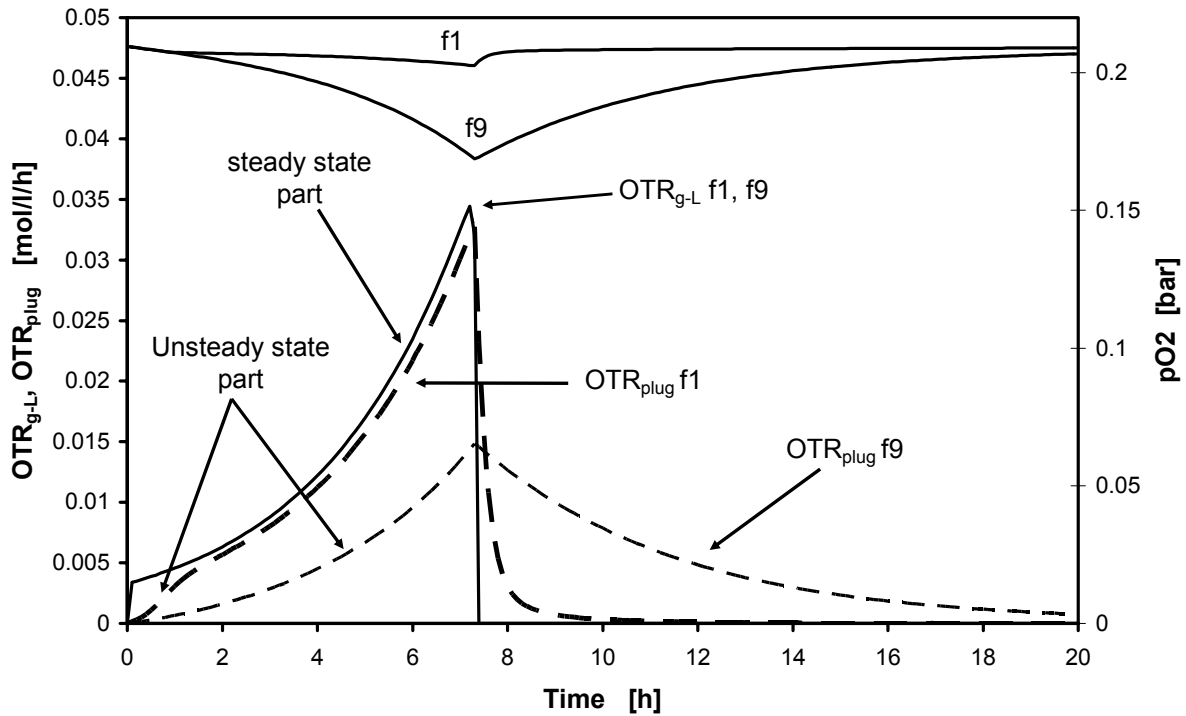
Figure 4.9: Model results for OTR_{plug}, OTR_{g-L} and pO_2 in the ventilation flasks f1 and f9. The input parameters were selected for fermentation of *C. glutamicum* DM1730 on 10 g/l glucose (n=400 rpm, V_L=10 ml, T=30 °C, d_o=5 cm, $Y_{x/s}$=0.48, $Y_{x/o2}$=53 g/mol, RQ=1, Xo=0.5 gr/l, f=0.23 calculated by Eq. 4.13, K_S=0.0045 gr/l, K_{O2}=10^{-6} mol/l, μ_{max}=0.32 h^{-1})
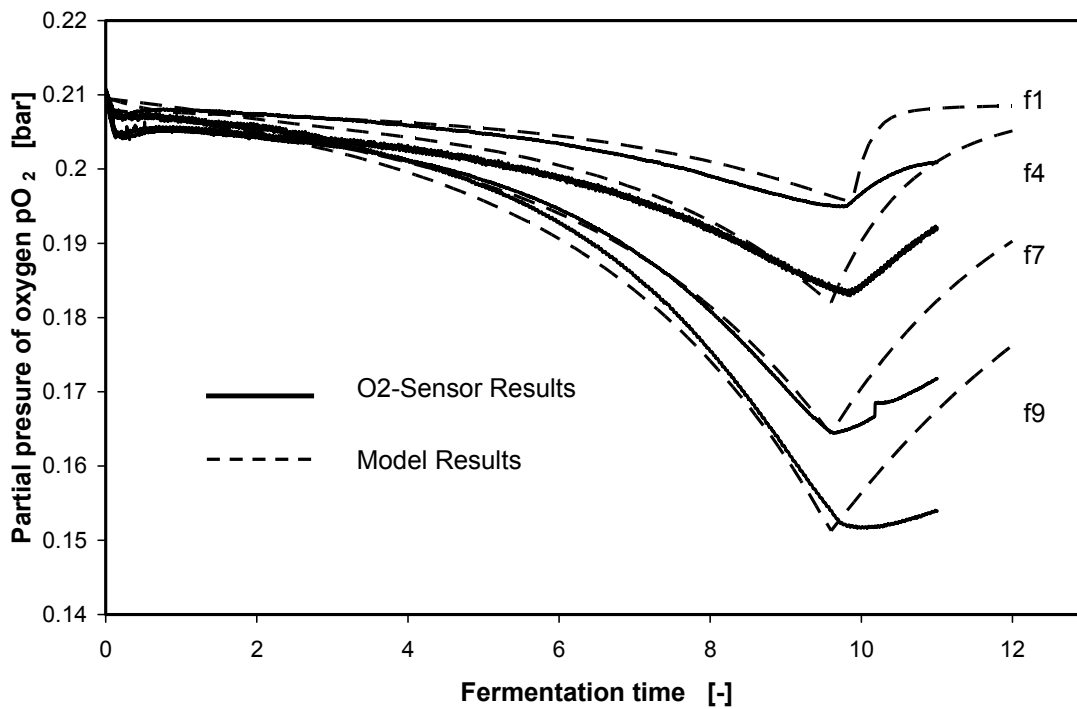
Figure 4.10: Comparison between unsteady state model and experimental results for the partial pressure of oxygen in the headspace of the ventilation flasks f1, f4, f7, f9 obtained for the fermentation of *C.glutamicum* DM 1730 on 10 g/l glucose and 21 g/l MOPS (V_L=10 ml, n=400 rpm, T=30 °C, d_o=5 cm, $Y_{x/s}$=0.48, $Y_{x/o2}$=53 g/mol, RQ=1 [5]).

The pO_2 was recalculated using the data of the oxygen sensor (Eq.2.1). The experimental and model results were compared in Figure 4.10. A good agreement between both results confirmed that the unsteady state model is valid for a biological system. The difference between the experimental and model results after 9.6 hours of fermentation may be due to the differences in the values of O_2 and CO_2 diffusion through the sterile closure as described in the Figures.3.5 and 3.6.

4.5   Conclusion

The mass transfer resistance of the sterile closure of a shake flask has a widely neglected effect on the performance of microbial cultures. If the characteristics of the sterile closure are considered at all, only simple models assuming steady state conditions are applied. In this work the influence of the mass transfer resistance of the sterile closure on oxygen partial pressure in the head space of a flask (pO_2) and on total oxygen transfer is investigated using a chemical model reaction (sulfite oxidation) and a biological system. It has been shown that the mass transfer resistance of the sterile closure should not be represented just by a constant parameter (k_{plug} or D_{eO2}). The model of Henzler and Schedel [23] should be used, which correctly describes the spatially-resolved change of the gas partial pressures inside the sterile closure. From this extended model a representation of the mass transfer resistance of the sterile closure which is closer, to reality and dependent on the mass flow through the plug, can be obtained [57]. This representation of the mass transfer resistance of the sterile closure is then incorporated into an unsteady state model. It could be shown that large discrepancies are obtained between the simple steady state and the new unsteady state simulations. This was proven by two kinds of validation experiments applying two different measuring methods. The extension of the error depends on the level of mass transfer resistance of the sterile closure and the total amount of oxygen consumed by the chemical or biological reaction in the liquid, e.g. total time of the experiment. The conventional approach neglects the "buffer capacity" of the head space of the flask and, therefore, generally underestimates the oxygen transfer, especially at the beginning of an experiment.

The presented unsteady state model may become a useful tool for correct prediction of gas transfer in shaken bioreactors under a wide range of values of k_{plug} and k_La. The findings could be a key point for the optimization of the experimental conditions of microbial cultures avoiding oxygen limitation.

As mentioned in the following Chapter, the introduced ventilation flasks are applied to investigate the effect of aeration and of CO_2 produced by the cultures and accumulated at different partial pressures in ventilation flasks f1-f9 on the performance of different microbial systems.

Chapter 5

A New Aeration Strategy from a

Ventilation to an Aerated Flask

5.1   Introduction

The sterile closures of the shaken bioreactors play an important role in the aeration. Aeration in shake flasks is achieved by a simple gas liquid contact, supported by shaking in the reciprocating or rotary shaking machines [29 and 46].

As mentioned in Chapters 3 and 4, the gas transfer in ventilation flasks can be affected by the coefficients of the gas liquid interface (k_La) and the sterile closure (k_{plug}). Under a defined operation conditions, the values of resistance of sterile closure may become a critical factor for supplying the oxygen in aerobic fermentations. Use of manufactured cotton plug leads to poor understanding of physical parameters, e.g. gas transfer and aeration factor, in the normal shake flasks in comparison with aerated flasks [8 and 23]. Considering this promotion, it is proposed that the gas transfer in sterile closure can be characterized using a new dependency of k_{plug} on OTR_{plug} (Sec.4.3.6.2).

The aim of this Chapter is to validate a new strategy for aeration from the ventilation to flasks aerated (RAMOS device). By means of this new method, a better comparability based on obtaining the same gas concentration in the headspace of both flasks can be achieved. For this goal the values of specific aeration rate (q_{in}), calculated by the values of OTR_{plug} in ventilation flask, will be used for aerated flasks, e.g. measuring flask of RAMOS device. This could be advantageous for scaling -up from a shake flask to a stirred tank bioreactor.

5.2   Theory

Using the oxygen balance on the gas transfer through the sterile closure and the gas flow into the aerated flask, the equations 5.1 and 5.2 are derived, respectively:

$$OTR_{plug} = k_{plug} \cdot \frac{1}{V_L \cdot p_{abs}} \cdot (pO_{2,out} - pO_2) \tag{5.1}$$

$$OTR_{flow} = \frac{1}{p_{abs} \cdot V_{mo}} \cdot q_{in} \cdot (pO_{2,out} - pO_2) \tag{5.2}$$

OTR_{flow} is defined as the amount of oxygen transferred by aeration into a chemical or biological system in the aerated (measuring) flask, and q_{in} is the specific aeration rate (vvm) in this flask. In order to have an equivalent gas concentration (pO_2) in the headspace of both flasks, OTR_{plug} should be equal to OTR_{flow}. This gives the Eq.5.3:

$$q_{in} = \frac{V_{mo}}{V_L} \cdot k_{plug} \tag{5.3}$$

The values of k_{plug} were quantified using the dependency of k_{plug} an OTR_{plug} (Eq. 4.19). With substitution of Eq. 4.19 in Eq. 5.3, the following equation can be developed:

$$q_{in} = \frac{V_{mo}}{V_L} \cdot k_{plug} = \frac{V_{mo}}{V_L} \cdot \frac{a \cdot OTR_{plug}}{b + OTR_{plug} + \frac{OTR_{plug}^2}{c}} \qquad (5.4)$$

where a, b, c are given in the Table 4.1. Using the values of OTR_{plug} which are resulted by unsteady state model (Chapter 4), in the Eq. 5.4 a pattern for the aeration in the sterile closure during a sulfite reaction or a biological system can be simulated. From this simulation a maximum aeration rate (max. q_{in}) can be obtained. In this chapter, a new aeration strategy will be experimentally investigated, using the maximum q_{in} for aeration in the aerated flask.

5.3   Materials and methods

5.3.1   Ventilation flasks equipped with oxygen sensor

In this study the special ventilation flasks f1, f4, f7 and f9 equipped with oxygen sensors were employed as described in Chapter 2 (Sec. 2.1.4 and Figure 2.1-A).

5.3.2   A special aeration system for the measuring flask of the RAMOS device

In this study a RAMOS device with measuring flasks (Figure 2.1.C) was utilized (Sec. 2.1.). The aeration system of the RAMOS device [3 and 4] was modified for acquiring an equivalent gas concentration in the headspace of the measuring flasks to that in the ventilation flasks. The aeration system comprises of two mass flow controllers (5850TR, Brooks Instruments, Venendaal, NL), two gas distributors and capillary tubes with different length for adjusting the aeration rates. Uses of two mass flow controllers were due to obtain a better accuracy in supplying the low aeration rates in the aerated flasks. Figure 5.1 illustrates the developed aeration system for the measuring flasks of RAMOS device that allow parallel experiments with the ventilation flasks. The specific aeration rates (vvm) in the aerated measuring flasks of the RAMOS device (rf1, rf4, rf7 and rf9) were adjusted to the calculated amount of the maximum q_{in} for the parallel ventilation flasks. The flasks were fixed onto a shaker and the sensors were appropriately connected.

5.3.3   Unsteady state model to determine q_{in} in the aerated measuring flasks of the RAMOS device

In order to estimate the values of specific aeration rates (q_{in}), for the aerated measuring flasks of the RAMOS device that result in the same gas concentration as in the headspace of the ventilation flask. OTR_{plug} was calculated from the unsteady state model (Chapter 4) and inserted into Eq. 5.4. This model can simulate qin and OTR_{plug} during the sulfite reaction or

biological systems. As will be shown later q_{in} significantly changes with OTR_{plug} and time. Therefore, the maximum value of specific aeration rates (max. q_{in}) was arbitrarily chosen to be used in order to aerate in the measuring flask of the RAMOS device.
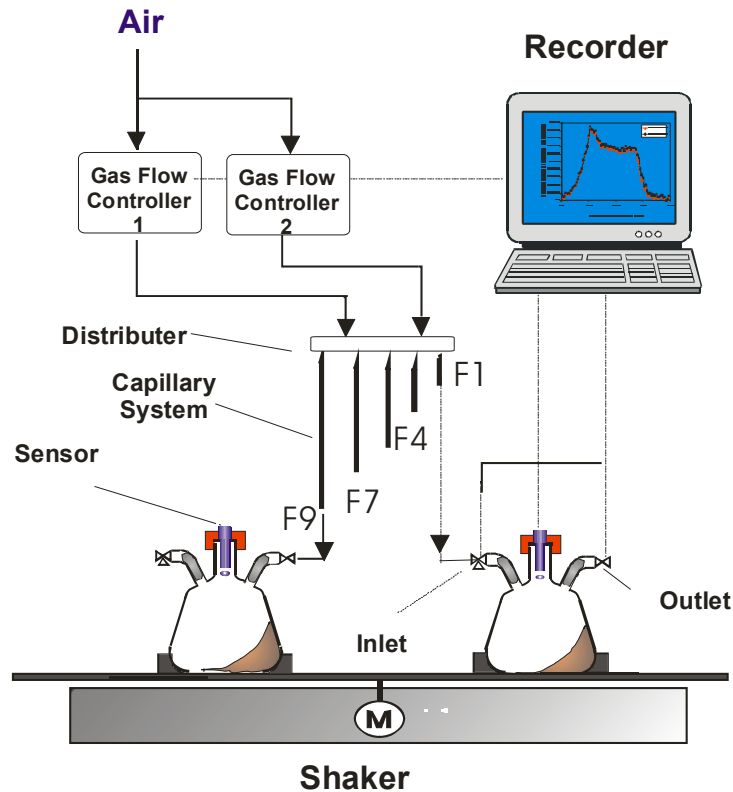
Figure 5.1: Development of the aeration system for the RAMOS device [3] employed in this study.

5.3.4   Model organisms and cultivation system

The *C. glutamicum* DM 1730 as a model organism was used. The mediums preparation and the cultivations system were given in section. 2.6.2. The operation conditions and the aeration rates are given in the Table 2.8 and Table 5.1, respectively.

5.4   Results and Discussions

5.4.1   Simulation of the specific aeration rate (q_{in}) in the ventilation flask

As noted in Figs. 4.7, 4.8 and 4.10, the unsteady state model was able to correctly simulate the gas transfer for a biological system in the ventilation flasks. In this study a modified unsteady state model was used (Sec. 5.3.3) for the calculation of the specific aeration rates (q_{in}) of an aerated measuring flask of the RAMOS device that result in the same headspace concentrations as in the ventilation flasks f1 and f9 for a biological system *C. glutamicum* DM 1730.

Figures 5.2 and 5.3 show simulations of OTR_{plug} in ventilation flasks f1 and f9 (see also Figure 4.9). The input parameters (Table 2.3) of this model are given in the legends of Figures 5.2 and 5.3. Also q_{in} was calculated for the aerated measuring flasks of the RAMOS device which provide equivalent conditions as in the respective ventilation flask The outcomes of this model for a sulfite reaction or a biological systems are given in Table 5.1. It is noted that, the small differences between the data of aeration rates in the aerated and ventilation flasks f4, f7 and f9 were due to the difficulty in adjusting the low aeration rates by the capillary system

As illustrated by Figure5.2 the values of the q_{in} increases with increasing ORT_{plug} until a maximum value of 1.45-1.5 vvm.

Table 5.1: Comparison between the maximum values specific aeration rates in ventilation flask (q_{in}), and those values in the (measuring) flask of RAMOS which are used in this study (V_L=15ml, d_o=5cm).

flasks	Specific aeration rate q_{in} [vvm]			
	0.5 M Sulfite system		Biological system	
	Calculated maximum value	Value adjusted in aerated flask	Calculated maximum value	Value adjusted in aerated flask
f1	1.21	1.85	1.47	1.5
f4	0.45	0.46	0.39	0.4
f7	0.18	0.16	0.19	0.21
f9	0.08	0.09	0.08	0.1

* Calculated unsteady state model
** These values were used in our experiments, provided by a special aeration system in RAMOS (Sec. 5.3.2)

Figure 5.3 shows OTR_{plug} for ventilation flask f9 (see also Figure 4.9)and the resulting specific aeration rate q_{in} for a respective aerated flask. In that case, maximum values between 0.07 and 0.08 vvm were calculated for the specific aeration rate.

These mentioned maximum values were calculated for the considered biological system under non-oxygen limited condition. Other simulations have shown that changing some input parameters such as filling volume, carbon source concentration and shaking frequency could lead to an oxygen limitation in ventilation flasks. Therefore, the maximum aeration rate was used in order to avoid oxygen limitation, since an oxygen limitation may occur from a lower aeration rate.
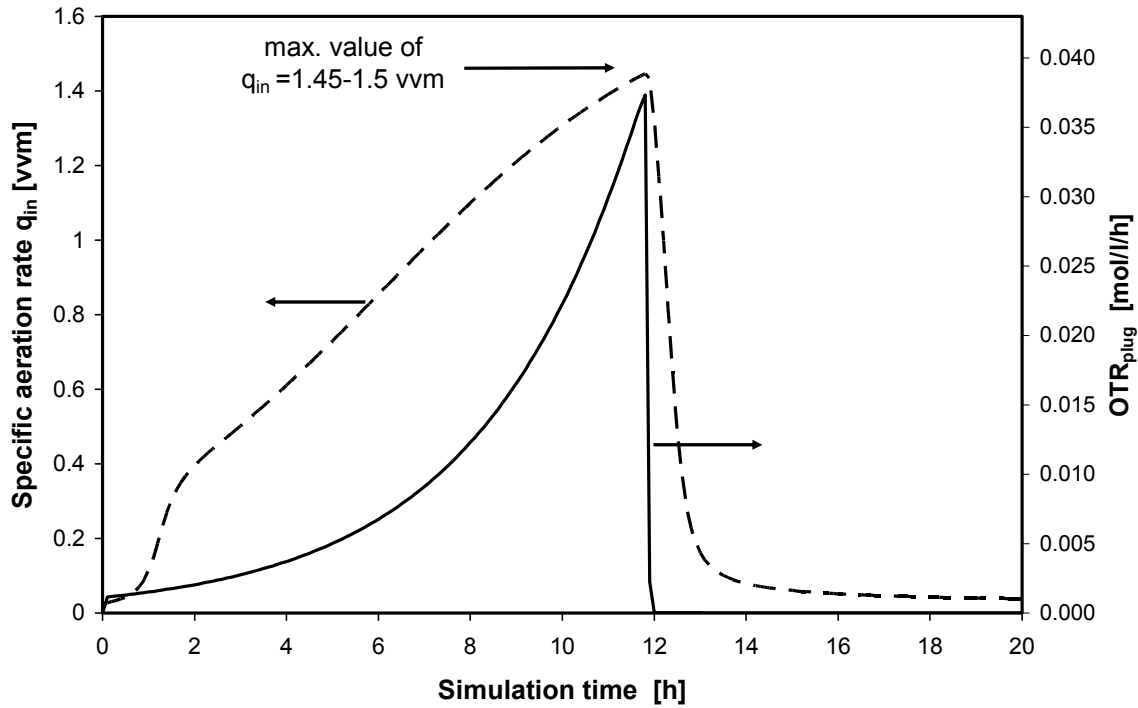
Figure 5.2: Simulation results of q_{in} for the aerated flasks of the RAMOS device resulting in the same headspace concentration as in ventilation flask f1, using the unsteady state model and Eq. 5.4 for fermentation of *C. glutamicum* DM1730 (n=350 rpm, d_o=5 cm, V_L=15 ml, 15 gr/l glucose, $Y_{x/s}$=0.48, $Y_{x/O2}$=53 g/mol, T=30 °C, μ_{max}=0.32 1/h, K_S=0.0045 gr/l, K_{O2}=10^{-6} mol/l [5, 68]).
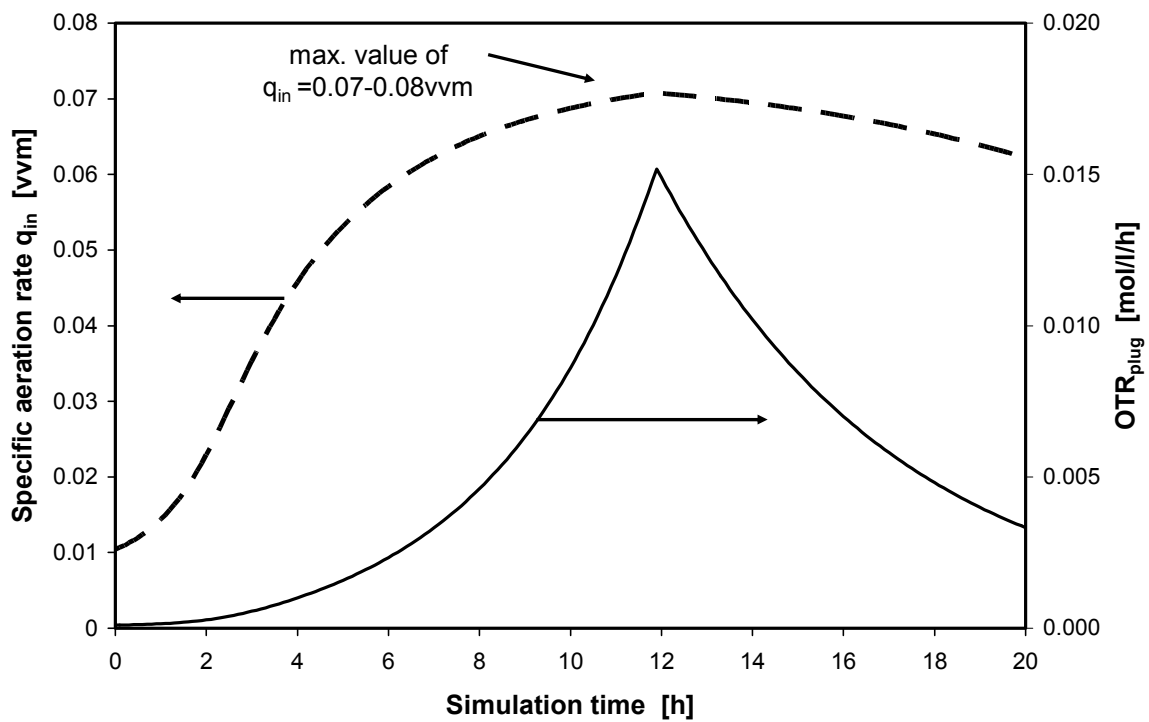
Figure 5.3: Simulation results of q_{in} for the aerated flasks of the RAMOS device resulting in the same headspace concentration as in ventilation flask f9, using the unsteady state model and Eq. 5.4 for fermentation of *C. glutamicum* DM1730 (n=350 rpm, d_o=5 cm, V_L=15 ml, 15 gr/l glucose, $Y_{x/s}$=0.48, $Y_{x/O2}$=53 g/mol, T=30 °C, μ_{max}=0.32 1/h, K_S=0.0045 gr/l, K_{O2}=10^{-6} mol/l [5, 68]).

In the next sections the new proposed aeration strategy under non-oxygen limited condition will be experimentally investigated, utilizing the maximum value of the specific aeration plug rate for the sulfite or a biological system in the measuring flasks, parallel to the respective ventilation flasksf1, f4, f7 and f9. The maximum values of q_{in} are given in the Table 5.1.

5.4.2   Validation of the method for the sulfite system

The usefulness of the new aeration method for the 0.5 M sulfite reaction, as a defined kinetic system (Sec. 4.3.3), was confirmed by a comparison between the results of the oxygen concentration in the headspace of the ventilation flasks (f1, f4, f7 and f9) equipped with oxygen sensors, and the respective aerated measuring flasks of RAMOS device. Specific aeration rates of 0.45, 0.16 and 0.08 vvm were adjusted in the aerated flasks. These values were almost equal to the maximum values of the specific aeration rates resulting from the conditions in the ventilation flasks f1, f4, f7 and f9 (Table 5.1). This aeration for aerated flask rf1 (1.85vvm) was selected %53 more than the maximum calculated value of qin in the ventilation flask f1 (1.21 vvm). The materials and preparation of the sulfite system were given in the Section 4.3.3. The aeration system was adjusted according to the Figure 5.1.
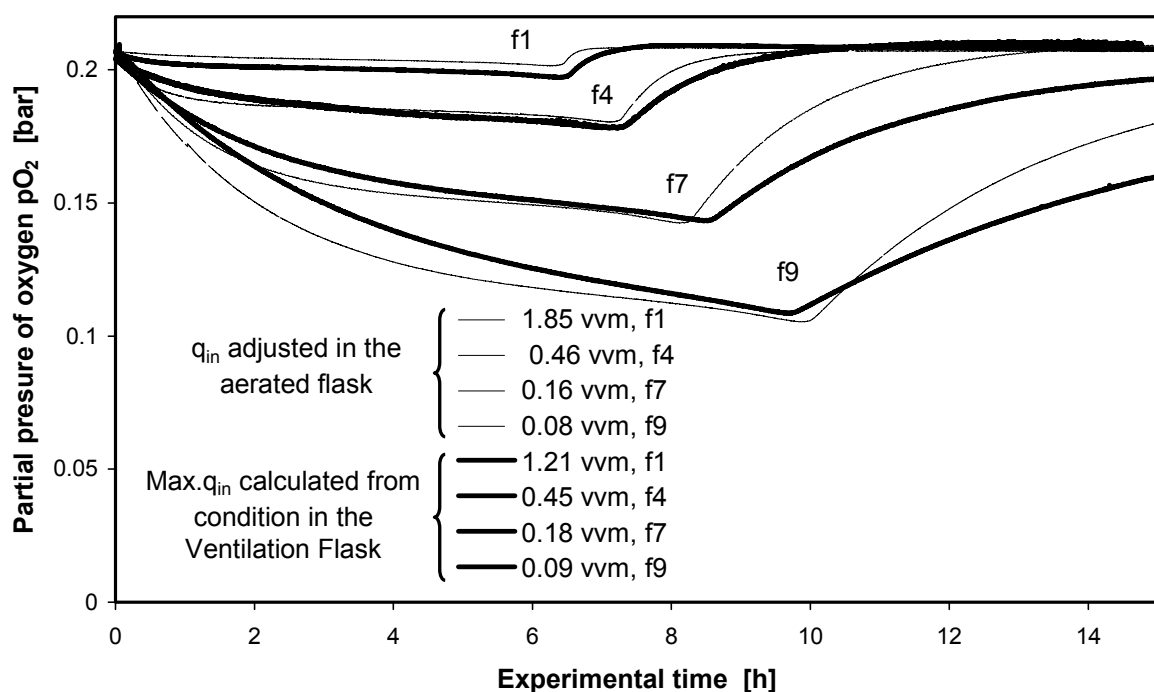
Figure 5.4: Comparison between the partial pressure of oxygen in the headspace of the ventilation flasks f1, f4, f7 and f9 and aerated flasks for 0.5 M sulfite system based on the new aeration strategy (n=300 rpm, d_o=5 cm ,V_L=15 ml, T=25 °C). The values of specific aeration rates are given in the legend and in Table 5.1.

Figure 5.4 demonstrates the results of detection of the oxygen concentration of the gas phase in the headspace of the ventilation and aerated flasks. This Figure shows a high similarity between the results of the pO_2 in the both ventilation and aerated flasks. This confirmed the validity of our purposed strategy. As depicted in Figure5.4 the values of pO_2 for ventilation flask f1 is less than that for the aerated flask rf1. This could occur due to the value of aeration in vf1, which was 53 % less than that in rf1. The effect of k_{plug} on the pO_2 has been discussed in section 4.4.3. Although the both values in the other flasks (f4, f7 and f9) show a similar behavior, there are some slight deviations between the results. This could be happened because of the incomplete mixing of the gas in the part of mounted sensor in ventilation flask (Figure 2.1.A).

5.4.3   Validation of the method for a biological system

The validation of the new aeration method for the cultivation of *C. glutamicum* DM1730 as model organism was performed by comparing the oxygen concentration in the headspace of the ventilation flasks f1 and f9 and the related measuring flask of the RAMOS device. The specific aeration rates in the measuring flasks were adjusted equal to the maximum of qin in ventilation flasks f1 and f9 (Table 5.1).
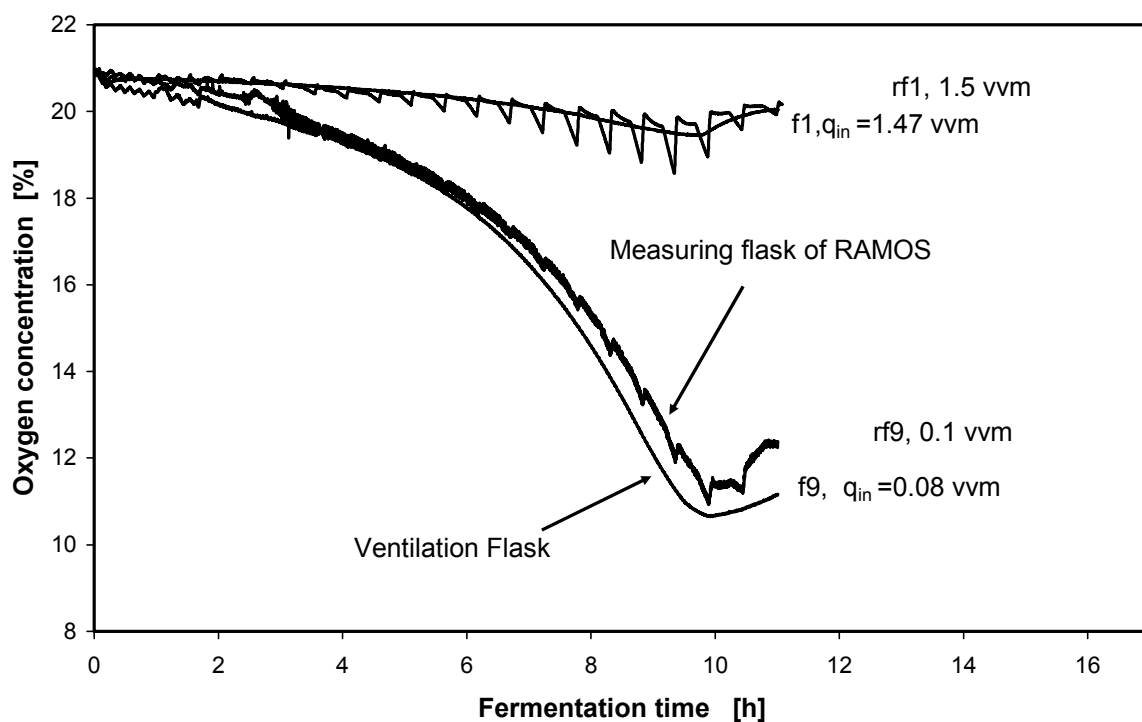
Figure 5.5: Comparison between the concentration of oxygen in the headspace of the ventilation flasks f1 and f9 and related measuring flasks for the fermentation of *C. glutamicum* DM1730 on 15 g/l glucose (21g/l MOPS, pH_{start}=7.2, V_L=15 ml, n=350 rpm, OD_{start}=1). The values of the specific aeration rates of the flasks, calculated based on the new aeration strategy, are given in Table 5.1.

The experiments were conducted under operation conditions, obtained using Eq. 5.4 and the unsteady state model. The aerations in measuring flasks were adjusted to 1.5 vvm and 0.1 vvm by the designed aerated system of the RAMOS device (Figure 5.1). The medium preparation and cultivation of the micro-organisms were explained in materials and methods (Sec. 2.6.2). The signals of the oxygen sensors are recorded by the control program of the RAMOS device for both flasks. The pO_2 was calculated from the oxygen sensor signal by Eq. 2.1.

Figure 5.6 shows the results of the O_2 concentration in the headspace of the ventilations and the measuring flasks. A good agreement between the oxygen concentration in the head space of both ventilation flask f1 and f9 and the related measuring flasks of the RAMOS device confirms the proposed new aeration strategy. The slight difference between the minimum values of the O_2 concentration in f9 may have occurred due to a higher adjusted value of the aeration in the measuring flask (0.1vvm) than that in the ventilation flask f9 (q_{in}=0.08vvm) and also properly incomplete mixing of the gas in the connector of the mounted sensor in the ventilation flask.

5.5   Conclusion

The biotechnologists desire to provide adequate oxygen for aerobic cultures and to control aeration, especially in scale up from shake flask to fermentor. In an aerobic fermentation in a shake flask with sterile closure there is in many cases no assurance that the aeration is sufficient [18 and 23]. It was the aim of this part of the work to present a new aeration strategy based on the values of aeration rate which are calculated in sterile closures using an unsteady state model and considering a dependency between k_{plug} and OTR_{plug} (Eq. 5.4). The method was confirmed, obtaining the same gas concentration the headspaces of ventilation and aerated flasks for a sulfite and a biological system (Figs. 5.4 and 5.5). This method addresses the problem of insufficient information on aeration in the shake flask as reported by different authors [8, 23, 36, 37, 66 and 75]. This strategy would be a very useful method for scaling up from a shake flask to a fermentor, comparing the results of the gas concentration in the gas phase. This method will be used in order to develop a new online CO_2 sensitivity monitoring of micro-organisms in Chapter 7 and a novel scale up method from shake flasks to stirred tank fermentors in Chapter 8.

Chapter 6

A Novel and Easy Method for the Quantification of CO$_2$ Sensitivity of Micro-organisms in small scale Bioreactors

6.1   Introduction

Carbon dioxide plays a major role in many aerobic and anaerobic fermentations. Many authors have reported the inhibitory effects of CO$_2$ on bacteria [19 and 54], yeasts [34] and fungal micro-organisms [12, 26 and 50] in a cultivation process. The most important effects mentioned by them are altering growth [12, 19, 34 and 41] and product formation [12 41, and 54]. The carbon dioxide in the metabolism of the micro-organisms by carboxylation reaction and decarboxylation reaction is the fundamental inhibitor stimulant for cell growth and productivity [34]. It can particularly play a significant role in industrial micro-organisms for the fermentation of some important bio products (e.g. amino acids, antibiotics and etc.) [60]. Table 6.1 summarizes some of the effects of carbon dioxide on several micro-organisms in industrial fermentation processes. As noted in the Table 6.1, the degree of growth or productivity inhibition by CO$_2$ is different, depending on the species of micro-organism and on environmental parameters (e.g. the composition, pH of medium and substrate).

In spite of these studies, the influence of CO$_2$ on cultivation systems is still not fully understood, as compared to the O$_2$ transfer in fermentation systems [30 and 31]. CO$_2$ inhibition can be the most important parameter in industrial scale fermentors, since, the dissolved CO$_2$ concentrations (D$_{CO2}$) is increased by increasing the hydrostatic pressure near to the bottom of the vessels [26 and 38].

Considering the importance of the CO$_2$ effects on productivity and growth rate of industrial microorganisms, several quantitative methods for evaluation of these effects have been reported [2, 19, 25-27, 50 and 51]. Some of these methods are summarized in Table 6.1. In these methods continuous gassing of batch, fed-batch and continuous cultures with a constant CO$_2$ concentration. The use of batch and fed batch methods have a number of limitations including a continuous change in cell concentration, culture age distribution, nutrient/by-product and dissolved CO$_2$ levels with time. The use of continuous cultures excludes most of the changes as noted above [51]. Bäumchen [6] has developed a continuous method based on a turbidostatic culture system under sufficient O$_2$ supply mixed with a certain concentration of CO$_2$ and nitrogen [45]. This method was set up and validated for *Corynebacterium glutamicum* (WT1320) [6]. This method was employed for investigating the effect of CO$_2$ on growth rate and amino acid production by *C. glutamicum* DM1730 [39].

Table 6.1: A summary of some methods employing bioreactors for CO_2 sensitivity evaluation of several micro-organisms in industrial fermentation processes [12, 28 and 34]

Micro-organism	Culture method	CO_2 gas phase	Bio-product	Effect of CO_2	Ref.
Brevibacterium flavum	Batch Air/ CO_2	Different concentration between 0.05-20% (v/V)	Histidine	Increased in production at all CO_2 concentration	[2, 25]
			Arginine	Optimal production at 12 % CO_2 (Increased below 12 %, decreased above 12%)	
Penicillium chrysogenum	Batch Air/ CO_2	3 % and	Penicillin	Slight or no reduction in metabolic activity at %3 CO_2	[26,27]
		5 % (v/V)		increased lag phase and decrease in penicillin at 5 % CO_2	
	Fed batch Air/ CO_2	12.6 %	Penicillin	40 % decrease in penicillin	
Aspergillus niger	Batch Air/CO2	5 % (v/v)	Citrate	32 % reduction in maximum cell mass; 20 % decrease in Citrate	[50]
		7.5 % (v/v)		35% reduction in maximum cell mass; 65.4 % decrease in Citrate	
	Continuous Air/ CO_2	2 and 4 % (v/v)	gluconate	No considerable change in biomass or product	[51]
		10 % (v/v)		22 % decrease in biomass; 50 % reduction in gluconate	
Saccharomyces cerevisiae	Continuous Air and N2/ CO_2	4.5-20 %(V/V) in exhaust gas	Ethanol	8 % increase in ethanol. No considerable change in biomass	[41]
C. glutamicum	Continuous Air and $O_2/N_2/$ CO_2	1-50 %(V/V) continuous air and N2/ CO_2	Lysine	Effect on growth rate and productivity	[6]

Although the mentioned methods in batch, fed-batch and continuous fermentors have brought valuable results, the operating cost, the time consumption and reproducibility are the limiting factors for using these methods. Furthermore, using the current methods for evaluation of the CO_2 sensitivity becomes tedious for researchers in laboratories for new industrial organisms created by DNA technologies or mutation.

Therefore, a novel, easy and economical method for the quantification of CO_2 sensitivity of micro-organisms in shake flask bioreactors will be presented. The results of this method will be compared with the results of current methods e.g. the continuous turbidostatic cultures.

6.2   Theory

Using a sterile closure leads to a reduction of O_2 and an accumulation of CO_2 in the gas phase of the headspace of the shake flask in an aerobic cultivation system [25, 66 and 80]. As it was described in Chapter 4 and 5, the decreasing of k_{plug} causes a reduction of O_2 concentration in the head space of the ventilation flask under an unsteady state condition. A correlation of the k_{plug} on OTR_{plug} is very useful to model the gas transfer in shaken bioreactors (Secs. 4.4.3 and 4.4.5) and also to calculate the specific flow rates in the ventilation flasks(Secs. 5.4.2 and 5.4.3).

6.2.1   Thermodynamic of the interactions of CO_2 and aqueous medium

The thermodynamics of the CO_2 in a culture media has been already investigated [12 and 34]. It has been reported that the CO_2 in the fermentation broth as can exist in various forms, e.g. dissolved CO_2 [$CO_{2,L}$], bicarbonate ion [HCO_3^-] and carbonate [CO_3^{-2}] [64]. Figure 6.1 shows the dissociation of dissolved CO_2 in a fermentation broth. It has been demonstrated that between these species, the dissolved CO_2 [$CO_{2,L}$] and bicarbonate [$H CO_3^-$] are generally microbial growth and productivity [12 and 34].

However, it is still difficult to find a distinct principal mechanism to elucidate an explicit role to any molecular species of CO_2 in the cultivation systems [52]. It was suggested that the microbial inhibition was due to an alteration in the properties of cell membrane, cytoplasm, enzymes and etc. [12]. Many studies on the mechanisms of CO_2 on the cell membrane and metabolism were summarized by Jones and Greenfield in 1982 [34].
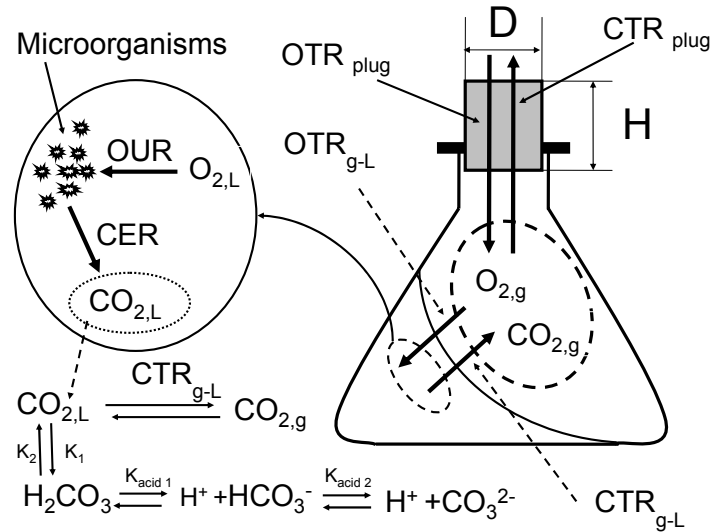
Figure 6.1: Schematic representation of the oxygen and carbon dioxide transfer in ventilation flask and association/dissociation of CO_2 in a biological system [64]. Where K_1, K_2 [sec^{-1}] are the constant rates for the illustrated reactions and K_{acid} [mol/m^3] is the dissociation constant value of carbonic acid.

The effects of the temperature, pH and solutes e.g. salts on the concentration of CO_2 species have already been studied [30, 34 and 64]. The concentration of dissolved CO_2 [$CO_{2,L}$] and bicarbonate [HCO_3^-] are calculated by the following Eqs. 6.1-4, considering the dissolution and dissociation of CO_2 in a culture medium with a range of pH between 5 and 8 [65]:

$$\frac{\partial [CO_{2,L}]}{\partial t} = -K_1 \cdot [CO_{2,L}] + K_2 \cdot [H_2CO_3] \tag{6.1}$$

$$[H_2CO_3] = \frac{10^{-pH} \cdot [HCO_3^-]}{K_{acid}} \tag{6.2}$$

$$\frac{\partial [CO_{2,L}]}{\partial t} = -K_1 \cdot [CO_{2,L}] + \frac{K_2}{K_{acid}} \cdot 10^{-pH} \cdot [HCO_3^-] \tag{6.3}$$

$$\frac{\partial [HCO_3^-]}{\partial t} = K_1 \cdot [CO_{2,L}] - \frac{K_2}{K_{acid}} \cdot 10^{-pH} \cdot [HCO_3^-] \tag{6.4}$$

where $K_1 = 0.058$ [sec^{-1}], $K_2 = 0.6$ [sec^{-1}] are the reaction rates for the indicated reactions, and $K_{acid} = 0.68$ [mol/m^3] is the dissociation constant of carbonic acid [61, 95].

6.2.2   Effect of pH on the CO_2

Regarding to the Eqs. 6.3 and 6.4, the value of pH can critically effect [$CO_{2,L}$] and [HCO_3^-]. The concentration of carbonic acid is always very small in comparison with that of the dissolved carbon dioxide at neutral pH [65]. The concentration of bicarbonate ions [HCO_3^-]

increases with increasing pH. It is equal to the dissolved CO_2 concentration at the pH of 6.3 and dramatically climbs at pH 7.3. In the low pH (pH<5.5) the largest part of CO_2 exists as dissolved CO_2 $[CO_{2,L}]$. Thus, dissolved CO_2 plays an important role by lowering the pH of the medium, and this acidity leads to a disturbance of some biological systems within the cells [34].

6.2.3 CO2 transfer in the ventilation flasks

As described in Chapter 4, the gas transfer rates (OTR_{g-L} and OTR_{plug}) can be modeled and expressed by the oxygen concentration in the headspace of the ventilation flasks. In the same way, the carbon dioxide transfer rate (CTR_{g-L} and CTR_{plug}) in a cultivation system can be expressed by the concentration of CO_2 of the gas phase in the headspace of the ventilation flask (pCO_2). The mass balance for CO_2 in the headspace of these flasks (Figure 6.1) is given as follows (Eq. 6.5)

$$\frac{\partial pCO_{2,g}}{\partial t} = CTR_{g-L} - CTR_{plug} \tag{6.5}$$

where CTR_{plug} is the carbon dioxide transfer through the sterile closure and CTR_{g-L} is the carbon dioxide transfer across the gas–liquid interface. In the following sections the effective factors necessary to calculate CTR_{plug} and CTR_{g-L}, and consequently, $pCO_{2,g}$ will be presented.

6.2.3.1 Gas-liquid carbon dioxide transfer rate (OTR_{g-L}) in a ventilation flask

For the determination of the gas liquid transfer rate of CO_2 (CTR_{g-L}), the thermodynamics of the different species of CO_2 in the culture media, which has been already explained in section 6.2.1, would be advantageous. The concentration of dissolved carbon dioxide $[CO_{2,L}]$ in a culture medium can be correlated to the partial pressure of carbon dioxide in the headspace of the ventilation flask ($pCO_{2,g}$) by Henry's law (Eq.6.6) [31]. This law only applies to infinitely diluted solutions.

$$[CO_{2,L}] = pCO_{2,g} \cdot H_{eCO2} \tag{6.6}$$

The Henry coefficient for carbon dioxide (H_{eCO2}) for pure water is available in literature [61 and 67]. The accumulation of a high concentration of carbon dioxide in the gas phase and good solubility of it in aqueous solution may invalidate the use of the Henry's law in the ventilation flasks. Nevertheless we assumed that the Henry's law is validated for the ventilation flasks. Hence, the concentration of the species of carbon dioxide in the liquid phase my become an important factor to calculate the values of dissolved carbon dioxide $[CO_{2,L}]$,

CTR_{g-L} and $pCO_{2,g}$. The CTR_{g-L} can be calculated by using the Eq. 6.7 which is expressed in the same way as for OTR_{g-L} [28] or by Eq. 6.8 obtained by a mass balance on the dissolved carbon dioxide $[CO_{2,L}]$:

$$CTR_{g-L} = (k_L a)_{CO_2} \cdot ([CO_{2,L}] - \frac{pCO_{2,g}}{He_{CO_2}}) \qquad (6.7)$$

$$CTR_{g-L} = CER - \frac{\partial [CO_{2,L}]}{\partial t} - \frac{\partial [HCO_2^-]}{\partial t} \qquad (6.8)$$

where $(k_L a)_{CO2}$ is the volumetric gas liquid mass transfer coefficient for CO_2 [1/s]. In these equations it is assumed that both the gas-phase and the liquid phase are well mixed. For the determination of CTR_{g-L}, the values of $CO_{2,L}$ in liquid phase, achieved by Eq. 6.3 and $(k_L a)_{CO2}$, calculated by Eq. 6.9, must be taken into an account [64].

$$\frac{(kLa)_{CO2}}{(kLa)_{O2}} = \left(\frac{D_{O2,L}}{D_{CO2,L}} \right)^{\frac{2}{3}} \qquad (6.9)$$

where $k_L a)_{O2}$ is the volumetric gas–liquid mass transfer coefficient for oxygen which can be calculated by Eq. 4.12 (Sec. 4.2.5).

6.2.3.2 Carbon dioxide transfer through the sterile closure (OTR$_{plug}$)

As already mentioned in Chapter 3, the O_2, CO_2, N_2 and H_2O flow rates through the sterile closure can be computed using the model of Henzler and Schedel [23]. The constant value of 0.123 cm²/s for D_{CO2} in the sterile closure of the ventilation flasks with the density of 0.15 g/cm³ resulted by using the water loss method (Sec. 3.4.2). The approximate values of $k_{plug,CO2}$ were obtained using D_{CO2} and different values of the neck geometry in Eq. 3.15 (Figure3.7). The activity of micro-organisms and the concentration of the compounds in the gas mixture can affect the value of OTR$_{plug}$ and CTR$_{plug}$. Therefore, the carbon dioxide transfer rate through the sterile closure (CTR$_{plug}$) can be calculated by Eq. 6.10 in the same way as the OTR$_{plug}$ calculation.

$$CTR_{plug} = k_{plug,CO2} \cdot \frac{1}{p_{abs} \cdot V_L} \cdot (pCO_{2,gas} - pCO_{2,out}) \qquad (6.10)$$

The approximate values of $k_{plug,CO2}$ obtained by $\frac{D_{CO2} \cdot A}{H \cdot V_{mo}}$ are given in Figure 3.6.

6.2.3.3   Equation for the determination of the CO_2 concentration in the headspace of the ventilation flasks

The effect of the kinetic parameters of the microbial metabolism (e.g. K_{CO2}, K_{O2}, K_S and μ_{max}), stochiometric parameters (e.g. $Y_{x/s}$, $Y_{x/O2}$ and RQ), carbon source concentration, operation conditions (e.g. VL, aeration and agitation), and the physicochemical parameters of the cultivation system (e.g. pH, temperature, gas solubility) on the concentration of O_2 and CO_2 in the gas phase of aerobic fermentations have been theoretically and experimentally discussed in several papers [5, 17 and 79]. Additionally, the effect of the overall gas transfer coefficient of the sterile closure (k_{plug}) on the concentration of gas components in the headspace of ventilation flasks was already described in Chapters 3, 4 and 5. These factors can be theoretically summarized by Eq. 6.11 with substituting Eqs. 6.3, 6.8 and 6.10 in Eq. 6.5.

$$\frac{\partial pCO_{2,g}}{\partial t} = K_1 \cdot [CO_{2,L}] - \frac{K_2}{K_{acid}} \cdot 10^{-pH} \cdot [HCO_3^-] - \frac{\partial [HCO_2^-]}{\partial t}$$
$$- k_{plug,CO2} \cdot \frac{1}{p_{abs} \cdot V_L} \cdot (pCO_{2,gas} - pCO_{2,out}) + \frac{RQ}{Y_{X/O2}} \cdot \mu \cdot X \tag{6.11}$$

where X is the biomass concentration (Eq. 4.8), μ is the specific growth rate depending on the substrate and oxygen concentration (Eqs. 4.9 and 4.10) and RQ is the respiration quotient (Eq. 6.12).

$$RQ = \frac{CER}{OUR} = \frac{CER}{OTR_{g-L}} \quad \text{(Non oxygen limitation)} \tag{6.12}$$

The RQ changes by the type of the substrates and products of the micro-organisms. It was argued that for cell cultures the RQ can be regarded as an important metabolic parameter for identifying suitable medium compounds [65]. It is proved that the oxygen uptake rate (OUR, Eq. 4.7) can be limited by the supplied oxygen from the gas phase of shake flask. Otherwise, the OUR can be considered equal to OTR_{g_L} (Eq. 4.5) [3, 72].

Furthermore according to Eq. 6.10, an increase in the values of the an accumulation of CO2 in the head space of the ventilation flasks can theoretically decrease CTR_{g-L} due to decreasing of the CO_2 driving concentration between gas and liquid phases. This leads to an increase of CO_2 concentration in the liquid phase ($CO_{2,L}$) produced by microorganism during the fermentation (CER, see the Figure 6.1). This results in an increase of the concentrations of CO_2 species in the liquid phase. The effect of these species on the activity of micro-organisms has been addressed in many papers as referred in section 6.2.1. As discussed in section 3.4.3, the

different levels of CO_2 transfer resistances are one of the properties of the ventilation flasks (Figure 3.6). Therefore, theoretically using the ventilation flasks for a cultivation system may result in different levels of CO_2 concentration in the head space of these flasks. On the other hand, this may lead to an decrease in the value of the removed $CO_{2,L}$ from culture broth. This is an essential base for the proposed method for the quantification of the CO_2 sensitivity of micro-organisms in shaken bioreactors. Figure 6.1 shows a general schematic representation of the oxygen and carbon dioxide transfer in a biological system in the ventilation flasks.

6.3   Materials and methods

6.3.1   Ventilation flasks

In this study the ventilation flasks f1-f9 (Figure 2.2) and also a specially designed ventilation flasks with a mounted oxygen or CO_2 sensor (Sec. 2.1.4 and Figure 2.1-A) were utilized. The characteristics of the ventilation flasks f1-f9 are given in Table 2.1.

6.3.2   Respiratory Activity Monitoring System (RAMOS)

For evaluation of the growth of micro-organisms in a cultivation system, a RAMOS measuring flasks (Figure 2.1-C) parallel with ventilation flasks were employed. This system was already explained in section 2.1.2

6.3.3   Model organisms and cultivation system

For the investigation of the purposed new method, experiments with *Arxula adeninivorans LS3*, *Corynebacterium glutamicum* (DM1730 and ATCC WT13032) and *Hansenula polymorpha* DSM70277 as model organisms in the ventilation flasks are performed. The medium preparation and the cultivation system and operation conditions were given in Sections 2.6.1 and 2.6.2. The fermentations in the RAMOS device were carried out with a normal aeration rate (1 vvm) and operated under the same conditions as the ventilation flask f1. The related operation conditions for the experiments were specified in the legend of the tables and Figures.

6.3.4 O_2 and CO_2 sensors

For detecting the partial pressure of oxygen and the concentration of CO_2 in the gas phase of headspace of the flask, the O_2 and CO_2 sensors were used (Sec. 2.1.4).

6.3.5   Calculation of CO_2 from the values of O_2 concentration

It was shown that aeration in aerobic fermentors may have an important role in the equilibrium between $CO_{2,g}$ and dissolved $CO_{2,L}$ [64]. Under equilibrium conditions CER becomes equal to

CTR$_{g-L}$. Therefore, under these condition and RQ equal to one the CO$_2$ concentration in the gas phase of the headspace can be estimated from the O$_2$ concentration in the head space of a ventilation flask (Eq. 6.13).

$$\%CO_{2,g} = 100 \cdot (0.2095 - pO_2) \tag{6.13}$$

6.3.6   Applied model

The modified unsteady state model was used to predict the operation conditions of biological system in the ventilation flasks (Sec. 4.4.5).

6.3.7   Sampling and analysis the of results

In our experiments we used 5 series of each ventilation flasks for the determination of the biomass concentration (bio dry weight), pH value, carbon source and product concentration (Sec. 2.4). Moreover, at the same time, additional experiments were performed with the RAMOS device for the determination of OTR, CTR and RQ in the cultivation system (Sec. 2.1.2).

6.3.8   Calculation of maximum specific growth rate (μ$_{max}$)

The maximum specific growth rate (μ$_{max.}$) in the exponential phase can be calculated by the results of the biomass concentration obtaining from sampling, during the fermentation [55].

$$\mu_{max} = \frac{\ln X - \ln X_0}{\Delta t} \tag{6.14}$$

6.4   Results and Discussions

6.4.1   Validity of the method

The effect of the mass transfer resistance of the sterile closures on the aeration of the ventilation flasks was quantified using an unsteady state model considering a dependency of k$_{plug}$ on OTR$_{plug}$ (Chapters 4 and 5). As described in those Chapters, a decrease of k$_{plug}$ is caused by a reduction of the O$_2$ concentration in the head space of the ventilation flasks (Figures 5.5 and 5.6). This reduction may lead to an accumulation of CO$_2$ in the gas phase of the headspace of a ventilation flask in an aerobic cultivation system [25, 60 and 66]. In this section, the validity of the proposed method was experimentally investigated using CO$_2$ and O$_2$ sensors (Figure 2.1.A). For these studies, the fermentation of *Hansenula polymorpha* DSM 70277 on 10 g/l glycerol and *Corynebacterium glutamicum* DM 1730 on 15 g/l glucose, were performed in the ventilation flasks equipped with the CO$_2$ and O$_2$ sensors.
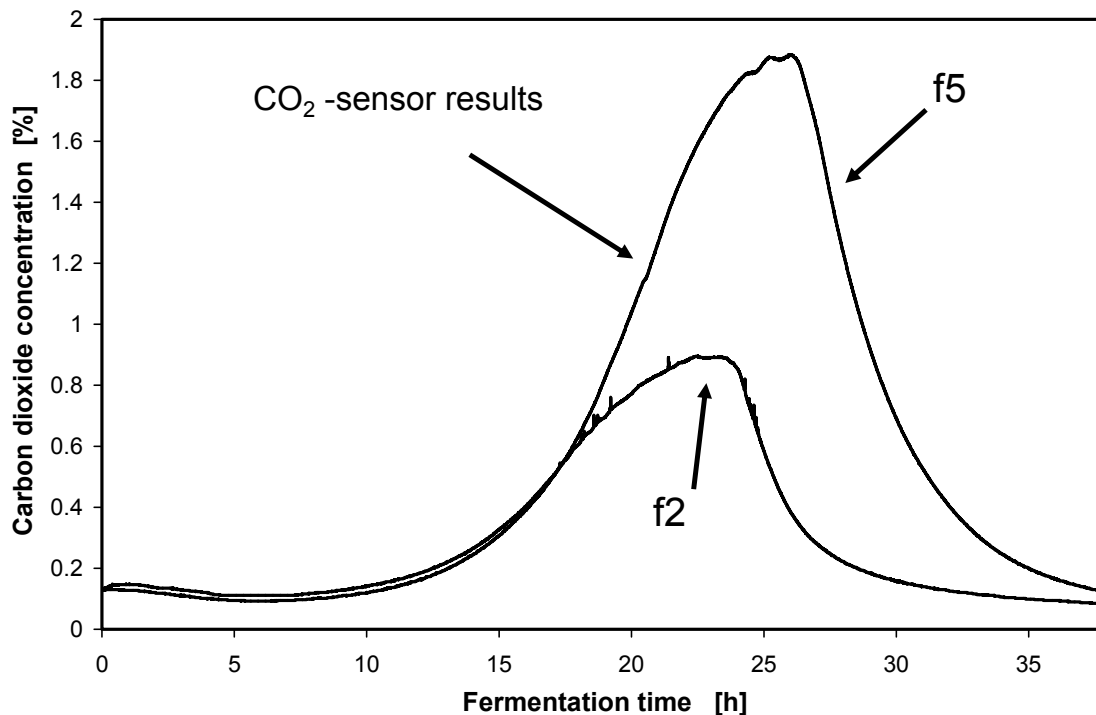
Figure 6.2: Validation of the method by employing a CO2-sensor during the fermentation of *Hansenula polymorpha* in the ventilation flasks f2 and f5 (15 g/l glycerol, Syn6+0.14 M MES, V_L=15 ml, pHstart=6.4, n=200 rpm), having different mass transfer resistances of the sterile closure.

The preparation of the media and cultivation methods were already explained in materials and methods for to each micro-organism (Sec. 2.6). The optimal operation conditions were predicted utilizing the unsteady state model (Chapter 4). The pH was controlled in the optimal ranges, regarded to the growth of micro-organisms using a suitable buffer solution. A parallel fermentation in the RAMOS device with the normal aeration (1 vvm) was carried out in the same way as described for the ventilation flask f1.

Figure 6.2 illustrates the accumulated CO_2 concentration for the fermentation of *Hansenula polymorpha* DSM70277 in the ventilation flasks f2 and f5 obtained by a CO_2-sensor. It is noted that the fermentations were operated under the same conditions and pH (between 5.5 and 6.4 using the 0.14 M MES buffer solution). Under these conditions the sensor results revealed that there was a significant difference between the maximum CO2 concentrations of 0.9 and 1.9 % in the ventilation flasks f2 and f5. This difference occurred as a result of the differences between the $k_{plug,CO2}$ values in these flasks (Figure 3.6).

The validity of the new method based on using a variety of mass transfer resistances of sterile closures was also confirmed by using an O_2 sensor mounted on the ventilation flasks f1, f4, f7 and f9 (Figure 2.1-A). The experiments were carried out for fermentation *Corynebacterium*

glutamicum DM 1730 on 15 g/l glucose (Sec. 2.6.2). The flasks were operated under the same conditions and pH (between 7.54 and 6.4 using 21 g/l MOPS buffer).
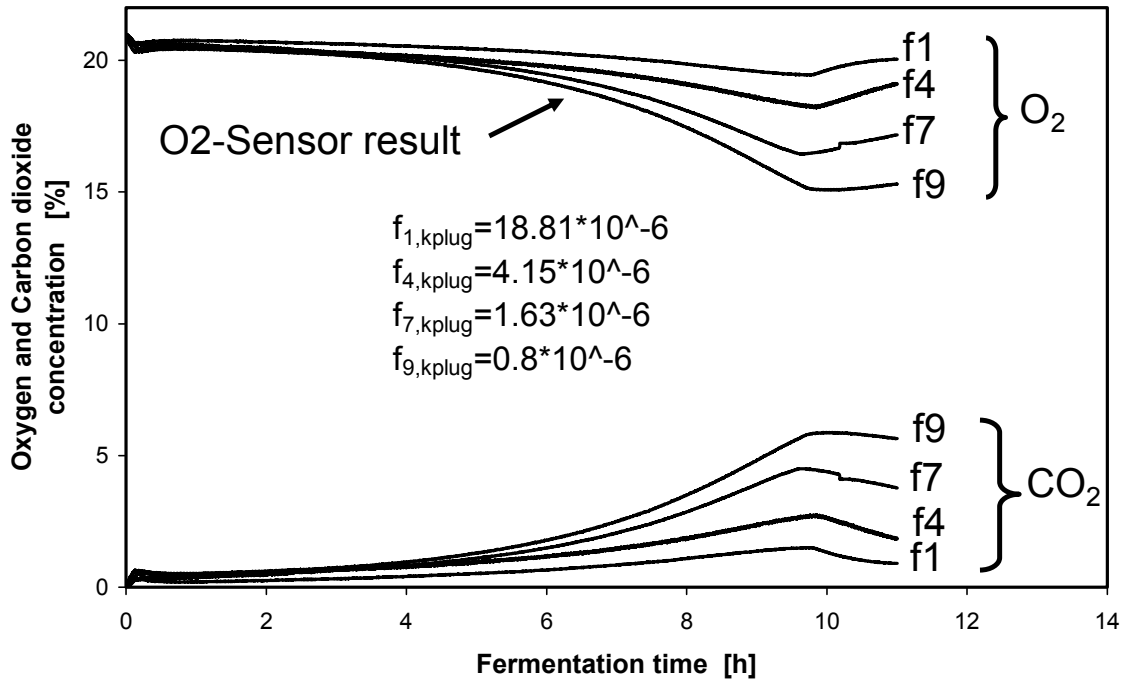
Figure 6.3: Results of fermentation of *C. glutamicum* DM173*0* in ventilation flasks (15 g/l glucose, 21 g/l MOPS, RQ=1, V_L=10 ml, n=350 rpm).

Figure 6.3 shows the O_2 concentration, detected by an oxygen sensor (Sec. 2.1.4). The CO_2 concentration was calculated using Eq. 6.13 in the headspace of the ventilation flasks f1, f4, f7 and f9. According to Figure 6.3, after 10 hours of fermentation, there is a significant difference between the minimum levels of 19.6, 18.3, 16.5, and 15.2 % for the O_2 concentration and also between the maximum accumulated CO2 of 1.4, 2.7, 4.5 and 5.2 % in the headspace of the ventilation flasks f1, f4, f7 and f9, respectively. This is due to the decrease of the mass transfer coefficient of the sterile closures in those ventilation flasks. It is noted that, the mass transfer coefficient of the sterile closure of flask f9 is was 23 times smaller than that of flask f1, as shown in the Figures. 3.5 and 3.6.

Furthermore, the OTR for those fermentations described above were simultaneously monitored using the RAMOS device. The OTR results are shown in Figure 6.4. Maximum OTR values of 0.017 and 0.043 [mol/l/h] for the fermentations of *Hansenula polymorpha* DSM70277 and *Corynebacterium glutamicum* DM1730 were obtained, respectively.
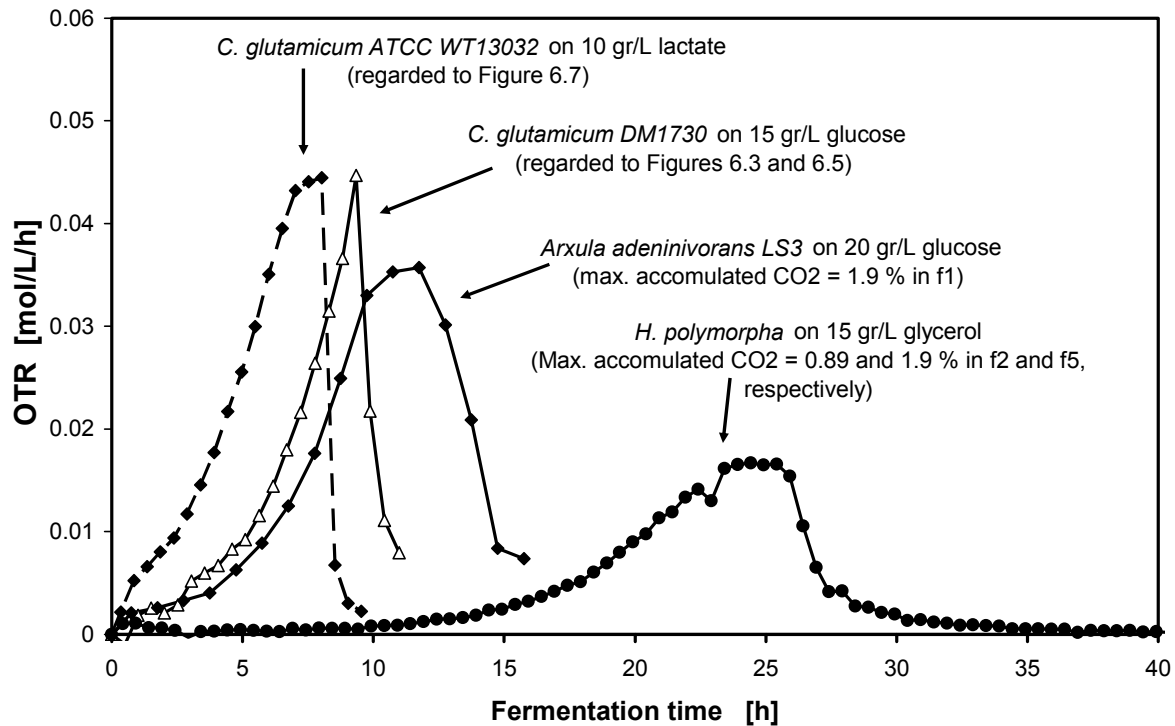
Figure 6.4: OTR results of the fermentation of *Arxula adeninivorans* LS3 (20 g/l glucose, n=200 rpm, RQ≈1, q_{in}=1 vvm, do=5 cm, V_L=10 ml; 0.14 M MES buffer, T=30°C, pH_{start} =6.4), *C. glutamicum* 13032WT (10 g/l Lactate, 21 g/l MOPS, n=350 rpm, T= 30°C, RQ≈1, q_{in}=1 vvm, do=5 cm, V_L=15 ml, pHstart=6.5), *C. glutamicum* DM1730 (15 g/l glucose, 21 g/l MOPS, RQ≈1, q_{in}=1 vvm, do=5 cm, V_L=10 ml, pH_{start}=7.5, n=350 rpm) and *Hansenula polymorpha* (15 g/l glycerol, 0.14 M MES buffer, RQ≈0.87, q_{in}=1 vvm, do=5 cm, V_L=15 ml, pH_{start}=6.4, n=200 rpm) obtained using the RAMOS device.

Above results revealed that the maximum An accumulation of CO2 value (5.2 %) was obtained with the highest resistance in the ventilation flasks f9, where *C. glutamicum* was properly cultivated on 15 g/l glucose, 10 ml of filling volume and a maximum value of OTR=0.043 mol/l/h. The capacity of the maximum accumulated CO_2 in the ventilation flask f9 as a distinct factor for the maximum range of application of the new method will be discussed in the next section.

6.4.2 Maximum capacity of accumulated CO_2 in the ventilation flasks under non oxygen limited condition

The maximum capacity of accumulated CO_2 under sufficient oxygen concentration in the headspace of the ventilation flasks is an important parameter for the application range of the proposed new method. As mentioned in section 6.2.3.3, a maximum accumulated CO2 in the headspace of the ventilation flasks can be theoretically derived by selecting optimal operation conditions (e.g. VL, aeration, k_{plug}, n) and culture parameters (e.g. RQ, carbon source, pH). Among these parameters the carbon source and filling volume (Eq. 6.7 and 6.10) become more important to increase the accumulated carbon dioxide in ventilation flasks, according to

Eq. 6.11. The relation between the carbon source and the value of RQ (Eq. 6.12) and consequently on the CO_2 produced by the metabolism of the micro-organisms has been already documented [65]. Thus, in the following section the effect of filling volume (V_L), as an important parameter, on the maximum accumulation of CO_2 in the ventilation flask f9 was experimentally investigated. Furthermore, to predict optimum fermentation conditions under non oxygen limited condition the unsteady state model was employed, considering all physico-chemical parameters (Chapter 4).
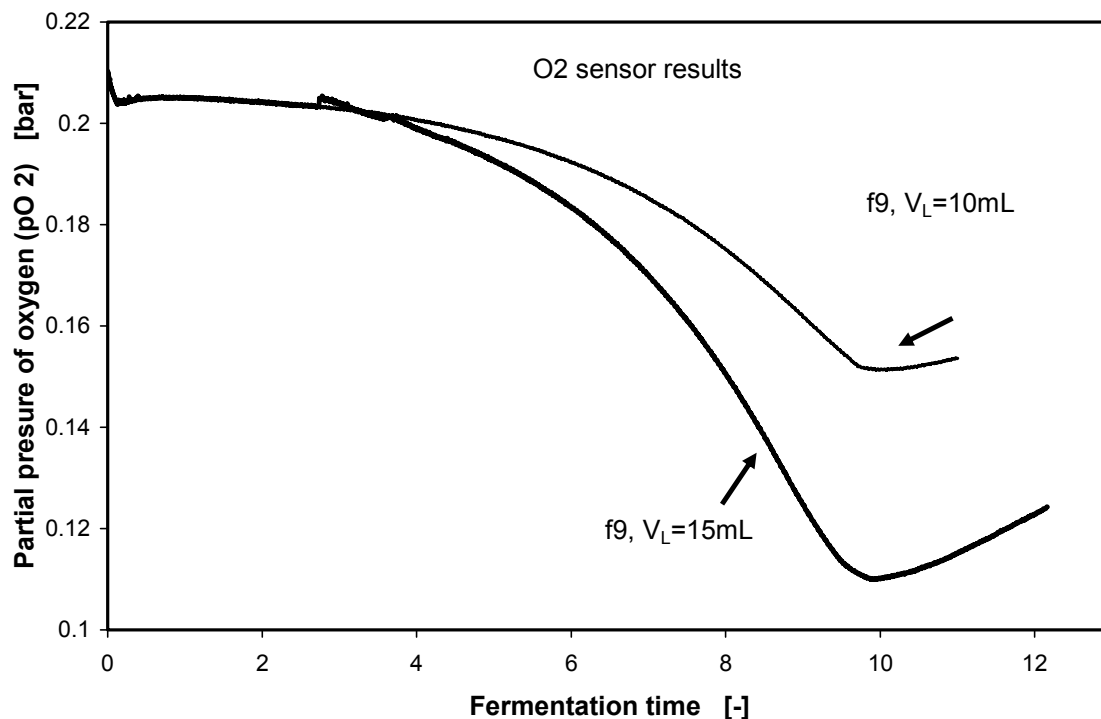
Figure 6.5: Effect of filling volume (10 and 15 ml) on the oxygen partial pressure in the headspace of the ventilation flask f9, resulted from the fermentation of *C. glutamicum* DM1730 on 15 g/l glucose, (21g/l MOPS, n=350 rpm, T=30 °C, do=5 cm, RQ=1). The oxygen partial pressure is measured using an oxygen sensor.

A fermentation of *C. glutamicum* DM1730 on 15 g/l glucose (RQ near one), and a sufficient buffer capacity to control pH (21 g/l MOPS), was carried out in the ventilation flask f9, equipped with an oxygen sensor. This fermentation was conducted under different filling volumes (10 ml and 15 ml). To avoid an oxygen limitation, the operation conditions (do=5 cm and n=350 rpm) were calculated by the unsteady state model (Sec. 4.4.5). The medium, equipment and cultures were prepared as mentioned in Sec. 2.6.2. Figure 6.5 shows the effect of filling volume (V_L) on the concentration of oxygen in the headspace of the ventilation flask f9. From this Figure, a significant variation of pO_2 with different filling volume is observed.

As mentioned before, the increase of filling volume from 10 to 15 ml leads to a decrease of pO_2 from 0.152 to 0.11 bar. Using Eq. 6.13, approximate values of 5.9 and 12 % for accumulated CO_2 concentration were calculated, respectively. This value could be the maximum possible amount of CO_2 for the investigation of the CO_2 sensitivity of micro-organisms by the new method under a non oxygen limitation condition.

6.4.3   Applications of the new method

In the following sections the CO_2 sensitivity of *Arxula adeninivorans* LS3 and two strains of *Corynebacterium glutamicum* (13032WT and DM1730) as model organisms will be quantified by the new method. After that, the results of *Corynebacterium glutamicum* (13032WT and DM1730) obtained by this method will be compared with the results of a continuous turbidostat method [6].

6.4.3.1 Assessment of the CO_2 sensitivity of micro-organisms in terms of biomass concentration

Samples obtained from the ventilation flasks during the fermentation, give an advanced knowledge of the quantitative effect of CO_2 on the activity of micro-organisms. Figure 6.6 indicates the results of samples (i.e. So (initial sample), S1, S2, S3, S4 and S5) during the fermentation of *Arxula adeninivorans* LS3 on 20 g/l glucose in the ventilation flasks f1, f3 and f6. The OTR and RQ were acquired using the RAMOS device.

Furthermore, values of 1.3, 3.6 and 6 % for the maximum accumulated CO_2 in the ventilation flasks f1, f3 and f6, respectively, were calculated using the unsteady state model (Chapter 4), by considering RQ=1 (Figure 6.6). As shown in the Figure 6.6, there was no difference between the biomass concentrations during the fermentation of this micro-organism under different accumulated CO_2 concentration. This means that the *Arxula adeninivoran* -LS3 has no sensitivity up to CO_2 concentration of 6 %. In the same way, the biomass concentrations of the two strains of *C. glutamicum* (13032WT and DM1730) were investigated by using the new method. Figure 6.7 shows the results. The accumulated CO_2 has a significant effect on the biomass concentration during the fermentation of *C. glutamicum* 13032WT and *C. glutamicum* DM1730 as a compared to *Arxula adeninivoran* LS3 (Figure 6.6).

Figure 6.6: pH, biomass, glucose concentration, resulted from sampling from the ventilation flasks f1, f3 and f6 during the fermentation of *Arxula adeninivorans LS3* on 20 g/l glucose (15 ml<V_L<10 ml, n=350 rpm, d_o=5cm, pH start=6.4, 0.14 M MES buffer , T=30 °C) based on the use of the new method.
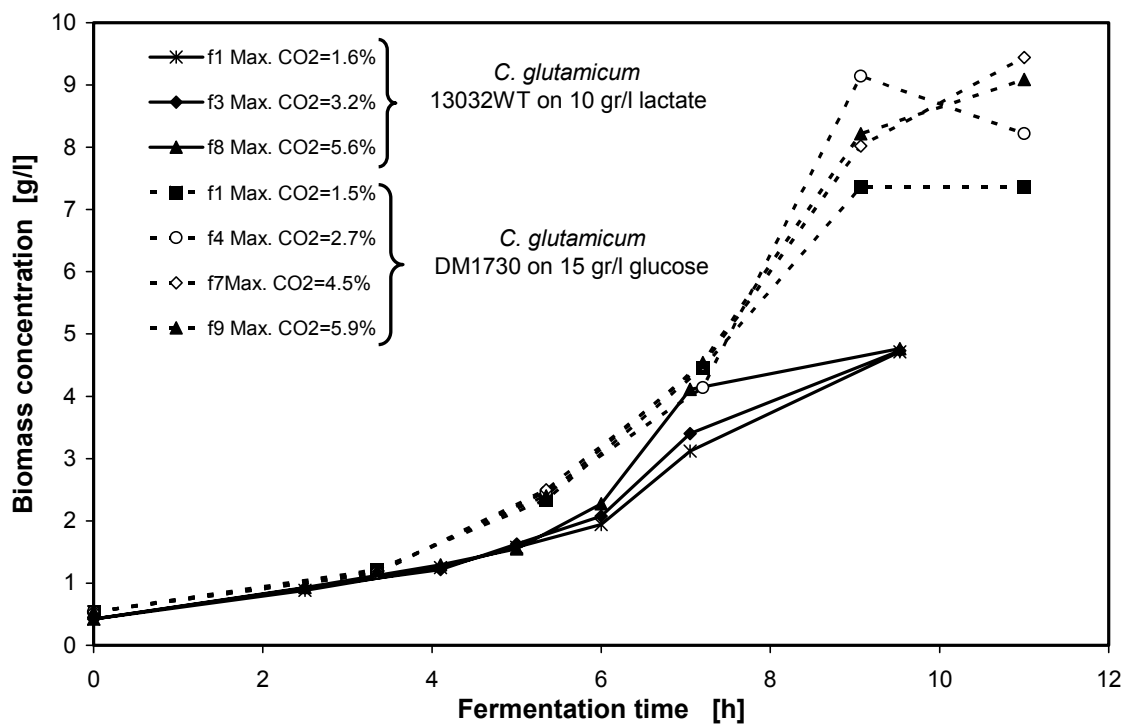
Figure 6.7: The effect of accumulated CO_2 on the biomass concentration, obtained from the fermentation *C. glutamicum* 13032WT on 10 g/l lactate (n=350 rpm, T=30 °C, RQ=1, do=5 cm, pH_{start}=6.5, 15 ml<V_L<10 ml) and *C. glutamicum* DM1730 on 15 g/l glucose(n=350 rpm, RQ=1, pH_{start}=7.5, V_L=10 ml, T=30 °C), in ventilation flasks.

At the beginning of the fermentation about 4 hours the oxygen demand of the culture was small, so a small amount of CO_2 accumulated in the ventilation flasks without any significant effect on the biomass concentration of both strains. Later, during the period of an intensive respiration (the OTR result in the Figure 6.4), the accumulated CO_2 reached maximum values 1.6, 3.2 and 5.6 % in the ventilation flasks f1, f3 and f8 and 1.5, 2.7, 4.5 and 5.9 % for ventilation flasks f1, f4, f7 and f9 for fermentation of *C. glutamicum* 13032WT and *C. glutamicum* DM1730, respectively. At these levels of accumulated CO2 the sensitivity of the micro-organisms become visible based on biomass concentration.

6.4.3.2 Assessment of the CO_2 sensitivity of the micro-organisms in terms of maximum growth rate

In this study maximum specific growth rate (μ_{max}) was used to evaluate the CO_2 sensitivity of micro-organisms. For the determination of μ_{max} Eq. 6.14 was applied considering the values of the biomass concentration, obtained by sampling from the ventilation flasks (refer to Sec. 6.4.3.1). The values of the biomass concentration of *Arxula adeninivorans* LS3 (Figure 6.7) resulted in the maximum value of 0.234 1/h for 1.3, 3.6 and 6.8 % specific growth rate maximum accumulated CO_2 in the ventilation flasks f1, f3 and f6, respectively. Figure 6.8 illustrates the μ_{max} over the values of maximum accumulated CO_2.
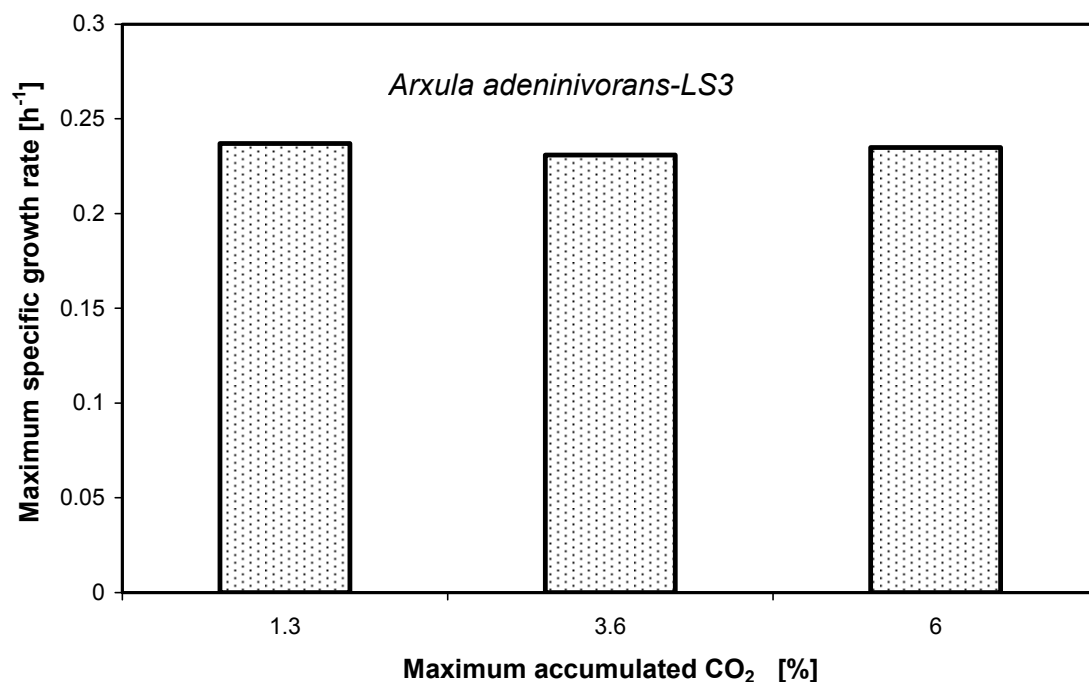
Figure 6.8: The effect of maximum accumulated CO_2 on the maximum specific growth rate of *Arxula adeninivorans* LS3. Results were obtained by using the values of biomass concentration (Figure 6.7).

This reveals that up to maximum value of 6 % for the concentration of CO$_2$ no significant effect on the growth rate of *Arxula adeninivorans* LS3 was detectable. In other studies yeast cells showed no sensitivity to the CO2 concentration below 20 % [34 and 41].

In the following section the validity of the new method for CO$_2$ sensitivity evaluation was investigated for two strains of *Corynebacterium glutamicum* (ATCC 13032WT and DM1730) in the ventilation flasks by comparing the results of a continuous turbidostatic culture method. The maximum specific growth rates of 0.31, 0.35 and 0.38 h^{-1} were calculated (Eq. 6.14) for *C. glutamicum* ATCC 13032 WT, grown on 10 g/l L-lactate as carbon source, under the maximum accumulated CO$_2$ values of 1.6, 3.2 and 5.6 % in the ventilation flasks f1, f3 and f8, respectively. These results together with the experimental values obtained by continuous turbidostatic culture [6] for this micro-organism are represented in Figure 6.9. According to this figure, there is a significant effect of the accumulated CO$_2$ on μ_{max} of *C. glutamicum* 13032WT demonstrated by both methods. The values of the maximum specific growth rate, obtained by the new method, are approximately 18 % less than those values resulted from continuous turbidostatic culture. Though, the overall tendency of these methods is almost the same.
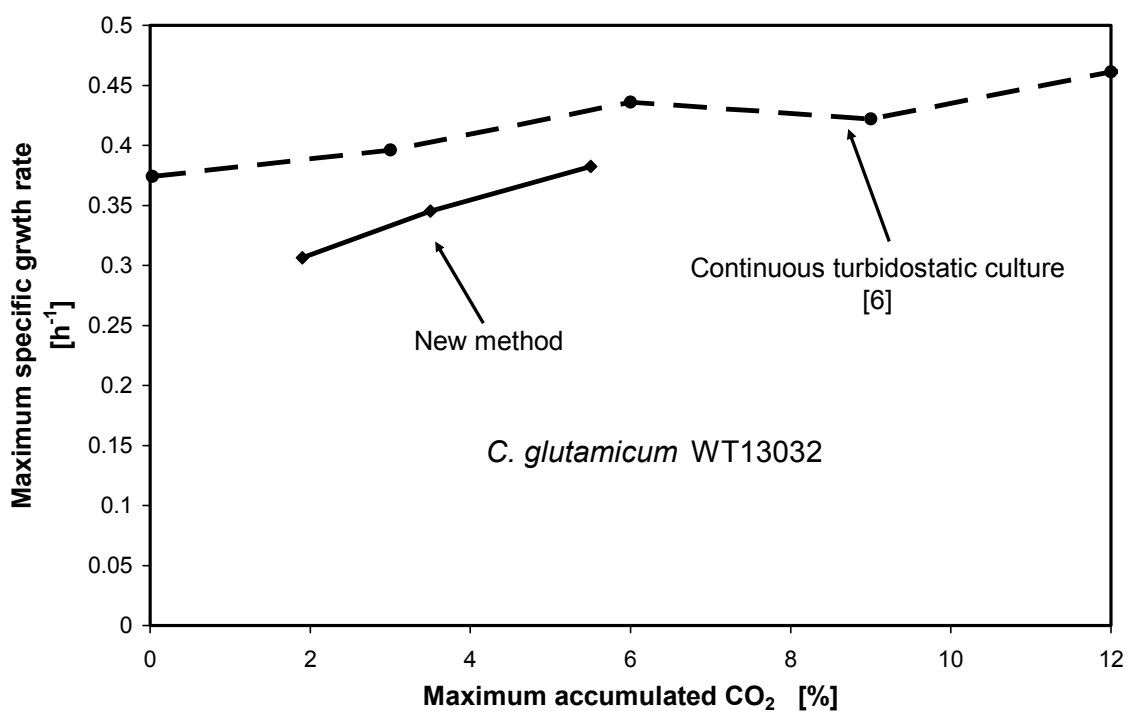
Figure 6.9: Comparison between the maximum specific growth rate of *C. glutamicum* WT13032 on 10g/l L-lactate, resulted by the new method in ventilation flasks (21 g/l MOPS, T=30 °C, d$_o$=5 cm, n=350 rpm, V$_L$=15 ml, pH$_{start}$=6.5) and a continuous turbidostatic culture in a fermentor (T=30 °C, q$_{in}$=1 vvm, n=1200 rpm, V$_L$=800 ml, pH$_{start}$=6.85) [6].

For the validation of the proposed method, the results of the growth rate of *C. glutamicum* DM1730 were compared with the results of the continuous turbidostatic [39]. These results are shown by Figure 6.10. Maximum accumulated CO_2 in the headspace of the ventilation flasks of 1.3, 4.6, 7.7 and 10.3 % were calculated, using the data of the O_2 sensor in Eq. 6.13. Under these conditions value of o.43, 0.41, 0.45 and 0.4 h^{-1} for the maximum specific growth rates (μ_{max}) of *C. glutamicum* DM1730 were computed, respectively. Considering Figure 6.10, these values have similar tendencies as the results of μ_{max} obtained by the continuous turbidostatic cultures [39].

It should be noted that in the Figures 6.8 and 6.9 there are some discrepancies between the results of both methods. They could occur due to the differences between the modes of adjusting the pH, the operation conditions and the procedure of the μ_{max} calculation. The values of μ_{max} determined for the continuous turbidostatic culture system, were expected to be higher than those of the batch experiments (e.g. ventilation flasks). In a continuous turbidostatic culture the microorganisms always grow at a μ_{max}. In this mode of operation, a high concentration of carbon source is available and the pH value is automatically regulated [6]. In the batch ventilation flasks the carbon source concentration decreases. Although a buffer is used, the pH changes (increase from 6.5 to 8.2, in the case of L-lactate consumption and decreased from 6.2 to 7.2 in the case of glucose) [7].
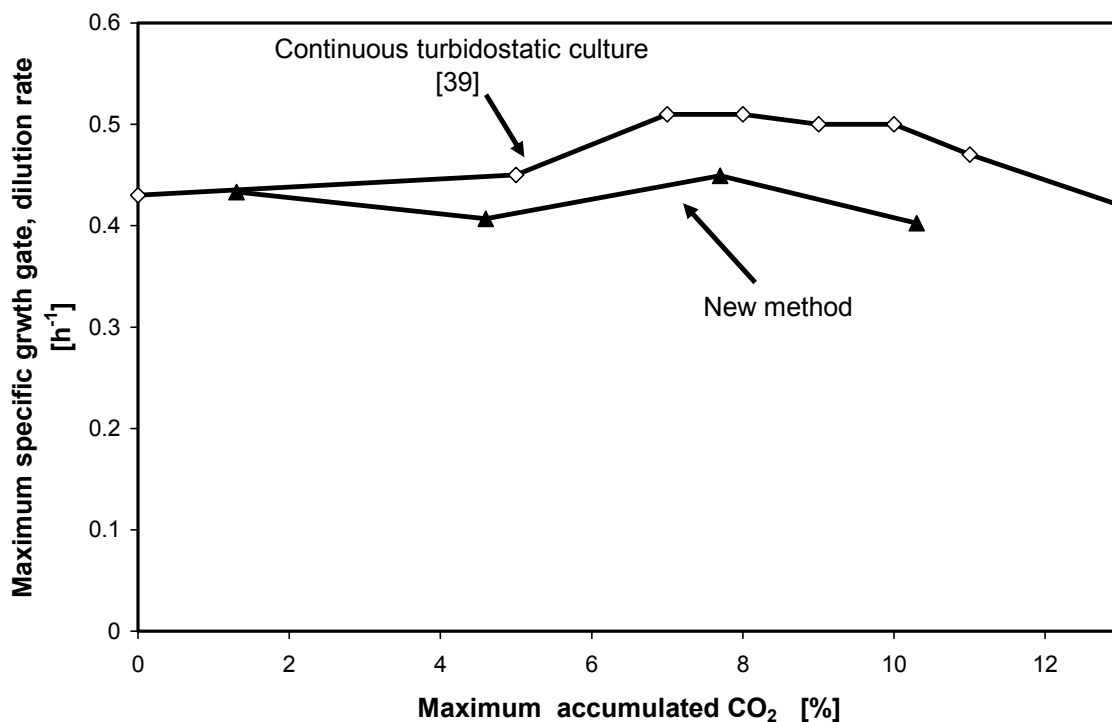
Figure 6.10: Comparison between the maximum specific growth rate of *C.glutamicum* DM1730 on 15 g/l glucose (21 g/l MOPS, T=30 °C, do=5 cm, n=350 rpm, V_L=15 ml, pH_{start}=7.18), using the new method in ventilation flask f1, f4, f7, f9 and a continuous turbidostatic culture (T=30 °C, q_{in}=1 vvm, n=1200 rpm, V_L=800 ml, pH_{start}=7) [39]

At the end of the batch phase, the growth curve is affected by all this change leading to a lower value of μ_{max} as illustrated in the Figures 6.9 and 6.10.

6.4.3.3 Assessment of the CO₂ sensitivity of the micro-organisms in terms of maximum specific productivity

Another goal of the new method was to evaluate the influence of different carbon dioxide concentrations on the product formation during the fermentation. For this aim, *C. glutamicum* DM1730 was used as a model organism for production of L-lysine. The cultivation in the ventilation flasks and sampling method during the fermentation of this micro-organism were explained in Secs. 2.4.5 and 2.6.2. The concentration of L-lysine formation was measured by HPLC analysis (Sec. 2.4.4). Figure 6.11 illustrates the concentration of L-lysine, produced by *C. glutamicum* DM1730 during the fermentation under different accumulated CO_2 values of 1.3, 4.6, 7.7 and 10.3 % in the headspace of the ventilation flasks f1, f4, f7 and f9, respectively. It becomes evident that there was a significant difference between the final amounts of 8.28, 4.8, 7.38 and 6.28 mmol/l accumulated L-lysine in these flasks, respectively.
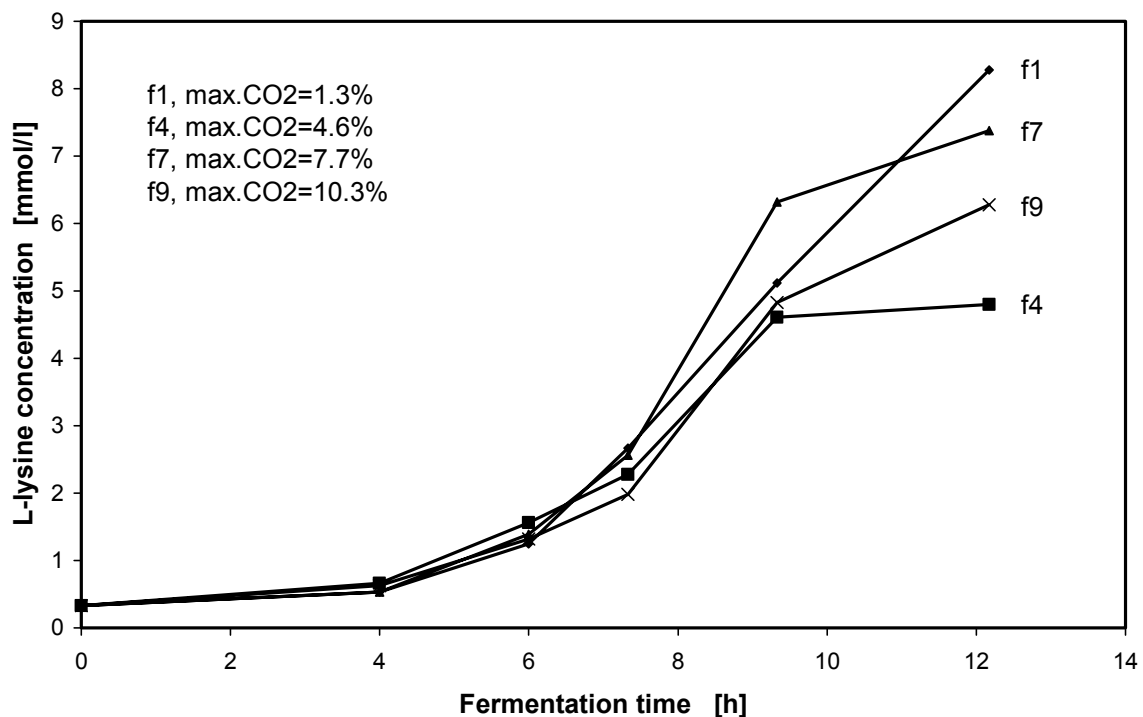
Figure 6.11: L-lysine concentration by fermentation of *C. glutamicum* DM1730 (15g/l glucose, 21 g/l MOPS, n=350 rpm, T=30 °C, do=5 cm, V_L=15 ml) under different level of accumulated CO_2 in the headspace of the ventilation flask f1, f4, f7 and f9.

For a better comparability of the obtained results, the maximum specific productivity of L-lysine in each ventilation flasks was calculated by dividing the concentration of L-lysine by

the biomass concentration and the period of the L-lysine formation. Figure 6.12 shows the dependency of the maximum specific productivity and also the maximum specific growth rate on the maximum accumulated carbon dioxide in the headspace of the ventilation flasks. The value of 0.08, 0.067, 0.1 and 0.072 mmol/gr biomass/h were obtained for the maximum specific productivity of L-lysine under different values of 1.3, 4.6, 7.7 and 10.3 % for accumulated CO_2 in the headspace of the ventilation flasks f1, f4, f7 and f9, respectively. The similar tendency of the maximum specific growth rate and the productivity that the productivity of L-lysine is dependent on the maximum specific growth ate (Figure 6.12).
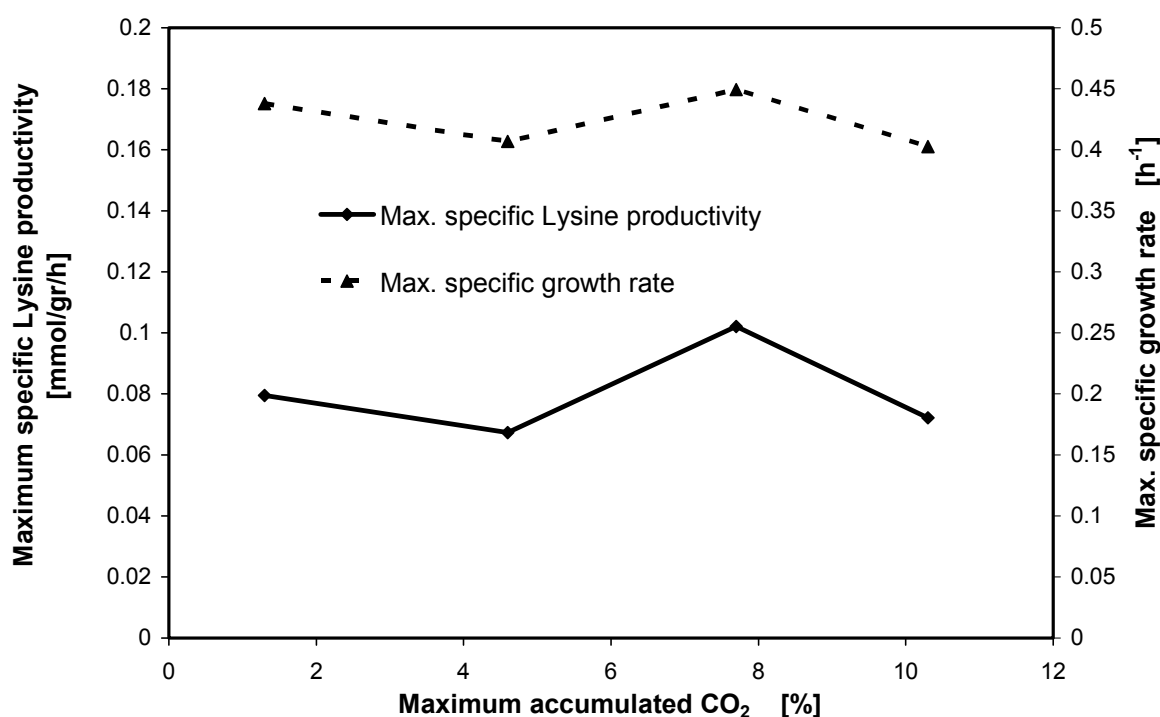
Figure 6.12: Dependency between the maximum specific productivity of L-lysine and the accumulated CO_2 concentration in the headspace of the ventilation flasks f1, f4, f7 and f9 for fermentation of *C. glutamicum* DM1730 (15 g/l glucose, 21 g/l MOPS, n=350 rpm, T=30°C, do=5 cm, V_L=15 ml).

6.5   Conclusion

Generally CO_2 is a grate challenge in some industrial fermentation in which An accumulation of CO2 can have an effect on the yield and fermentative capacity. The knowledge of the influence of carbon dioxide on growth and product kinetics of industrially important micro-organisms is essential for the interpretation of a bioprocess. The carbon dioxide sensitivity of micro-organisms should be investigated in early stages of a bioprocess designed for an accurate planning of an industrial unit.

Decreasing k_{plug} results in a reduction of O_2 concentration and an accumulation of CO2 in the gas phase of the headspace of the shaken bioreactors. In this study, a novel and easy method

for the quantification of CO_2 sensitivity of micro-organisms in shaken bioreactors (called ventilation flask) was investigated. The differences between the values of accumulated CO_2 and concentration of oxygen measured by a CO_2 and oxygen sensor in a culture system in ventilation flasks confirmed the validity of the method (Figures 6.2 and 6.3). The results obtained with this method were comparable with the results obtained with a continuous turbidostatic culture [6]. Using the new method, a significant effect of accumulated CO_2 on the biomass concentration and growth rate and lysine formation in the fermentation of *C. glutamicum* DM1730 was found (Figure 6.12). Applying this method for *Arxula adeninivorans* LS3 clarified that CO_2 has no effect on this micro-organism (Figures 6.6 and 6.8). Compared to the currently used method e.g. continuous turbidostatic culture, the presented method is simple, low in cost and produce similar results.

In this study the CO_2 sensitivity of micro-organism can be quantified up to a maximum concentration of 12 %, of accumulated CO_2 under non oxygen limited condition (Figure 6.5). This is possible, when the cultivation is carried out as follows:

  a- Operate the biological system at OTR values lower than the maximum oxygen transfer capacity of the bioreactor to avoid oxygen limitation.

  b- Use the same filling volume in ventilation flasks.

  c- Use appropriate media and buffer capacity to control the pH during the fermentation.

It is noted that the unsteady state model (Chapters 4 and 5) could be very useful to predict the optimal operation conditions not only for preventing oxygen limitation but also for obtaining a maximum accumulated CO_2 in the ventilation flasks.

Chapter 7

Online Monitoring of CO_2 Sensitivity of Micro-organisms

7.1   Introduction

The effect of aeration on the removal of volatile compounds, e.g. organic acids, NH_3, alcohols, hormones, CO_2 etc., from the fermentation broth have been demonstrated [15, 59 and 75]. As mentioned in the last Chapter, CO_2 has a stimulating and/or inhibiting effect on the growth and/or productivity of micro-organisms (Table 6.1). The oxygen transfer rate (OTR) is widely used to study the growth behavior of microbial and plant cell cultures (3, 17 and 47). Almost every physiological activity is joined to oxygen uptake in aerobic cultures making the OTR an excellent indicator of metabolic activity. Physiological responses of aerobic microorganisms to specific culture conditions (e.g. oxygen limitation, nutrient limitation, and inhibiting factors) are reflected by OTR [3]. A device for measuring the respiration activities (OTR and CTR and RQ), so called Respiratory Activity Monitoring System (RAMOS) in shaken bioreactors has been presented and developed [3 and 4]. This device for the determination of the optimal operating conditions, avoiding limitations in shaken bioreactors, and gaining important information for scaling up to stirred fermentors has been already applied [72].

As described in Chapter 5, a similar composition of the gas mixture in the headspace of ventilation and measuring (aerated) flask of the RAMOS device can be obtained by using a specific aeration rate. This aeration was calculated by considering the Eq. 5.4 for the dependency of k_{plug} on OTR_{plug}, in the unsteady state model. The results indicated that a decrease in the aeration led to a reduction of O_2 in the headspace of the aerated flask of the RAMOS device (Figures 5.4 and 5.5). It has been reported that the reduction of the aeration in an aerobic fermentor led to an increase of the autogenously CO_2 produced by micro-organisms [43]. The CO_2 sensitivity of micro-organisms, using batch and continuous fermentor has been addressed in many paper [2, 6, 19, 25, 26, 27, 41 and 50], but till date no report is available on the online monitoring and quantification of CO_2 sensitivity of micro-organisms in small scale bioreactors e.g. shake flask.

In Chapter 6, a new method for the quantification of CO_2-sensitivity of micro-organisms in shaken bioreactors, based on the variety of resistance of sterile closure was presented. In this Chapter, a new online monitoring method for the quantification of the CO_2 sensitivity of micro-organisms, based on the values of the respiration factors (OTR, CTR), obtained by using the RAMOS device with considering a variety of aeration rates in the measuring flask, will be investigated.

7.2   Theory

The gas transfer in the measuring flask of the RAMOS device based on the steady state gas transfer assumption has already been modeled [45]. The respiratory activities (e.g. OTR, CTR and RQ) are calculated by using the values of the partial pressure of oxygen, detected by an oxygen sensor.

In Chapter 4, we concluded that a variety of k_{plug} led to an unsteady state condition in the ventilation flasks. In an aerated flask this phenomenon will occur, if a low value of aeration rate is used (Figure 5.5). In the following sections, the effect of the aeration rate on the gas transfer and the results of OTR, obtained by the RAMOS device, will be discussed.
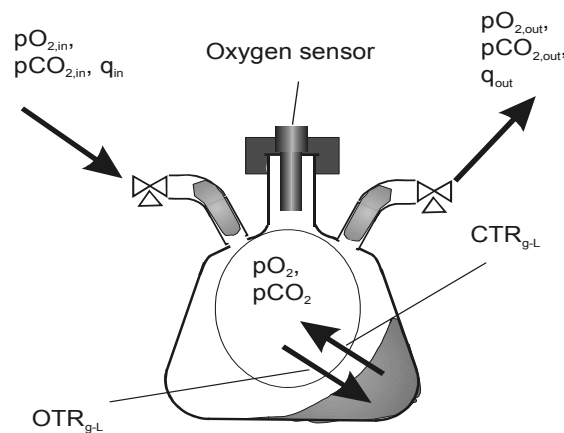
Figure 7.1: A schematic drawing of gas transfer in a measuring flask of the RAMOS device [3].

7.2.1   Determination of the OTR, CTR and RQ in the RAMOS device

The equations to calculate the values of OTR, CTR, and RQ based on the data of partial pressure of oxygen in the headspace of a measuring flask (Figure 7.1), detected by an oxygen sensor, have already been introduced [3 and 4]. During the fermentation in the RAMOS divice, a measuring cycle is continuously repeated, which is divided into the measuring and rinsing phase. The time interval of the measuring and rising phase depends on the cultivation system used. The continuous breathing activity of the micro organisms leads to the change of the oxygen partial pressure in the gas of the measuring flask. For instance, Figure 7.2 shows the sensor signal during each measuring cycle for the fermentation of *C. glutamicum* DM1730. In order to determine OTR, CTR and RQ during the measuring phase, a dynamic method has been employed [3]. At an exact time interval for each period, the inlet and outlet valves of the measuring flasks are closed (q_{in}=0). After the measuring phase, the gaseous products are removed by flowing fresh gas during the rising phase. At the end of the rising phase, the signal

normally reaches a stationary value (U^{α}). After this stationary condition, the signal drops in a linear manner with a slope (m) in the measuring phase. Using the values at the beginning (t1, U1) and end (t2, U2) of the measuring phase, the value of slope (m) can be calculated as follows:

$$m = \frac{U2 - U1}{t2 - t1} = \frac{dU}{dt} = \text{const.} \tag{7.1}$$
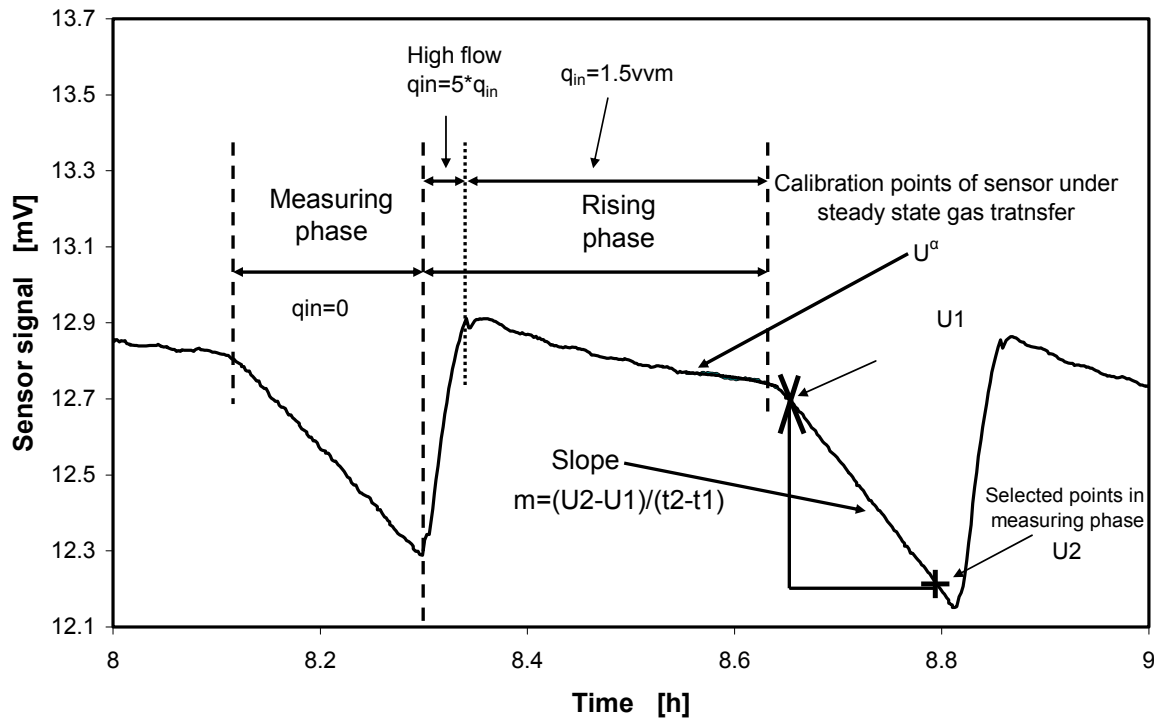
Figure 7.2: A measuring cycle of a fermentation of *C. glutamicum* DM 1730 in the measuring flask of the RAMOS device with a specific aeration rate of 1.5 vvm. After measuring phase a high aeration rate or a short time is used. The term 'm' is the slope in the measuring phase which is calculated by Eq.7.1. U^{α} is the values of the sensor signal in the end of rising phase and U2 is a value of the sensor signal nearly at the end of measuring phase.

where 'm' is the slope of the sensor signal in the measuring phase [V/h] (Figure 2.7). For the conversion of the sensor signal into the oxygen partial pressure, a sensor calibration must be done. For the compensation of a possible sensor drift (refer to the part of normal aeration in rising phase in the Figure 7.2) and/or for the avoidance of measuring errors by slow changes of the environmental conditions (e.g. the change of climate and temperature), the sensor is calibrated before the measuring period (refer to the point U^{α} in Figure 7.2). For a correlation between the value of the voltage signal changes and the value of the oxygen partial pressure, the following proportional equation is presented [10]:

$$\frac{\partial p_{O_2}}{\partial t} = \frac{pO_2^{\alpha}}{U^{\alpha} - U^{0}} \cdot m \tag{7.2}$$

Where $\dfrac{pO_2^{\alpha}}{U^{\alpha} - U^{0}}$ is defined as a calibration factors (C_f). Assuming a constant value of the calibration factor (C_f), a stationary gas transfer near the end of the rising phase during the fermentation is considered (Figure 7.2). In that case, the value of pO_2^{α} becomes a stationary value at the end of the rinsing phase which is dependent on the OTR $^{\alpha}$, RQ and q_{in}. Under steady state condition the vaue of pO_2^{α} can be calculated using an overall mass balance (e.g. O_2, CO_2 and N_2) in the measuring flask of RAMOS device (Figure 7.1) as follows [10]:

$$pO_2^{\alpha} = \frac{pO_{2,in}^{\alpha} \cdot q_{in} - p_{abs} \cdot V_{mo} \cdot OTR^{\alpha}}{q_{in} - V_{mo} \cdot OTR^{\alpha} \cdot (RQ - 1)} \tag{7.3}$$

where OTR^{α} is the oxygen transfer rate at the end of the rising phase. During the measuring phase, OTR, CTR and RQ can be calculated and monitored using the sensor signal values by a programming system [3 and 45]. The following equations result from a mass balance for O_2 and CO_2 in the headspace of the measuring flasks, considering the ideal gas law [3]:

$$OTR = \frac{V_G}{V_L} \cdot \frac{1}{R \cdot T} \cdot \frac{\partial pO_2}{\partial t} \tag{7.4}$$

$$CTR = \frac{V_G}{V_L} \cdot \frac{1}{R \cdot T} \cdot \frac{\partial pCO_2}{\partial t} \tag{7.5}$$

The oxygen transfer rate and the carbon dioxide transfer rate are connected by the respiration quotient (RQ).

$$RQ = \frac{CTR}{OTR} \tag{7.6}$$

Since the oxygen partial pressure is correlated to the nonlinear signal of the sensor (Eq. 7.2), the oxygen transfer rate can be continuously calculated by substitution of Eq. 7.2 into Eq. 7.4:

$$OTR = \frac{V_G}{V_L} \cdot \frac{1}{R \cdot T} \cdot C_f \cdot m \tag{7.7}$$

According to the Eqs. 7.1, 7.2 and 7.7, under defined operating conditions (such as V_L, aeration rate (q_{in}), physical parameter (p, Temperature, Vg)), the calibration factors (C_f) and,

consequently, pO$_2{}^\alpha$ play an important role to calculate the value of OTR in the RAMOS device.

As discussed in Chapter 5, a variety of aeration rates led to an unsteady state condition in the aerated flasks (Figures 5.5 and 5.6). This condition, especially at low aeration rate could affect the stationary values of pO$_2{}^\alpha$, and consequently on the constant value of C$_f$. This may lead to an error to calculate the OTR (Eq. 7.7). Therefore, in this study an unsteady state model to calculate the gas transfer in a headspace of an aerated flask was developed. Under this condition the partial pressure of oxygen can be calculated at the end of rising phase as following:

$$\frac{\partial p_{O2}}{\partial t} = (OTR_{conv.} - OTR_{g-L}) \cdot \frac{R \cdot T \cdot V_L}{V_g} \tag{7.8}$$

where OTR$_{conv.}$ is the rate of oxygen transferred by convection flow (aeration) through the aerated flask of the RAMOS device. OTR$_{conv.}$ can calculate as follows:

$$OTR_{conv.} = \frac{q_{in}}{V_{mo}} \cdot (pO_{2,in} - pO_2) \cdot \frac{1}{p_{abs}} \tag{7.9}$$

For a correlation between the values of the sensor voltage and the oxygen partial pressure at the end of rising phase, the following proportional equation is presented:

$$\frac{\Delta p_{O_2}{}^\alpha}{\Delta t} = C_f \cdot \frac{\Delta U^\alpha}{\Delta t} \tag{7.10}$$

Where the C$_f$ is the calibration factor at unsteady state condition and can be calculated by substitution of Eqs. 7.8 and 7.9 in Eq.7.10:.

$$C_{f,unst.st} = \frac{pO_2{}^\alpha}{U^\alpha - Uo} = \frac{\dfrac{pO_{2,in}^\alpha \cdot q_{in}}{p_{abs} \cdot V_{mo}} - OTR{}^\alpha{}_{g-L}}{\dfrac{U_1 \cdot q_{in}}{p_{abs} \cdot V_{mo}} + \dfrac{\Delta U}{\Delta t}} \tag{7.11}$$

Therefore the oxygen transfer rate can be continuously calculated considering the Eqs. 7.7, 7.8 and 7.9:

$$OTR = \frac{pO_{2,in}}{\dfrac{1}{m} \cdot (U1 \cdot \dfrac{R \cdot T \cdot V_L}{V_g} + \dfrac{\Delta U}{\Delta t} \cdot \dfrac{V_{mo} \cdot p_{abs}}{q_{in}}) - \dfrac{V_{mo} \cdot p_{abs}}{q_{in}}} \tag{7.12}$$

where the term of $\dfrac{\Delta U}{\Delta t} \cdot \dfrac{V_{mo} \cdot p_{abs}}{q_{in}}$ is for rising phase which will be zero if the rising phase become a steady state condition.

In this study we implemented the Eq.7.11 and 7.12 into an analyzing program, so called OTR analyzer, the correct values of OTR can be calculated using the data of oxygen sensor.

7.3 Material and Method

7.3.1 RAMOS with a special aeration system

In this study OTR was measured using the Respiration Activity Monitoring System (RAMOS, Hitec Zang, Herzogenrath, Germany) with a special aeration system developed our purpose (Sec. 5.3.1). The measuring flasks (Figure 7.1) were fixed onto a shaker, the oxygen sensors (Sec. 2.1.4) appropriately connected, and then operated under conditions which are given in the Table 2.3. The required values (e.g. temperature, air pressure, filling volume, aeration rates, measuring and rising time for the RAMOS device etc.) were entered in the programming system, and the air flow rates were adjusted using the mass flow controller (5850TR, Brooks Instruments, Venendaal, NL). The measuring and rising times were selected as 10 and 20 mins, respectively.

A high aeration rate, 5 times higher than a normal aeration rate at the beginning of the rising phase, for a short time (2.3 min) was used (Figure 7.2). In this way stationary conditions were reached in a shorter time. For further information on the general set-up of the RAMOS device, refer to the literature [3].

7.3.2 Program to analyze the OTR results of the RAMOS deice

In order to control and correct the results of RAMOS, obtained under a variety of aeration rate (particularly, at low aeration rate) an analyzing program was applied. The modified equations for calculating OTR (Eqs. 7.11 and 7.12) were implemented in an Excel-Makro (Excel 97) in Visual Basic for Applications [10]. Using this program, the value of the calibration factor (C_f) was calculated before the periodic measuring phase. This program also automatically recalculates the correct values of OTR, based on the corrected value of the calibration factor (C_f).

7.3.3 Model organisms and cultivation

For the investigation of the new method, fermentations of *Arxula adeninivorans* WT-LS3, *Corynebacterium glutamicum* (DM1730 and 13032WT), *Pseudomonas fluorescens* DSM50090 and *Hansenula polymorpha* RB11-FMD-GFP as model organisms were performed in the measuring flasks of the RAMOS device. The medium preparation and the cultivation method were described in Sec. 2.6. The operating conditions of the experiments are

provided in Table 2.3. The fermentations in the RAMOS device were carried out under a variety of aeration rates (between 3 and 0.08 vvm), which were calculated using the unsteady state model (Sec. 5.3.3). It is noted that the details of the operation conditions of the experiments are specified in the legend of Tables and Figures.

7.3.4 Applied model

The modified unsteady state model for the prediction of operation conditions of a biological system in measuring flasks was used (Secs. 5.4.1 and 5.4.3) in order to avoid oxygen limitation.

7.3.5 Calculation of the CO₂ concentration

For an aerobic fermentation, with RQ equal to 1, the concentration of accumulated CO_2 could be easily estimated from the value of pO_2 (Eq. 7.13).

$$CO_{2,g} = 100 \cdot (0.2095 - pO_2) \ [\%] \tag{7.13}$$

7.3.6 Calculation of the maximum specific growth rate (μ_{max})

The maximum specific growth rate in the exponential phase ($\mu_{max.}$) can be deduced from the maximum exponential slope of the OTR [72]:

$$\mu_{max.} = \frac{\ln OTR_t - \ln OTR_{t_0}}{t - t_0} \tag{7.14}$$

7.3.7 Calculation of the oxygen consumption during the fermentation

The amount of oxygen consumed over the fermentation time was calculated by integration of OTR according to the Eq. 7.15.

$$C_{O2} = \int_0^t OTR \cdot dt \tag{7.15}$$

7.4 Results and Discussions

Considering the importance of the carbon dioxide for industrial aerobic bioprocesses, the new method for quantification of the CO_2 sensitivity of microorganisms presented in the Chapter 6, was developed via an online monitoring system. In the following sections, this method will be firstly validated by carrying out a fermentation of *Arxula adeninivorans* WT-LS3, *Corynebacterium glutamicum* (DM1730 and 13032WT), *Pseudomonas fluorescens* DSM50090 and *Hansenula polymorpha* RB11-FMD-GFP as model organisms in the

measuring flasks of the RAMOS device. Then, the effect of aeration rate on the calibration factor (C_f), and consequently on OTR will be discussed.

Finally, the CO_2 sensitivity of the microorganisms, based on the values of OTR will be investigated. In that case, the values of the maximum specific growth rate, calculated by OTR values and the productivity, will be used.

7.4.1   The effect of aeration rate on the partial pressure of oxygen

In the Chapter 5, it was indicated that a pattern for the specific aeration rate (q_{in}) in the ventilation flasks could be calculated using the unsteady state model considering Eq. 5.4. By utilizing maximum values of q_{in} (refer to the Figures 5.2 and 5.3) for aeration of the measuring flasks of the RAMOS device, the same gas concentration of O_2 and CO_2 in the headspace of both flasks under a non oxygen limited condition obtained (Figure 5.6). Therefore, different levels of accumulated CO_2 in the headspace of the aerated flasks could be adjusted by using different aeration rates.
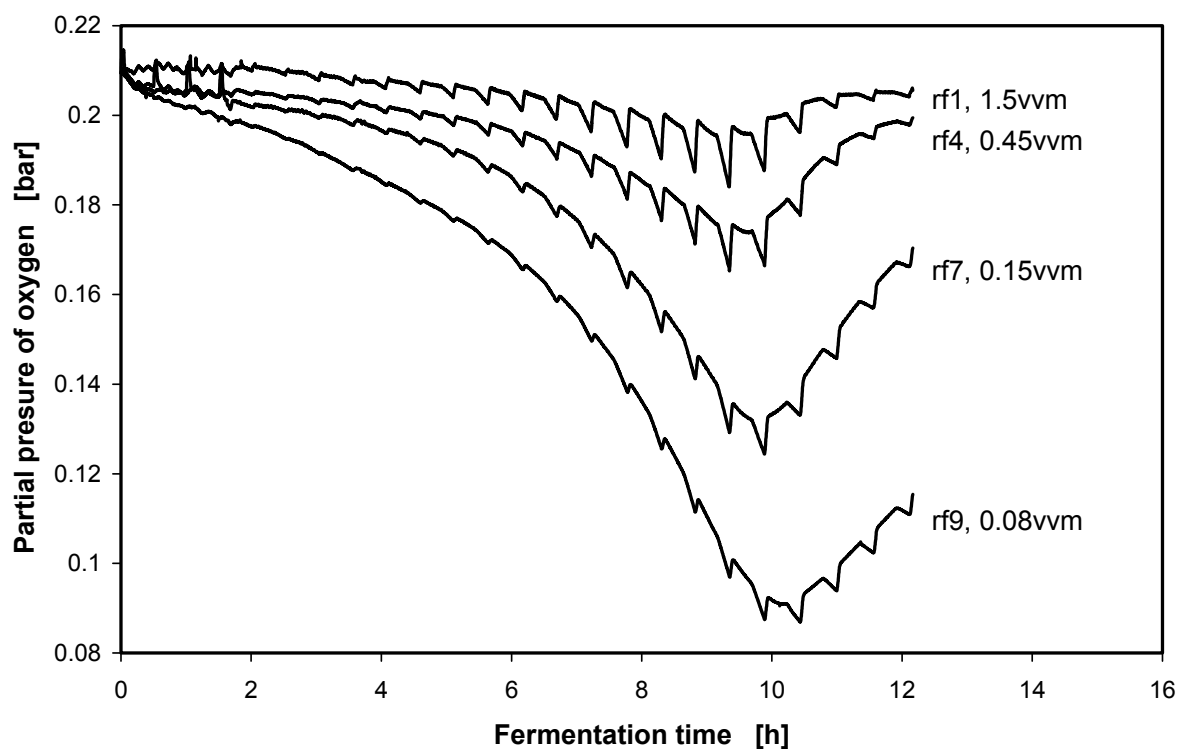
Figure 7.3: The effect of aeration rates on the partial pressure of oxygen in the headspace of the measuring flasks (rf1, rf4, rf7 and rf9) of the RAMOS device for a fermentation of *C. glutamicum* DM1730 on 15g/l glucose (21 g/l MOPS, pH_{start}=7.18, V_L=15 ml, n=400 rpm). The values of the aeration rates for the flasks were obtained by the unsteady sate model.

In order to investigate the effect of aeration on the concentration of the components of the gas mixture (O_2 and CO_2) in the headspace of the measuring flasks of the RAMOS device, the fermentation of *C. glutamicum* DM1730 on 15 g/l glucose (21 g/l MOPS, pH_{start}=7.18, V_L=15

ml, n=400 rpm) was performed based on different aeration values of 1.5, 0.45, 0.15 and 0.08 vvm for aerated flasks rf1, rf4, rf7 and rf9, respectively. These aeration rates were calculated by the unsteady state model (Sec. 7.3.4). Figure 7.3 illustrates the results of this fermentation in the measuring flasks. After 10.2 hours of the fermentation there are significant differences between the minimum levels of the partial pressure of O_2 (0.196, 0.174, 0.134, and 0.09 bar). Values of 1.5, 3.7, 7.8 and 11.9 % for the maximum accumulated CO_2 were obtained in the headspace of the aerated flasks rf1, rf4, rf7 and rf9 using Eq. 7.13, respectively.

These results revealed that the uses of different values of aeration rates in the RAMOS device are advantageous for quantifying the CO_2 sensitivity of micro-organisms, as an online monitoring method. This method is based on the effect of CO_2 on the values of the oxygen uptake rate. In the following sections the validity of this method will be experimentally demonstrated.

7.4.2 Validation of the OTR results of the RAMOS device obtained by the new method

For the investigation of the effect of a variety of aeration rates (new method) on the values of OTR resulted by the RAMOS device, fermentations were performed with *C. glutamicum* 13032WT on 10g/l L-lactate (n=350 rpm, T=30 °C, do=5 cm, pH_{start}=6.4), in the measuring flasks with different specific aeration rates of 1.03, 0.55 and 0.23 vvm. Figure 7.4 shows the oxygen values of the partial pressure in the headspace of the measuring flasks during this fermentation. This figure indicates that the use of different aeration rates of 1.03, 0.55 and 0.23 vvm for the measuring flasks resulted in minimum value of 18.46, 16.73, and 12.9 % for the concentration of O_2 in the headspace of these flasks, respectively.

The values of OTR were calculated using the partial pressure of oxygen, detected by oxygen sensor (Sec. 2.1.4) in the programming system. These OTR values are presented in the Figure 7.5. As illustrated by that Figure, there is a significant discrepancy in the slopes of OTR curves. This could be interpreted as a criterion for the effect of CO_2 on the *C. glutamicum*. Although the total oxygen consumptions calculated by the integration of OTR over the fermentation time for all flasks should be the same (Eq. 7.11), the obtained results were different. Those differences clarified that there was an error in the calculation of the OTR, specially, for the low aeration rate of 0.23vvm. For this reason of the calibration factor (C_f) and the OTR were calculated using the oxygen sensor's signals. This result is shown in the Figure 7.5. Interestingly, it was found that the values of the calibration factor (C_f) were strongly changed during the fermentation with low aeration rate (0.23vvm) in comparison with the high aeration rate (1.03vvm). The highest variation of C_f values was obtained around the maximum OTR for the low aeration in which unsteady state conditions strongly occurred.
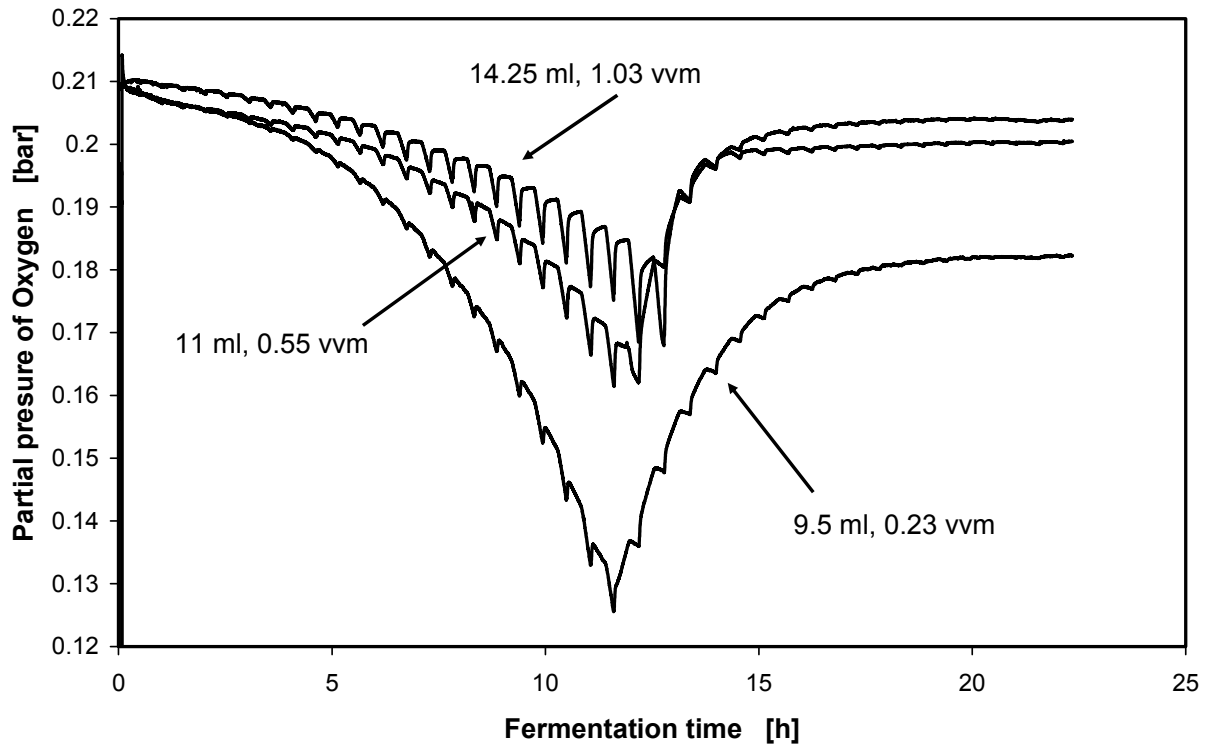
Figure 7.4: The effect of the specific aeration rates on the partial pressure of oxygen in the headspace of the measuring flasks of the RAMOS device for a fermentation of *C. glutamicum* 13032WT on 10 g/l lactate (n=350 rpm, T=30 °C, do=5 cm, pH$_{start}$=6.4).
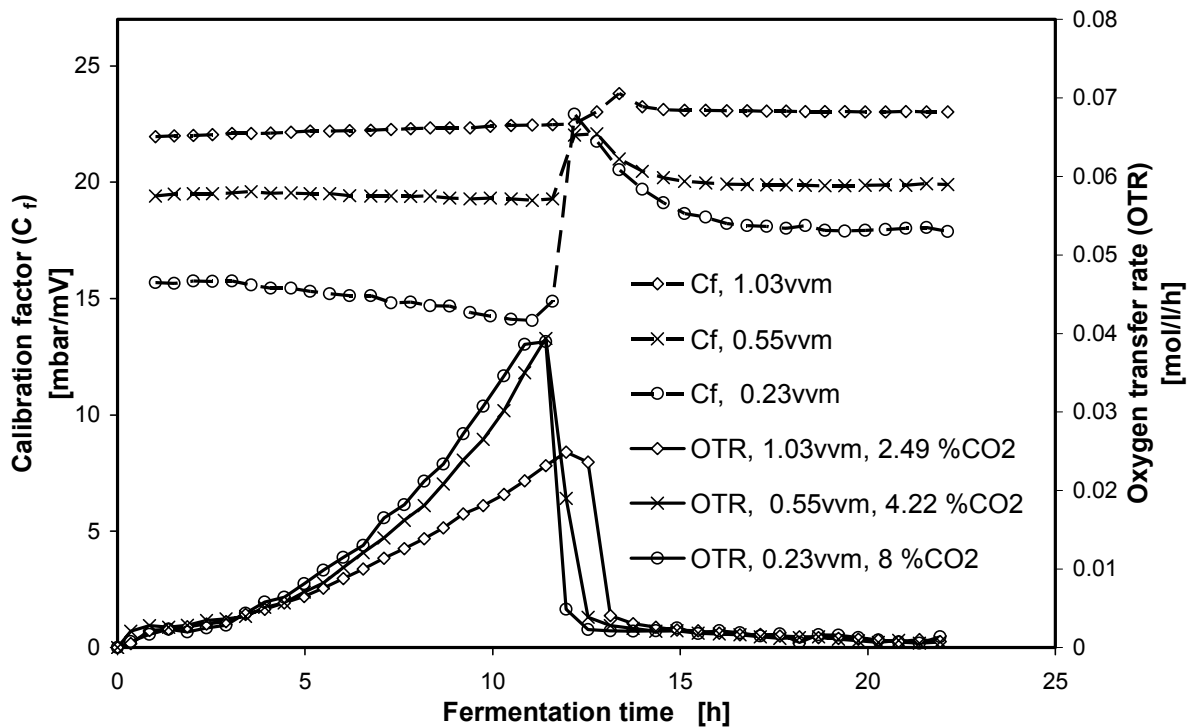
Figure 7.5: The effect of the specific aeration rate (1.03, 0.55 and 0.23 vvm) on the calibration factor (C$_f$) and OTR for fermentation of *C. glutamicum* 13032WT on 10 g/l lactate (n=350 rpm, T=30 °C, do=5 cm, pH$_{start}$=6.4) in the RAMOS device.

The values of C_f and OTR were recalculated by the OTR analyzer. Figure 7.6 illustrates the recalculated values of OTR and the corrected value of C_f considering the real value of pO_2, before each periodic of the measuring phase. According to this method, the same values of oxygen consumption for the fermentation of *C. glutamicum* 13032 WT on 10 g/l L-lactate were obtained. In the following section, the new method accompanied with the OTR analyzer will be presented for the investigation of the CO_2 sensitivity of micro-organisms.
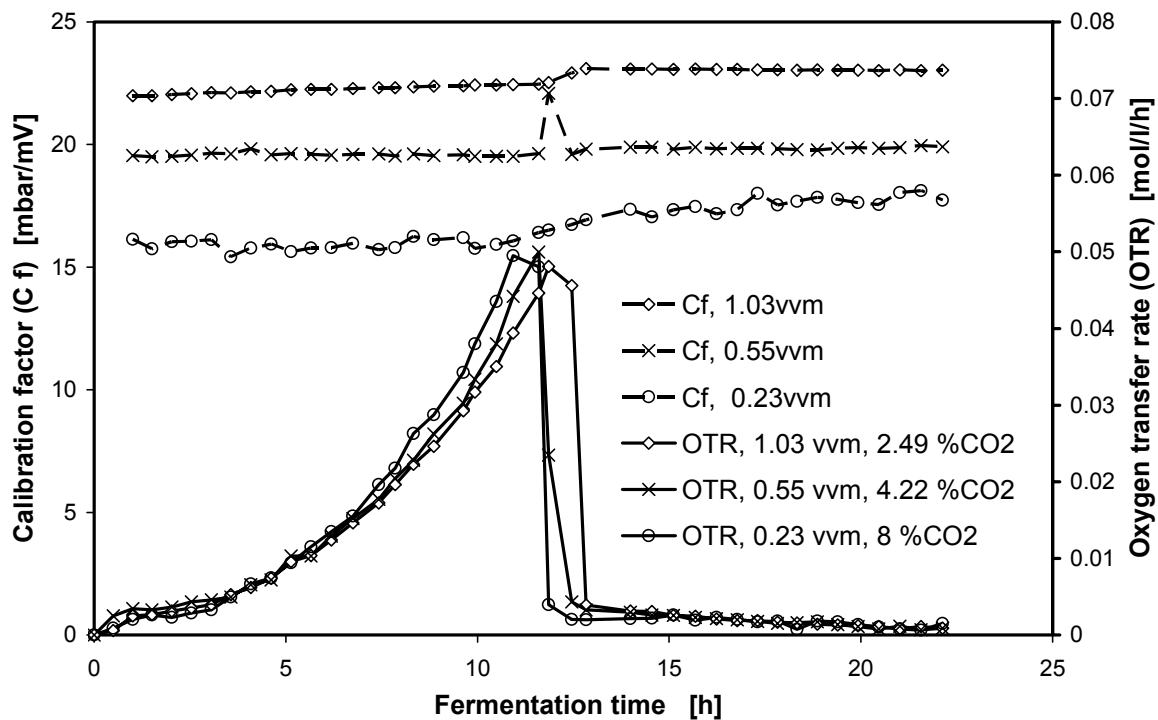
Figure 7.6: The recalculated values of OTR and calibration factor (C_f), for the fermentation of *C. glutamicum* 13032WT on 10g/l lactate (n=350 rpm, T=30 °C, do=5 cm, pH_{start}=6.4), by an OTR analyzer

7.4.3 Evaluation of the CO_2 sensitivity of micro-organism using OTR values

In aerobic cultures, the OTR is a very useful parameter to reflect the physiological responses of micro-organisms to specific culture conditions [3]. Thus, the OTR values, obtained by the RAMOS dev ice were applied for the investigation of the CO_2 sensitivity of micro-organisms.

Culture experiments were performed with *Arxula adeninivorans* WT-LS3, *Corynebacterium glutamicum* (DM1730 and 13032WT), *Pseudomonas fluorescens* DSM50090, as model organisms in the RAMOS device, under a variety of aeration rates. The values of OTR, obtained by the RAMOS device were recalculated, in advance, by the OTR analyzer. The results shown in the Figure 7.6 clarify that there is a significant discrepancy between the slope of OTR, recalculated by OTR analyzer, for fermentation of this organisms under the different

maximum accumulated CO_2 values of 2.49, 4.22 and 8 % related to the aeration rates of 1.03, 0.55 and 0.23 vvm in the measuring flasks, respectively. On this basis, it can be inferred that *C. glutamicum* 13032WT is sensitive to the values of CO_2. The CO_2 sensitivity of this microorganism has been already reported by a continuous turbidostatic culture system [6]. *Pseudomonas fluorescens* DSM 50090 as an especially sensitive organism to CO2 which agrees with literature [19] was fermented (Table 2.11) in the measuring flasks of the RAMOS devive under different specific aeration rates of 2.14, 0.17 and 1 vvm.

The results of OTR recalculated by the OTR analyzer, and pO_2 detected by an oxygen sensor (Sec. 2.1.4) are illustrated by Figure 7.7. As shown in this figure, minimum pO_2 values of 0.20, 0.19 and 0.18 bar were obtained after 5.1 hours of fermentation under different aeration rates of 2.14, 0.17 and 1 vvm in measuring flasks, respectively. Maximum accumulated CO_2 values of 0.9, 2.2 and 3.2 % were computed by Eq. 7.14. Under these conditions, different slopes of the OTR curves were obtained, and consequently, different values of 0.4, 0.34 and 0.23 h^{-1} for the maximum specific growth rate (μ_{max}) were calculated by Eq. 7.14. From these results it can be concluded that this micro-organism was sensitive to CO_2 as reported in literature [19].
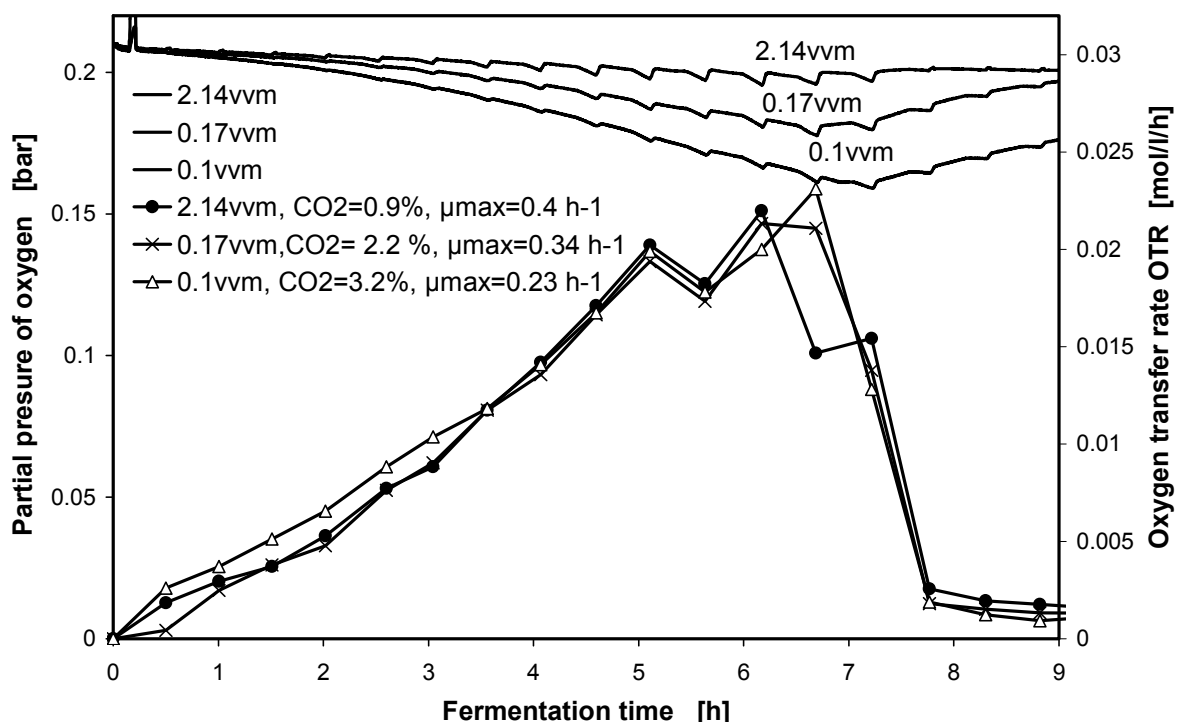
Figure 7.7: The results of pO_2 and OTR for a fermentation of *Pseudomonas fluorescens* DSM50090 on 5 g/l glucose and 2 g/l yeast extract (21 g/l MOPS, n=350 rpm, V_L=10 ml, T=30 °C, d_o=5 cm, pH_{start}=7.0, pH_{final}=7.1), under different values of accumulated CO_2 in the measuring flasks of the RAMOS device, obtained by the new method. The vales of OTR were recalculated by the OTR analyzer, based on constant values of the calibration factor (Eq.7.11), before the periodic the measuring phase.

In the same way, the CO_2 sensitivities of *C. glutamicum* DM 1730, *C. glutamicum* WT 13032 and *Arxula adeninivorans* LS3 were evaluated by the online monitoring method. Figure 7.8 shows the OTR results of these microorganisms.

The results for *Arxula adeninivorans* LS3 on 20 g/l glucose (0.14 M MES buffer, n=350 rpm, RQ≈1, do=5 cm, T=30 °C, pH_{start}=6.4), indicated that there was no significant difference between the values of OTR after 13.4 hours of the fermentation (in the exponential phase) under the maximum accumulated CO_2 values of 2.5 and 8 %. Furthermore, the same value of 0.30 h^{-1} for the maximum specific growth rate was calculated.

In case of the fermentation of *C. glutamicum* DM1730 on 15 g/l glucose (21 g/l MOPS, RQ≈1, do=5 cm, V_L=10 ml, pH_{start}=7.5), a significant effect of the accumulated CO_2 (4, 4.7 and 7 %) on the slope of the OTR and maximum growth rate (0.35, 0.32 and 0.31 h^{-1}), was found. Moreover, the results depicted in Figure 7.8 indicated that there was a noticeable effect of accumulated CO_2 (2.2 and 8 %) on the slopes of OTR and maximum specific growth rate (0.24 and 0.28 h^{-1}) in the fermentation of *C. glutamicum* WT13032.
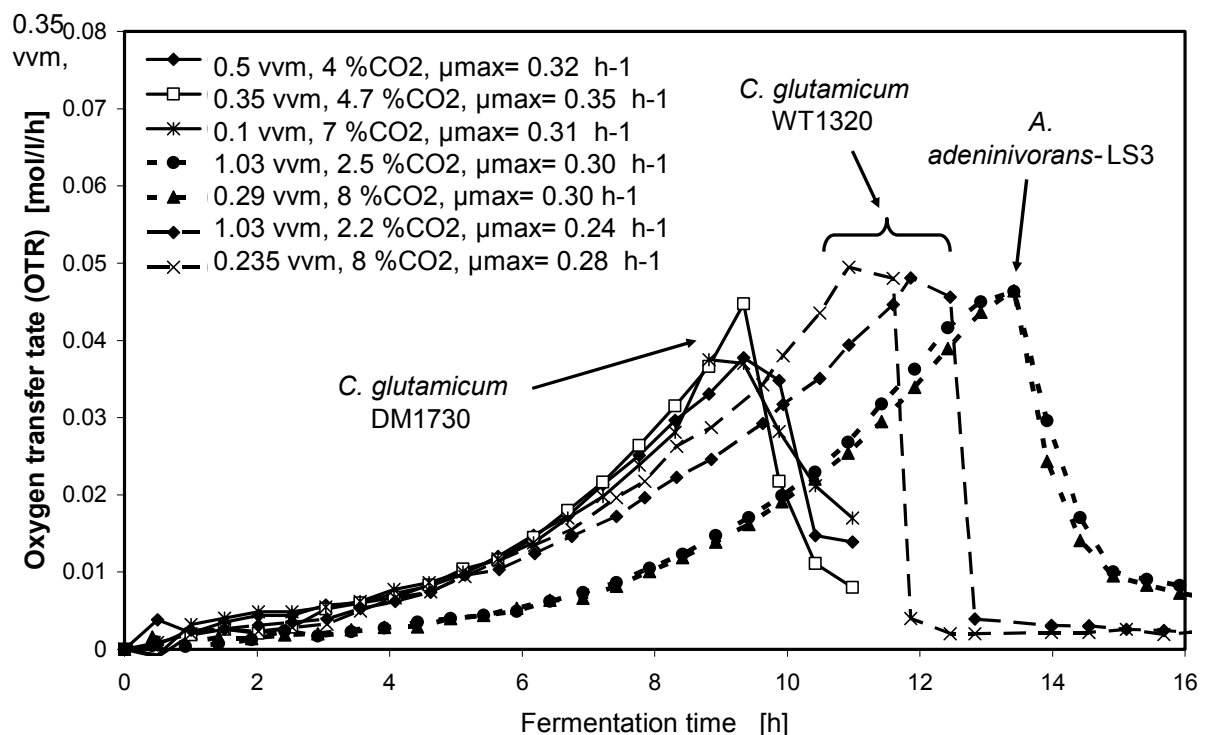
Figure 7.8: Comparison between the CO_2 sensitivities of *Arxula adeninivorans* LS3 on 20 g/l, glucose (0.14 M MES buffer, n=350 rpm, RQ≈1, do=5 cm, T=30 °C, pH_{start}=6.4); *C. glutamicum* 13032WT on 10 g/l lactate (n=350 rpm, T=30 °C, do=5 cm, pH_{start}=6.5) and *C. glutamicum* DM1730 on 15 g/l glucose (21 g/l MOPS, RQ≈1, do=5 cm, V_L=10 ml, pH_{start}=7.5) using the on line monitoring method based on the OTR results.

7.4.4 Results of the online monitoring method versus those of the continuous turbidostatic culture method

For the validation of the online monitoring method, the results of CO_2 sensitivity of *Corynebacterium glutamicum* 13032WT as a model organism obtained by the new method were compared with the results of the continuous turbidostatic culture system [6]. This comparison is shown in Figure 7.9. As depicted in this figure, the values of μ_{max} obtained with the turbidostat system are slightly higher than the values calculated by our method. However, the overall tendencies are the same. As mentioned in the Sec. 6.4.3.2, the difference between the results of both methods may be due to the differences between adjusting the pH and the calculation procedure of μ_{max}. On the basis of the explanations in that section, the values of μ_{max} obtained by the online monitoring method in the RAMOS device were validated to quantify the CO_2 sensitivity of micro-organisms. According to all mentioned results, our new method is reliable.
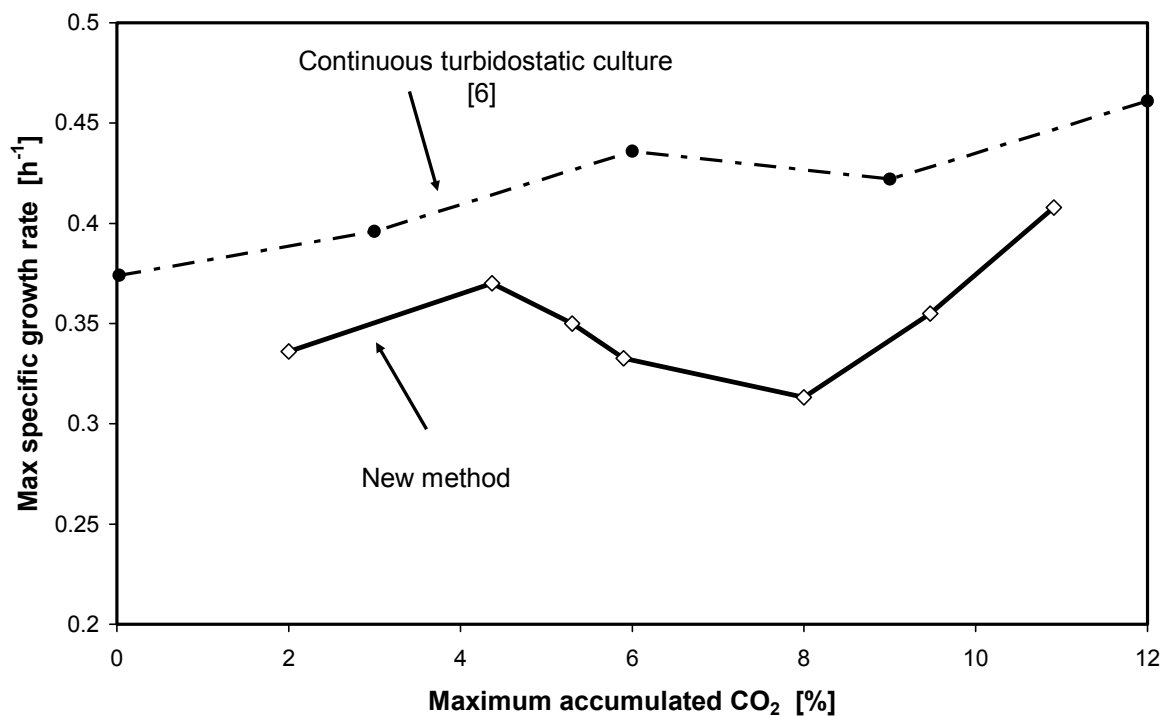
Figure 7.9: Comparison between the maximum specific growth rate of *C.glutamicum* WT13032 on 10 g/l lactate resulted by the online monitoring method in the RAMOS device (21 g/l MOPS, 30°C, do=5 cm, n=350 rpm, VL=15 ml, pH$_{start}$=7.05, pH$_{final}$=8.2) and the continuous turbidostatic culture method (T=30 °C, qin=1 vvm, n=1200 rpm, V$_L$=800 ml, pH$_{start}$=6.85) [6]

7.4.5 Quantification of the CO2 sensitivity in terms of the maximum specific growth rate

The quantification of the CO_2 sensitivity of *Arxula adeninivrtans* WT LS3, *Corynebacterium glutamicum* (DM1730 and 13032WT), *Pseudomonas fluorescens* DSM50090 and *Hansenula*

polymorpha RB11-FMD-GFP were investigated by performing series of experiments based on the online monitoring method in the RAMOS device. The values of the maximum specific growth rate were calculated using the values of OTR in Eq. 7.10.

Figure 7.10 indicates the effect of maximum accumulated CO_2 concentration on the maximum specific growth rate of these microorganisms. The sensitivities of these microorganisms can be quantified at the maximum accumulated CO_2 range of 12 % using the online monitoring method.

From these results, it could be easily concluded that *Arxula adeninivorans* LS3 and *Hansenula polymorpha* as yeasts are not sensitive to CO_2 [34], and the bacterial strains of *Corynebacterium glutamicum* (DM1730 and 13032WT) are sensitive to autogeneously produced CO_2. *Pseudomonas fluorescens* (DSM50090) was found to be a especially sensitive organism [19].
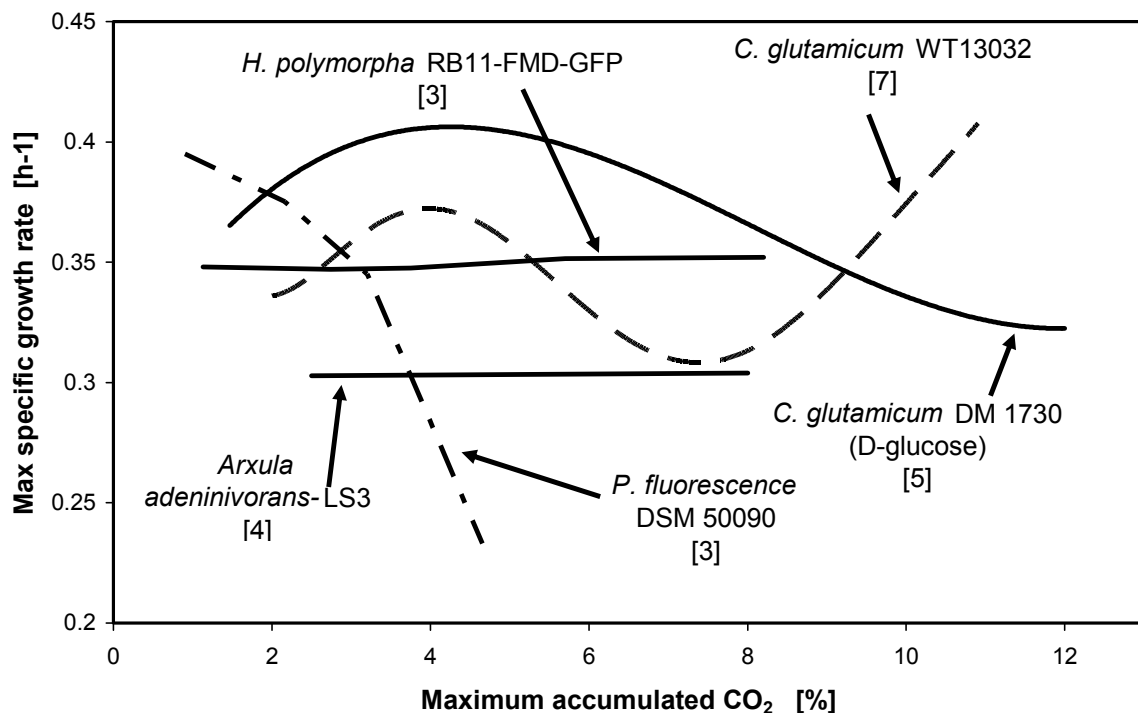
Figure 7.10 Maximum specific growth rate over the maximum accumulated CO_2 for several micro-organisms obtained using the online monitoring of CO_2 sensitivity method. The experiments were repeated several times and its reproducibility is indicated in brackets.

7.5   Conclusion

The measurement of OTR in shake flask cultures provided valuable data during screening. The OTR profiles displayed the time dependent course of the screening cultures and reflected the metabolic activity with respect to different screening conditions. The quantification of CO_2 sensitivity of micro-organisms could be easily detected using an online monitoring method in

the RAMOS device, based on the data of OTR obtained under different aeration rates. In order to see the function of the online monitoring method, experiments with several microorganisms in the measuring flasks of the RAMOS device were carried out. A maximum value of 12 % for accumulated CO_2 could be derived by applying a low flow rate of 0.1 vvm (Figure 7.3), under the appropriate conditions (e.g. V_L, do and n) and culture parameters (e.g. RQ, carbon source, pH and etc.). In order to predict these conditions an unsteady state gas transfer model in shaken bioreactors would be very advantageous. The data of OTR obtained by the RAMOS device were analyzed and recalculated by a program considering the calibration factor (C_f) (Eq. 7.11). An approximate constant value for this factor confirms the OTR results (Figure7.6). Based on the analyzed OTR, the CO_2 sensitivity of micro-organisms was quantified by the assessment of the slope of the OTR curves or the values of maximum specific growth rate (Figures 7.8 and 7.10).

The major advantage of the new method is the possibility to determine the metabolic activity, independent of manual sampling.

Chapter 8

A New Scale-up Method from Shake Flask to Stirred Tank Fermentor Based on the Effect of CO$_2$ Ventilation

8.1   Introduction

Scale up in fermentation processes is a procedure for the design and assembly of a large scale system considering the results from small-scale cultures and devices (e.g. micro titre plates and shake flasks). The scale-up of a fermentation process can be divided into three steps [33 and 35]:

a- laboratory scale, in which elementary studies are carried out in shaken bioreactors;

b- pilot scale, where the process optimizations are performed;

c- plant scale or production scale, where the process is used to fabricate economic products.

Biotechnologists are requested to control aeration, especially in scale up from shake flask to fermentors in order to provide sufficient oxygen for aerobic culture [8, 74 and 75]. The scale up from shake flasks to stirred tank bioreactors is often very complex and time consuming [8]. Generally, the oxygen transfer rate and the specific power input have been used to scale up bioprocesses from shaken bioreactors to stirred tank fermentors [8]. The suitability of scale up methods are usually confirmed by experimental results, which show that there is no difference between fermentation results in various types of small and large scales, carried out under the same oxygen transfer rate [21]. Under this condition, the divergence between the values of CO_2 ventilation in both scales could lead to a discrepancy between the results of both scales [15, 59 and 75]. Ventilation is defined as the removal rate of volatile compounds such as carbon dioxide, alcohols or auto-inducers, from the fermentation broth [15, 39, 43 and 56]. Inhibition of the cell growth, product formation, exhaustion of volatile substrates and incomplete induction may happen due to insufficiently adjusted ventilation. The rate of ventilation mainly depends on the aeration rate in a fermentation system [30, 58, 59 and 75]. It has been shown that at high aeration rates the carbon dioxide concentration in fermentation broth is reduced leading to higher inosine formation from shake [69]. Tanaka et al. [75] have introduced the ventilation of a bioreactor as an additional scale up criterion. They have concluded that the degree of ventilation between shake flasks and a stirred bioreactors could be different, and scale up problems may occur. The impossibility of scale up from a shake flask with sterile closure to a stirred tank bioreactor and the possibility of it from aerated flasks to stirred tank bioreactor have been reported. This was attributed to the effect of CO_2 ventilation [37].

The dependency of the gas transfer coefficient (k_{plug}) and the oxygen transfer rate (OTR_{plug}) in the sterile closure of the ventilation flasks was well described in Chapter 4. Based on this dependency a new aeration strategy to determine the specific aeration rate from a ventilation

flask to an aerated (measuring) flask was introduced in Chapter 5. A goal of this chapter is the investigation of a new scale-up method from a shake flask to a stirred tank fermentor, based on the effect of CO2 ventilation. This method is quantified using the aeration strategy presented in Chapter 5. Figure 8.1 shows a schematic illustration of this method.

$$q_{in}(plug) = \frac{V_{mo}}{V_L} \cdot k_{plug}$$

Calculated by Model

Scale-up

q_{in} (fermentor) = Max.q_{in} (plug)

20.95% O_2
0.03% CO_2
q_{in}

Ventilation flask   Fermentor
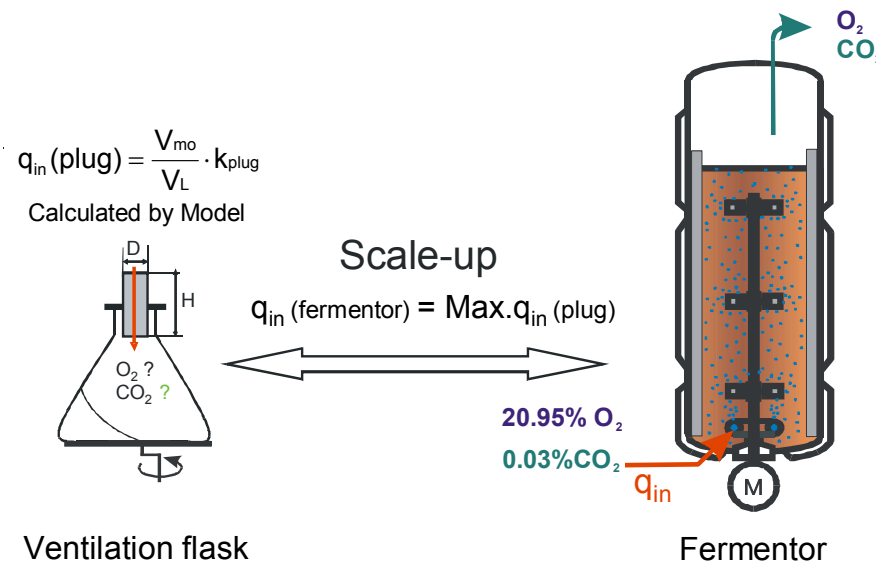
Figure 8.1: Schematic illustration of a scale up method based on the ventilation criterion

8.2   Material and Method

8.2.1   Ventilation flask

In this study, the ventilation flasks f1, f4 and f9 (Figure 2.2) were used. For measuring the pO_2, special designed ventilation flasks with mounted oxygen sensors (Figure 2.1-A) were employed. The characteristics of these flasks are given in Table 2.1.

8.2.2   Respiratory Activity Monitoring System (RAMOS)

In order to evaluate the activity of micro-organisms during the fermentation, a the RAMOS device with a special aeration system (Figure 5.1) explained in Chapter 5, as a system used in parallel to ventilation flasks f1, f4 and f9, was used. More details are given in Secs. 2.1.2 and 7.3.1.

8.2.3   Laboratory scale fermentor

In this study a foil fermentor (Visual Safety- Fermentor (VSF), Bioengineering AG, Wald, CH) was used. The fermentor is sterilized in situ. The pH electrode (Mettler Toledo) is attached to a measuring amplifier. The temperature control is formed by the internal cooling system. The aeration rate is adjusted by a mass flow controller (5850TR, Brooks of

instrument, Venendaal, NL). The optical density is measured on-line with the help of a flow cuvette (170 QA, layer thickness 0,5mm, Hellma). Data acquisition is made by Adam modules (4250 + 4018, ADAM). These record the data of CO_2 and O_2 from the exhaust gas analyzer and pO_2, pH, OD, temperature, aeration rate and agitation from other equipments. All data are transmitted to the process computer, analyzed and stored. The fermentor with the operating volume of 1800 ml was prepared, autoclaved and then filled with a medium, and finally inoculated by 5 % of a pre-culture. Fermentations in the fermentor were performed at 30°C. Specific aeration rates of 1.43, 0.37, 0.1 vvm were selected and the agitation was switched on between 300 and 1000 rpm, in order to avoid an oxygen limitation. The operation conditions and some important information of the experiments in the fermentor are given in Table 2.2. The pH value was controlled utilizing 21 g/l MOPS buffer.

8.2.4   Sampling and analysis of the results

Five series of each ventilation flask and several samples from the fermentor were taken for the determination of the biomass concentration (bio dry weight), pH value and optical density (600 nm), carbon source and L-lysine concentration (Sec. 2.4). Furthermore, at the same time, additional experiments were performed in the RAMOS device for determination of OTR, CTR and RQ.

8.2.5   Model organisms and cultivation

For the investigation of the scale up method, fermentation of *Corynebacterium glutamicum* DM1730 as model organism was performed in the ventilation flasks, measuring flasks and fermentor. The medium preparation, the cultivation system and operation conditions are given in section 2.7. The fermentations in the RAMOS device and fermentor were carried out under specific aeration rates of 1.43, 0.37, 0.1 vvm, which are calculated using the unsteady state model (Chapter 5). It is noted that the operation conditions for the experiments are specified in the legend of the tables and Figures.

8.2.6   Determination of O_2 and CO_2 in the headspace of flasks

For detecting the partial pressure of oxygen in the gas phase of the headspace of the ventilation and measuring flasks O_2 sensors were employed (Sec. 2.1.4). The values of CO_2 concentration were calculated by using the data of pO_2 in the Eq. 7.10.

8.2.7 O_2 and CO_2 concentration in the exhaust gas of the fermentor

The exhaust gas left the fermentor through an exhaust gas cooler and a sterile filter and was led to the gas analyzer in order to monitor the O_2 and CO_2 concentrations in the outlet stream. This gas analyzer was previously calibrated with a commercial gas of defined composition (5% (v/v) O_2, 25% (v/v) CO_2 and 70% (v/v) N_2; Westfalen, Germany).

8.3   Results and Discussions

In order to investigate the scale up method based on the effects of CO_2 ventilation, fermentations of *C. glutamicum* DM1730 on 15 g/l glucose were simultaneously examined in the ventilation flasks equipped with an oxygen sensor, measuring flasks of the RAMOS device and a stirred tank fermentor. Different specific aeration rates of 1.5, 0.39, 0.1 vvm for the measuring flasks and for the fermentor, related to the maximum aeration rate calculated for ventilation flasks f1, f4 and f9 were utilized as described in Sec. 5.4.1. The pH was controlled using 21 g/l MOPS as a buffer. The agitation in the fermentor was adjusted, so that the dissolved oxygen was above 25 % of saturation. This was essential for a scale up from shake flask to a fermentor under sufficient oxygen supply [33]. The fermentation results in these vessels are compared by observing the gas concentrations in the gas phase (O_2 and CO_2), maximum oxygen transfer rate (OTR), cell dry weight (biomass) concentration, maximum specific growth rate and L-lysine formation. It is noted that in the following sections the terms f1, f4 and f9 will be used as short forms of the different conditions for the different scales.

8.3.1   Validation of the method based on the comparison of the concentration of CO_2 and O_2 in the ventilation flask and the fermentor

In order to study the method, the oxygen concentrations in the headspace of the ventilation and measuring flasks and in the exhaust gas of the fermentor were measured using an oxygen sensor and exhaust gas analyzer, respectively. Experiments with *C. glutamicum* DM1730 as a model organism were performed. Figure 8.2 illustrates those results. As indicated in this figure, the O_2 concentrations in the gas phase obtained in the measuring flasks and the stirred tank bioreactor considering different specific aeration rates of 1.5, 0.39 and 0.1 vvm, were comparable to those obtained from ventilation flasks f1, f4 and f9, respectively. Moreover, there a significant difference between the average minimum values of 19.4, 16.5 and 10.2 % for O_2 concentrations in the gas phase of all scales (f1, f4 and f9).
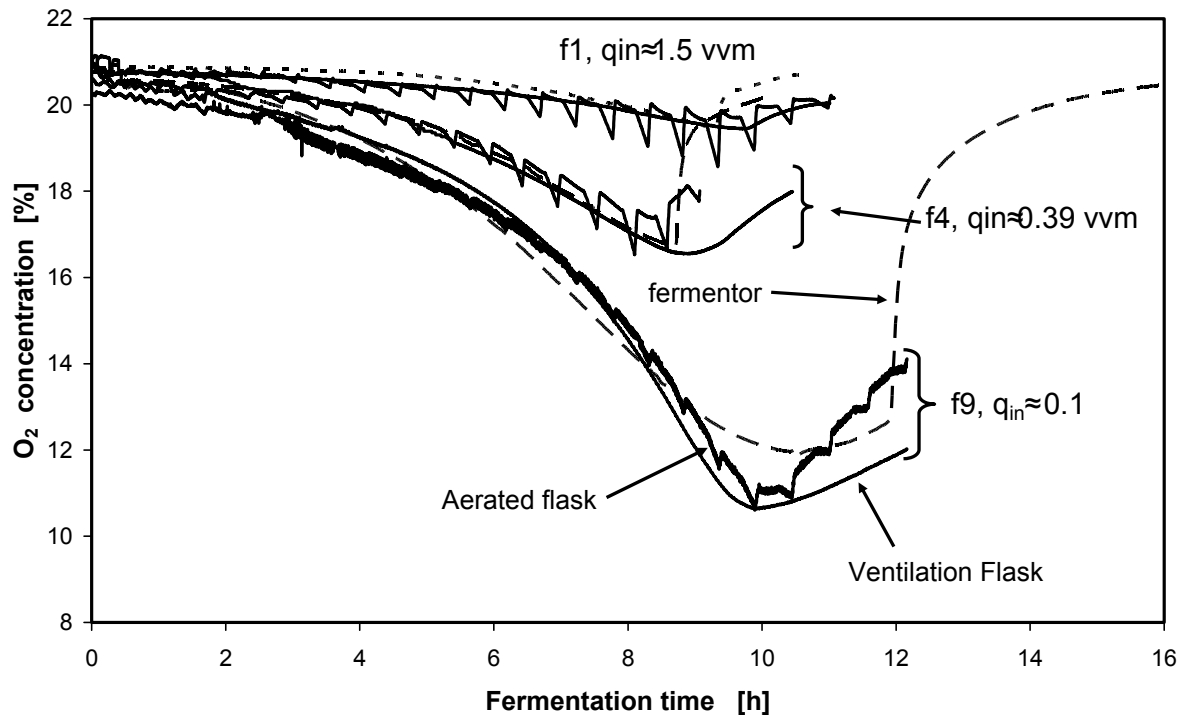
Figure 8.2: Comparison between the oxygen concentration for a fermentation of *C. glutamicum* DM1730 in ventilation flasks, aerated flasks (14 g/l glucose, 21 g/l MOPS, pH_{start}=7.18, V_L=15 ml, n=350 rpm)) and a foil fermentor (15.5 g/l glucose, 21 g/l MOPS, pH_{start}=7.18, V_L=1800 ml, n=300-1000 rpm)) with different specific aeration rates calculated using the Eq. 5.

As mentioned in Chapter 7, the approximate maximum accumulated CO_2 values of 1.5, 3.4 and 11 % could be calculated by the values of O_2 concentration by Eq. 7.10, providing a RQ=1. Accordingly, the values of CO_2 for the ventilation and measuring flasks were calculated and compared with the values of CO_2 from the fermentor. The values of CO_2 for the different scales were compared together in Figure 8.3. This figure also indicates very good comparable results for each group of CO_2 concentrations in the headspaces of ventilation flasks f1, f4 and f9 with measuring flasks and fermentor.

Regarding Figures 8.3 and 8.4, a plateau becomes clear after 9.6 hours of the fermentation in the fermentor, operated under a specific aeration rate of 0.1vvm. This could be due to the presence of a low aeration rate (0.1 vvm). This may causes a temporal delay between the fermentor and the exhaust gas analyzer cabinet. Therefore, although the concentrations of the O_2 and CO_2 in the gas exhaust of the fermentor are often measured, these concentrations do not show the actual concentrations in the gas phase of the fermentor under dynamic conditions. Figure 8.4 illustrates the OTR of a fermentation *of C. glutamicum DM1730* in the foil fermentor with different specific aeration rates of 1.5, 0.39 and 0.1 vvm. This figure indicates that, there is a significant discrepancy between the total amount of oxygen consumption, calculated by Eq. 7.15, for a low specific aeration rate (0.1vvm) and other aeration rates (1.5 and 0.39 vvm).
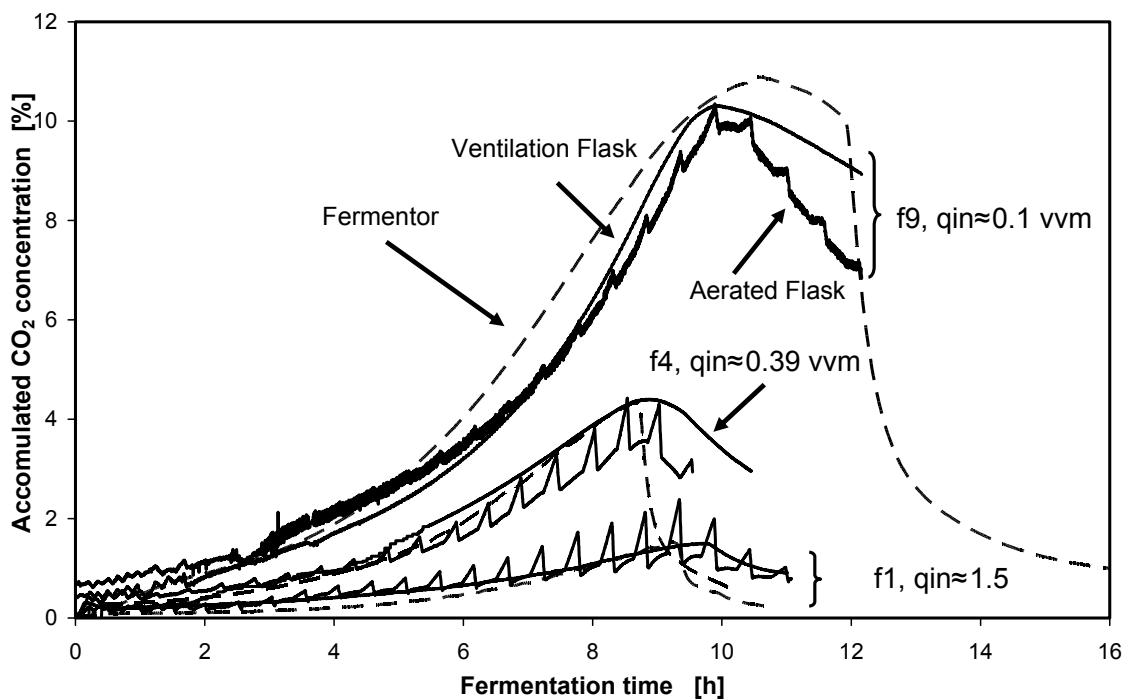
Figure 8.3: Comparison between the carbon dioxide concentration for a fermentation of *C. glutamicum* DM 730 in ventilation flasks, aerated flasks (14 g/l glucose, 21 g/l MOPS, pH_{start}=7.18, V_L=15 ml, n=350 rpm)) and a foil fermentor (15.5 g/l glucose, 21 g/l MOPS, pH_{start}=7.18, V_L=1800 ml, n=300-1000 rpm) with different specific aeration rates of 1.5, 0.39 and 0.1 vvm.
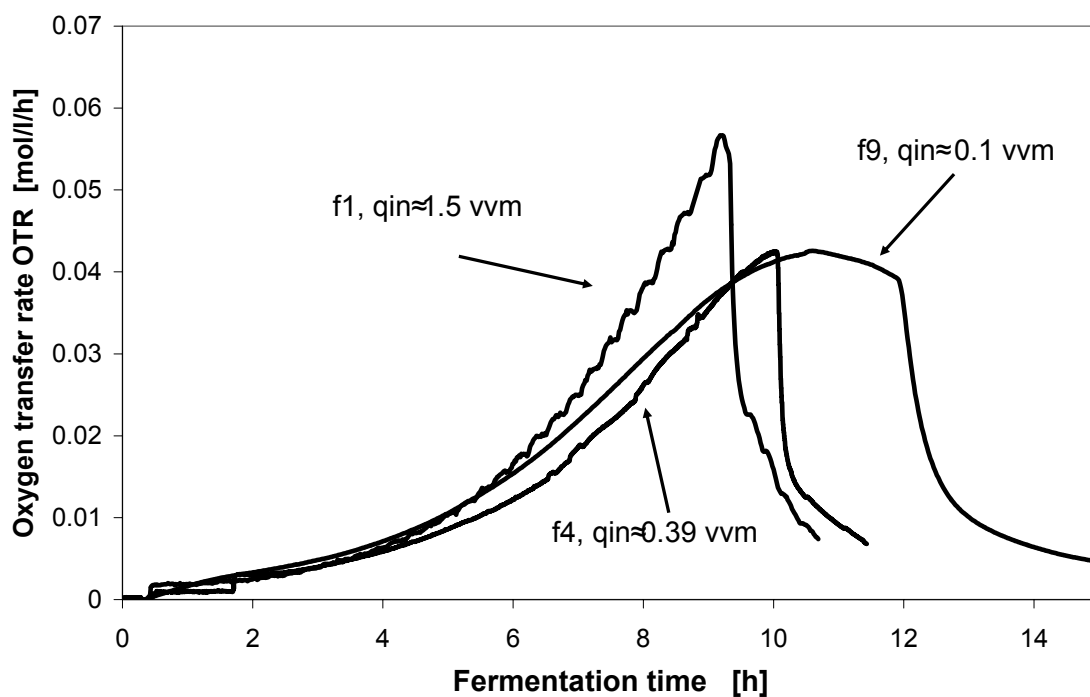
Figure 8.4: Comparison between ORT results of a fermentation of *C. glutamicum* DM1730 (15.5 g/l glucose, 21 g/l MOPS, pH_{start}=7.18, V_L=1800 ml, n=300-1000 rpm) in the foil fermentor with different specific aeration rates of 1.5, 0.39 and 0.1 vvm.

In the following step, the proposed method will be investigated, comparing between both scales in terms of OTR, cell dry weight (biomass) concentration, maximum specific growth rate and L-lysine formation.

8.3.2 Comparison between the maximum OTR in the ventilation flask and the fermentor

Obtaining the same oxygen transfer rate (OTR) in small and large scale can be a suitable scale up method [21]. Figure 8.5 shows the comparison between both scales in terms of OTR for a fermentation of *C. glutamicum* DM1730 in the measuring flasks (f1, f4 and f9) and the fermentor under different specific aeration rates of 1.5, 0.39 and 0.1 vvm. An average difference of 3 % between the values of maximum OTR in both scales were obtained this indicates that there is no noticeable difference between the values of the maximum OTR in the measuring flasks and the fermentor. This could confirm a reliable scale up from our shake flasks (ventilation and measuring) to foil fermentor. Noted that the results of the ventilation flasks and the measuring flasks could be compared, providing that they are operated under the same aeration strategy (Chapter 5).
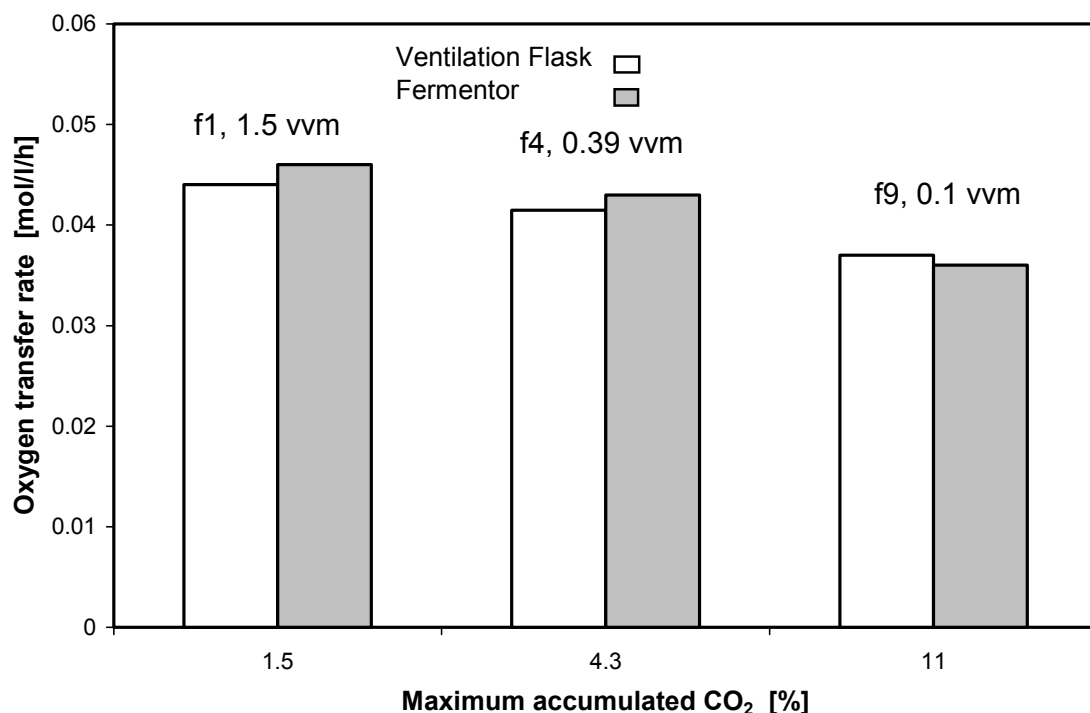
Figure 8.5: Comparison between the OTR results of a fermentation of *C. glutamicum* DM1730 in the measuring flask and the fermentor under different maximum accumulated CO_2.

Figure 8.5 also reveals that there was a remarkable deviation of 6 and 19 % between the average maximum OTR values of 0.042 and 0.037 mol/l/h under the conditions of f4 and f9, in comparison to the f1 (0.045 mol/l/h), in both scales. This points out that the different levels

of the accumulated CO2 could have affected the oxygen consumption of *C. glutamicum* DM1730 on glucose [6]. The slight divergence between both scales each condition of f1 and f4 could be due to the difference between the amounts of glucose concentration (10 %) [1 and 68]. In the case of the f9, the maximum OTR in the fermentor is slightly lower than that in the measuring flask. As mentioned above, this could occur because of utilizing a low aeration for fermentor.

8.3.3 Comparison between the cell dry weight (biomass) concentrations in the ventilation flasks and the fermentor

Figure 8.6 (A, B and C) exemplifies the cell dry weight (biomass) concentrations of a fermentation of *C. glutamicum* DM1730 in ventilation flasks f1, f4 and f9 and relevant fermentors. As demonstrated there is a good similarity between the results from the ventilation flasks and the fermentor. 12 % deviations between the maximum biomass concentrations in both scales were observed, which was due to the differences between the glucose concentrations (the glucose in the medium of ventilation flasks was about 10 % lower than that of the fermentors). The approximate range of pH values between 7.4 and 6.3, controlled by 21 g/l MOPS buffer, indicates that the activity of the micro-organisms was not inhibited by this factor [1, 7 and 68].

8.3.4 Comparison between the maximum specific growth rate in the ventilation flasks and the fermentor

Using the values of cell dry weight (biomass) concentration in Eq. 6.14, the values of the maximum specific growth rates in the ventilation flasks and the fermentor under the conditions of f1, f4 and f9 were calculated. Those results are shown in Figure 8.7. There is no significant discrepancy between both scales of each condition of f1, f4 and f9 for the maximum specific growth rates. Only a small deviation of 3 % was obtained. Therefore, these results also confirm the validity of our proposed new method.

The average of the maximum specific growth rates of 0.37, 0.316 and 0.266 h^{-1} were calculated for both scales under maximum accumulated CO_2 values of 1.5, 4.3 and 11% , respectively. They specify that the CO_2 ventilation affect the growth rate of this micro-organism in the fermentor as in the ventilation flasks. This effect has been reported in literature [6] and also in Chapter 6.
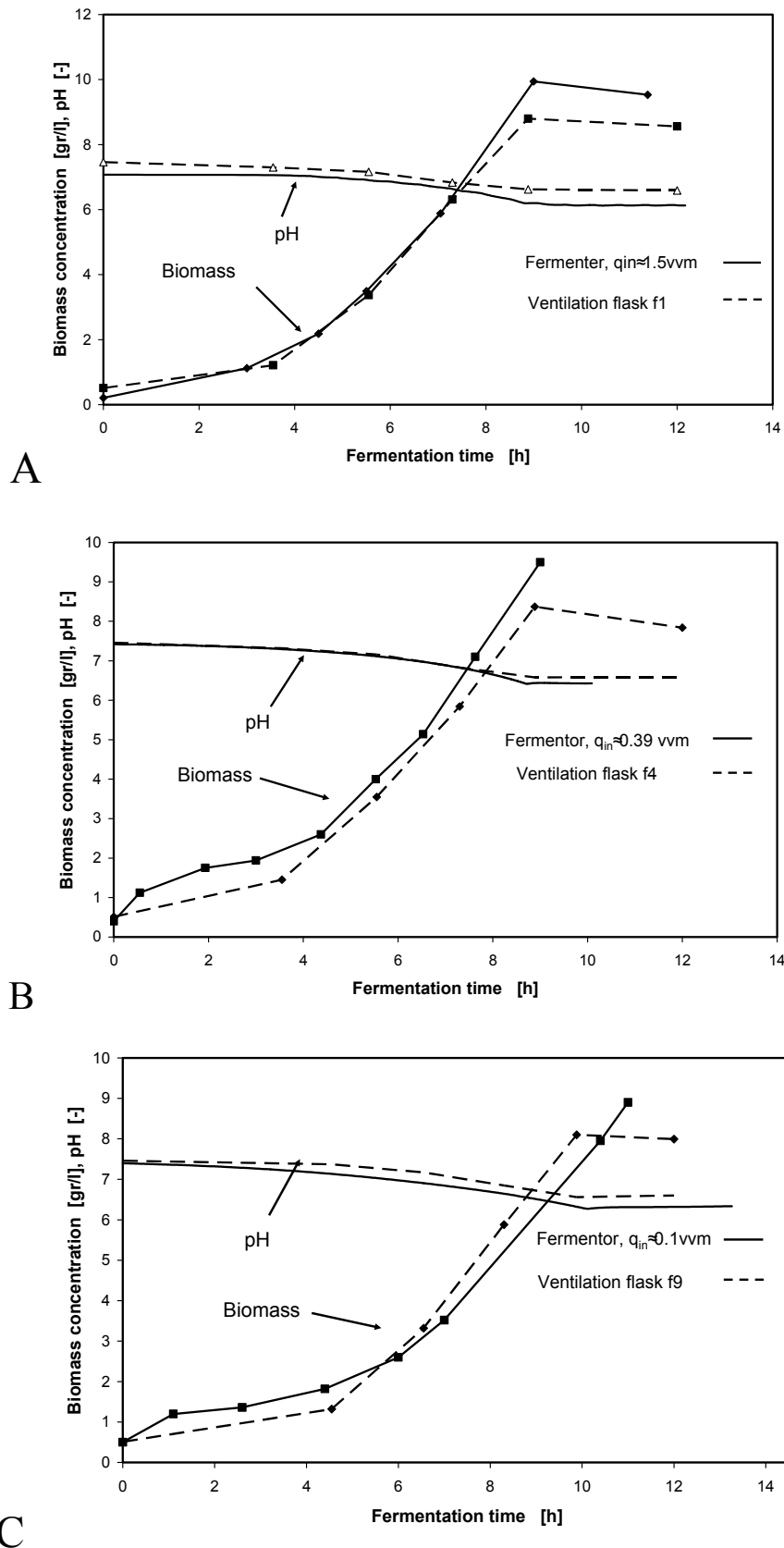
Figure 8.6: Comparison between the cell dry weight (biomass) concentrations for fermentations of *C. glutamicum* DM1730 in the fermentor and the ventilation flasks, obtained by the new method for scale up based on the effect of CO_2 ventilation. A: f1, 1.5 vvm, B: f4, 0.39 vvm, C: f9, 0.1vvm. (N0 points are shown for the fermentor, because the gas analyzer proceedes a continuous signal.
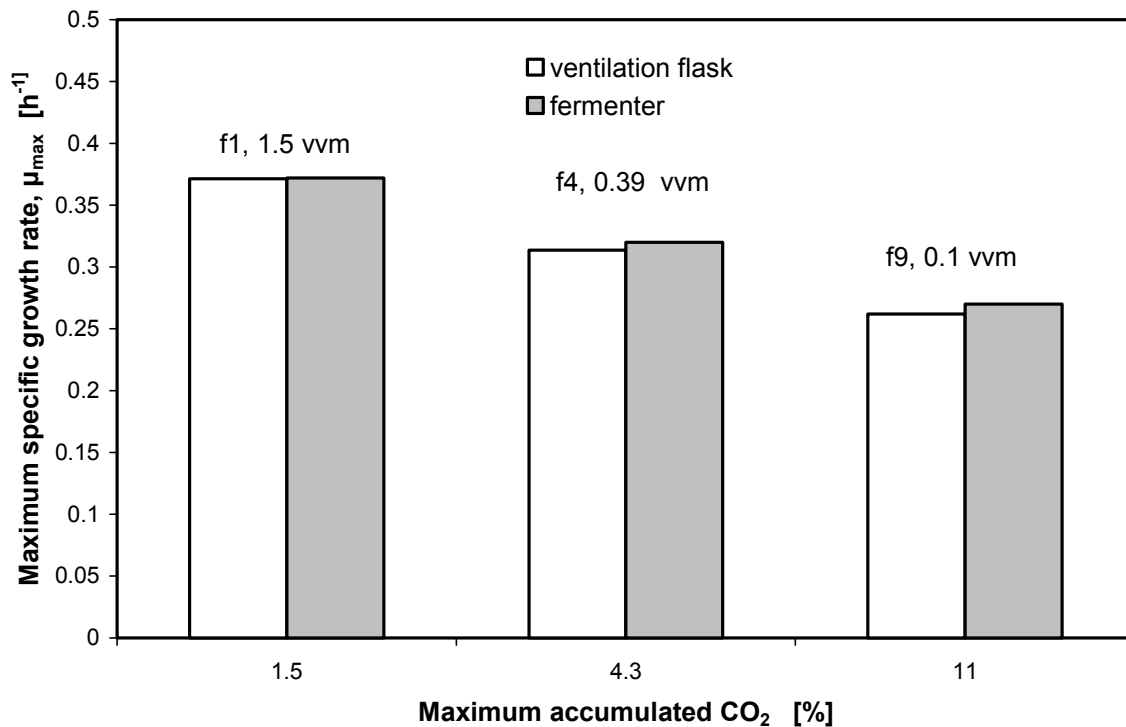
Figure 8.7: Comparison the maximum specific growth rates of *C. glutamicum* DM1730 from fermentations in the ventilation flasks and the fermentor, using the new method for scale up based on the effect of CO2 ventilation.

8.3.5 Comparison between the L-lysine formation in the ventilation flasks and the fermentor

In Figure 8.8 the L-lysine concentrations obtained by a fermentation of *C. glutamicum* DM 1730 in the ventilation flasks f4 and f9 and a fermentor are illustrated. This figure demonstrates that the L-lysine formations, obtained from the fermentor with specific aeration rates of 0.39 and 0.1 vvm, were quite close to those obtained from the ventilation flasks f4 and f9, respectively. It was also found that the different levels of CO_2 ventilation (max. 4.3 and 11 %) have a significant effect on the L-lysine production (in average 0.057 and 0.071 mmol/l), due to the different conditions of f4 and f9. It is remarkable that in the fermentor a higher L-lysine concentration was reached. This could be due to the higher glucose concentration (10 %) used in fermentor.
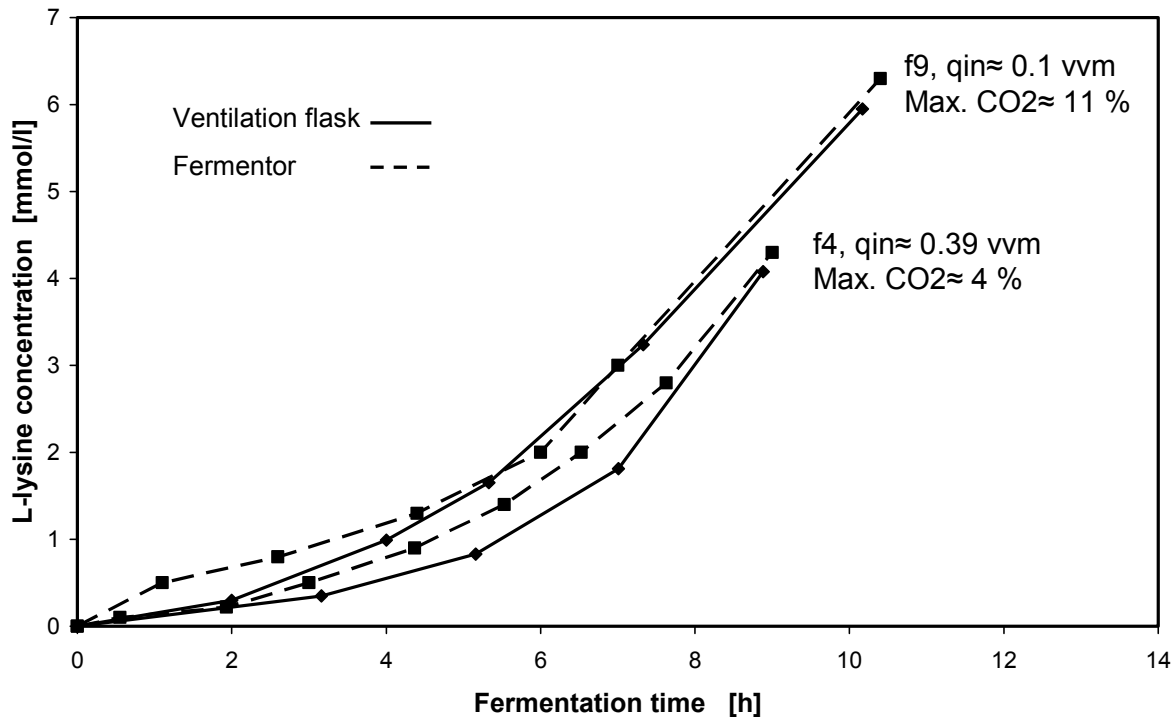
Figure 8.8: Comparison of the L-lysine concentration, of a fermentation of C. glutamicum DM 1730 in the ventilation flasks and the fermentors, using the new method for scale up based on the effect of CO2 ventilation.

8.4 Conclusion

The data from the shake flasks can be valuable for a bioreactor scale up. While scaling-up a fermentation process, it is very important to reproduce the shake flask data in a stirred tank fermentor with a minimum number of runs in a pilot fermentation. Furthermore, a direct method for scaling-up from a shake flask to a commercial-scale fermentor is suitable to reduce research expenses and shorten the research time. In this manner, the values of aeration and ventilation might be important criteria for bioreactors scale up, especially in the case of CO_2 sensitive micro-organisms. The scale up from shake flasks to stirred tank bioreactors is often very complex and time consuming because of distinctions between the results obtained in different scales. Based on the values of k_{plug} of the ventilation flasks, specific aeration rates of aerated flasks and stirred tank bioreactors were calculated, using the unsteady state model (Chap. 5).

Moreover, a new aeration strategy to scale up from Erlenmeyer flasks to aerated fermentation systems (e.g. measuring flask and fermentor), based on the effects of CO_2 ventilation was investigated. By applying this method, the concentrations of CO_2 and O_2 in the gas phase

obtained from aerated flasks and stirred tank bioreactors were comparable to those obtained from ventilation flasks (Figs. 8.2 and 8.3). Under these conditions similar trends in the results of the maximum OTR, cell dry weight (biomass) concentration, maximum specific growth rate (μ_{max}) and L-lysine formation for fermentation of *C. glutamicum* DM1730 as a model organism were found in both scales.

As a conclusion of these results there is a possibility for scaling up from ventilation flasks to stirred tank bioreactors based on the effect of the CO_2 ventilation criterion.

Summary
and
Future Work

In this work a novel and easy method to quantify the CO_2 sensitivity of micro organisms in shaken bioreactors has been described (Chapters 6 and 7). A new aeration strategy for scale up from a shake flask to aerated fermentation system (measuring or aerated flask and stirred tank bioreactors) is presented, as well (Chapters 5 and 8). For these aims, at first a variety of the gas transfer coefficients through the sterile closure (k_{plug}) of specially designed shake flasks, so called ventilation flasks, were obtained. The values of k_{plug} calculated using constant values of 0.162 and 0.123 cm^2/sec for D_{eo2} and D_{CO2} (Figs. 3.4 and 3.5) which are obtained by the water evaporation method and the extended model of Henzler and Schedel [23 and 57]. From this extended model a representation of the mass transfer coefficient (k_{plug}) of the sterile closure can be obtained which is closer to reality and which is dependent on the mass flow through the plug (OTR_{plug}) (Eq. 4.19). Then, it was found that unsteady state conditions in the ventilation flasks have to be considered, since the current steady state model can not express the large discrepancies between calculated and experimental results. Therefore, an unsteady state model was prepared to characterize the gas transfer in shaken bioreactors. The method was experimentally validated for the sulfite and biological systems for a variety of k_{plug} (Figs. 4.7, 4.8 and 4.10). In the next step, a new aeration strategy from shake flasks to aerated flasks was initiated with implementing equation 4.19 into the unsteady state model, and then the specific aeration rates in the ventilation flasks were clarified (Figure 4.5 and 4.6). Using these varieties of k_{plug} in ventilation flasks and aeration in measuring (aerated) flasks different levels of O_2 and CO_2 in these flasks were established (Figures 6.2, 6.3 and 7.3). According to these results, a new and easy method to quantify the CO_2 sensitivity of micro-organisms in shaken flask bioreactors of the RAMOS device was established. These methods were tested on several micro-organisms (Figure 7.10). A significant effect of accumulated CO_2 on the biomass concentration, growth rate and lysine production of *C. glutamicum* DM1730 was found. Applying this method for *Arxula adeninivorans* LS3 and *Hansenula polymorpha* (WT ATCC 34438 and RB11-FMD-GFP) indicated that the CO_2 has no effect on these microorganisms. *Pseudomonas fluorescens* (DSM 50090) and *Corynebacterium glutamicum* (ATCC WT13032 on lactate) was found to be especially sensitive organisms. This method was confirmed by comparison of the results with the results reported in literature [6, 19, 34 and 39]. In this study, the CO_2 sensitivity of micro-organisms could be quantified up to 12 % of accumulated CO_2 under non oxygen limited condition (Figure 6.5). When the cultivation was carried out under proper conditions (e.g. appropriate media and buffer capacity to control the pH, the OTR lower than the maximum oxygen transfer capacity to avoid oxygen limitation and the use of the same filling volume) the above value of CO_2 can be provided. Finally, concerning the

aeration strategy, a new scale up method from shaken flasks to stirred tank bioreactors was successfully developed based on the effect of CO_2 ventilation on *C. glutamicum* DM 1730 as a model organism.

In future, efforts can be made as follows:

a- Modify the unsteady state model for simultaneously solving the partial differential equation for partial pressure of the gas mixture (O_2, CO_2, N_2) in the headspace of the ventilation flasks and the spatially-resolved gas concentration in the sterile closure (Eq. 3.1) with the model of Henzler and Schedel [23] in an appropriate software program (e.g. g-PROMS). This will reduce the discrepancies between the observed and theoretically predicted results (Figures 4.8 and 4.10).

b- Implement the calibration factor (C_f) in to the programming system of the RAMOS device to eliminate the errors observed in the OTR results of the RAMOS device.

c- Apply the proposed method to quantify the CO_2 sensitivity of fungal, plant and mammalian cells.

d- Use the ventilation flasks for quantification of the effects of other volatile compounds (e.g. alcohols, organic acids, hormones, NH_3 etc.) in the fermentation broth on the activity of organisms based on the aeration strategy.

e- Identify the influence of carbon dioxide on metabolic fluxes dependent on the autogenously produced CO_2 by the organisms.

f- Controlling the aeration in stirred tank bioreactors based on CO_2 ventilation, considering the aeration strategy for scale up from a shake flask. This will give a better comparability between both scales' results.

References

[1] Abdul Haleem Shah, Abdul Hameed, Safia Ahmad and Gul Majid Khan (2002) Optimization of culture conditions for L-lysine fermentation by *Corynebacterium glutamicum*. On Line Journal of Biological Sciences 2(3), 151-156

[2] Akashi k., Shibia h. Hirose Y. (1976) Inhibitory effect of CO_2 and O_2 in amino acid fermentation. J. Ferment. Technol. 57(4), 317-320

[3] Anderlei T., Büchs J. (2001) Device for sterile online measurement of the oxygen transfer rate in shaking flasks. Biochem. Eng. J. 7(2), 157-162

[4] Anderlei T., Zang W., Büchs J. (2004) Online respiration activity measurement (OTR, CTR, RQ) in shake flasks. Biochem. Eng. J. 17(3), 187-194

[5] Atkinson, B. and Mauritura, F., (1991) Biochemical Engineering and Biotechnology Handbook. (The Nature Press)

[6] Bäumchen C., Knoll A., Bernward H., Seletzky J., Meier B., Dietrich C., Amoabediny Gh., Buechs J., (2006) Effect of Increased Dissolved Carbon Dioxide Concentrations on Growth of *Corynebacterium glutamicum* on D-Glucose and L-Lactate, J. of Biotechnology. (Submitted)

[7] Büchs J., (1988) Immobilisierung von aeroben Mikroorganismen an Glassintermaterialam Beispiel der L-Leucin Produktion von *Corynebakterium glutmicum*. PhD thesis at Forschungszentrum Jülich (TU Hamburg-Harburg, Germany)

[8] Büchs J., (2001) Introduction to advantages and problems of shaken cultures. Biochemical Engineering Journal 7(2), 91-98

[9] Chain E. B., Gualandi G., Morisi G. (1966) Aeration studies. IV. Aeration conditions in 3000-liter submerged fermentations with various micro-organisms. Biotechnology and Bioengineering 8 (4), 595-619

[10] Daub A. (2005) Etablierung eines industriellen Fermentationsprozesses mit erhöhter Viskosität im Mikrotiterplattenmaßstab, Diplom Thesis at RWTH Aachen University

[11] Demain A. L. and Davies J. (1999) Manual of Industrial Microbiology and Biotechnology 2nd ed. Washington, D.C: ASM Press

[12] Dixon N. M and Kell D. B. (1989) The inhibition of CO_2 of the growth and metabolism of micro-organisms. J. Appl. Bacteriol. 67, 109-136.

[13] Dixon N.M. and Kell D.B. (1990) The control and measurement of "CO_2" during fermentations. J. Microbiol. Methods 10, 155-176

[14] Dixon, N.M. and Kell, D.B. (1997) The inhibition of CO_2 of the growth and metabolism of micro-organisms. Journal of Applied Bacteriology 67, 109-136

[15] Dronawat S.N., Svihla C.K. and T.R. Hanley (1995) the Effects of agitation and aeration upon the production of Gluconic Acid by *Aspergillus niger*. Appl. Biochem. & Biotechnology 52/52, 347-354

[16] Rose D., Winston F. and Hieter P. (1990) Laboratory Course Manual for Methods in Yeast Genetics. Cold Spring Harbor, New York

[17] Fan D, Shang L, Yu J. (1996) Research on fermentation scale-up based on the OUR obtained from a shake flask. Chin J Biotechnol. 12 (3), 177-184

[18] Gaden, E. (1962) Improved shaken flask performance. Biotechnol. Bioeng. 4, 99-103

[19] Gill C. O. and K. H. Tan. (1979) Effect of carbon dioxide on growth of *Pseudomonas fluorescens*. Appl. Environ. Microbiol. 38, 237-240

[20] Gros J., B., Dussap C.G. and Catte M. (1999) Estimation of O_2 and CO_2 solubility in microbial culture media. Biotechnol. Prog. 15, 923-927

[21] Gupta A. and Rao G. (2003) A study of oxygen transfer in shake flasks using a non invasive oxygen sensor. Biotechnol. Bioeng. 84 (3), 351-358

[22] Hens j. g. Hoopen T., Walter M. Vanoulik, Jurrian E. Schlatman, Paulo R. H: Moreno, J. L. Vike, J. J. Heijnen and Robert Verporte (1994) Ajamalicine production by cell cultures of *Catharanthus seus*: from shake flask to bioreactor. Plant Cell, Tissue and Organ Culture 38, 85-91

[23] Henzler H.J.and Schedel M. (1991) Suitability of the shaking flask for oxygen supply to microbiological cultures. Bioprocess Eng. 7, 123-131

[24] Hermann R., Walther N., Maier U. and Büchs J. (2001) Optical method for the determination of the oxygen-transfer capacity of small bioreactors based on sulfite oxidation. Biotechnol. Bioeng. J. 74, 355-363

[25] Hirose Y, Sonada H, Kinoshita K, Okada H. (1966) Studies on oxygen transfer in submerged fermentations IV. Determination of oxygen transfer rate and respiration rate in shaken cultures using oxygen analyser. Agr. Biol. Chem. 30, 49-58

[26] Ho C. S., Smith M. D. (1986a) Effect of dissolved carbon dioxide on penicillin fermentations: mycelia growth and penicillin production. Biotechnol Bioeng 28, 668-677

[27] Ho C. S., Smith M. D. (1986b) Morphological alterations of *Penicillium chrysogenum* caused by carbon dioxide. J Gen Microbiol 132, 3479-3484

[28] Ho C. S., Smith M. D. and Shanahan J. F. (1987) Carbon dioxide transfer in biochemical reactors. Adv Biochem Eng Biotechnol 35, 83-125

[29] Ikeno Y. and Ozaki A. (1968) Factors affecting oxygen transfer into shaken flask. Agr. Biol. Chem. 32 (7), 912-915

[30] Ishizaki A., Shibai H., Hirose Y. and Shiro T. (1971) Dissolution and dissociation of carbon dioxide in the model system. Part I: Studies on the ventilation in submerged fermentations. Agric. Biol. Chem., 35 (11), 1733-1740

[31] Ishizaki A., Hirose Y., and Shiro T. (1971) Quantitative studies on the dissolution and dissociation of carbon dioxide in culture system. Part II: Studies on the ventilation in submerged fermentations. Agric. Biol. Chem. 35 (12), 1852-1859

[32] Jensen A.L. and J. S. Schultz (1966) Apparatus for monitoring the oxygen uptake and carbon dioxide production of fermentation. Biotechnology and Bioengineering VIII, 539-548

[33] Jin ZH, Lin JP and Cen PL. (2004) Scale-up of rifamycin B fermentation with *Amycolatoposis mediterranei*. J Zhejiang Univ Sci. 5 (12), 1590-6

[34] Jones R. P. and P. F. Greenfield (1982) Effect of carbon dioxide on yeast

growth and fermentation. Enzyme Microb. Technol. 4, 210-223.

[35] Ju L. K., and Chase G. G. (1992) Improved scale-up strategies of bioreactors. Bioprocess Engineering 8, 49-53

[36] Kato I. and Tanaka H. (1998) Development of a novel box-shaped shake flask with efficient gas exchange capacity. Journal of Fermentation and Bioengineering, 85(4), 404-409

[37] Kato I. and Tanaka H. (1998a) Influence of CO_2 ventilation on microbial cultivation in shake-flasks. Biotechnol. Tech. 12, 325–328

[38] Knoll A. et al. (2005) The oxygen mass transfer, carbon dioxide inhibition, heat removal and energy and cost efficiencies of high pressure fermentation. Adv. Biochem. Eng. Biotechnol. 92, 77-99

[39] Kremer A. (2006) Bestimmung der Reaktion von *C. glutamicum* Stämmen auf erhöhte CO_2 Konzentrationen. Diplom Thesis at RWTH Aachen University

[40] Kunze G. and Kunze I. (1996) Arxula adeninivorans (Nonconventional yeast in biotechnology a handbook). springer-verlageBerlin Klauswolf

[41] Kuriyama H., Matsul S. and Kobayashi H. (1993) Effect of pCO_2 on growth and metabolism yeast continuous fermentation. Biotechnology letters, 15(2), 186-193

[42] Linek, V. and Vacek, V. (1981) Chemical engineering use of catalysed oxidation Kinetics for the determination of mass transfer characteristics of gas-liquid contactors. Chem. Eng. Science 36(11), 1747-1768

[43] Longan Shang, Min Jiang, Chul Hee Ryu, Ho Nam Chang, Soon Haeng Cho, and Jong Won Lee (2003) Inhibitory effect of carbon dioxide on the fed-batch culture of Ralstonia eutropha: Evaluation by CO2 pulse injection and autogenous CO_2 methods Biotechnology and Bioengineering. 83(3), 312-320.

[44] Maier, U. and Büchs, J. (2001) Characterisation of the gas-liquid mass transfer in shaken bioreactors. Biochem. Engng. J. 7 (2), 99-106

[45] Maier U. (2002) Gas/Flüssigkeits-Stofftransfer und Hydrodynamik im Schüttelkolben ,Ph.D thesis at RWTH-Aachen, Aachen University

[46] Maier, U., Losen, M. and Büchs J. (2004) Advances in understanding and modeling the gas-liquid mass transfer in shake flasks. Biochem. Engng. J. 17, 155-167

[47] Maria Papagianni,(2004) Fungal morphology and metabolite production submerged mycelia processes , Biotechnology Advances 22 189–259

[48] Mateles, R. I. (1971) Calculation of the oxygen required for cell production. Biotechnology and Bioengineering 13, 581

[49] McDaniel, L.E. and Bailey, E.G. (1969) Effect of shaken speed and type of closure a shake flask cultures. Appl. Microbiol. 17, 286-290

[50] McIntyre, M., and B. McNeil. (1997). Dissolved carbon dioxide effects on morphology, growth and citrate production in *Aspergillus niger* A60. Enzyme Microb. Technol. 20, 135–142.

[51] McIntyre, M., and B. McNeil (1997b) Effect of carbon dioxide on morphology and product synthesis in chemostat cultures of *Aspergillus niger* A60. Enzyme Microb. Technol. 21, 479-483

[52] McIntyre M. and B. McNeil (1998) Morphogenetic and biochemical effects of dissolved carbon dioxide on Flamentous fungi in submerged cultivation Appl Microbiol Biotechnol. 50, 291-298

[53] Mitz M A (1979) CO_2 biodynamics: a new concept of cellular control. J Theo Biol 80(4), 537-51

[54] Molin G.(1985) Effect of carbon dioxide on growth of *Pseudomonas putida* ATCC 11172 on asparagine, citrate, glucose, and lactatee in batch and continuous culture. Can. J Microbiol. 31 (9):763-6.

[55] Monod J (1949) The Growth of Bacterial Cultures, Ann Rev Microbiol 3, 371-94

[56] Mostafa S S, Gu X (2003) Strategies for improved dCO2 removal in large-scale fed-batch cultures, Biotechnol Prog 19 (1), 45-51

[57] Mrotzek, Ch., Anderlei, T., Henzler, H. and Büchs, J (2001) Mass transfer resistance of sterile plugs in shaken bioreactors Biochem. Engng. J. 7(2), 107-112

[58] Nyiri L., Z. L. Lengyel (1968) Studies on ventilation of culture broths. I. Behavior of CO2 in model systems Biotechnology and Bioengineering 10(2), 133-150-

[59] Nyiri L. and Z. L. Lengyel (1965) Studies on automatically aerated biosynthetic processes. I. The effect of agitation and CO_2 on penicillin formation in automatically aerated liquid cultures. Biotechnology and Bioengineering, 7(3), 343-354

[60] Onken U. (1990) Batch and Continous cultivation of psedomonas fluorescence at increased biotechnology and bioengineering. 35, 983-969

[61] Perry, R. H. and Green, D. (1994) Chemical Engineers Handbook. McGraw-Hill Publishing Company, Sixth Edition, Section 3

[62] Pfefferle W.; Möckel, B.; Bathe, B.; Marx, A. (2003) Biotechnological manufacture of lysine. in microbial production of L-amino acids. Adv Biochem Eng Biotechnol, 79, 59-112.

[63] Reith, T. and Beek, W.J. (1973) The Oxidation of Sodium Sulfite Solutions. Chem. Eng. Sci. 28, 1331-1339

[64] Royce, Patrick N.C., Thornhill and Nina F. (1991) Estimation of Dissolved Carbon Dioxide Concentrations in Aerobic Fermentations. AIChE J., 37(11), 1680 - 1686

[65] Royce and Patrick N.C., (1992) Effect of Changes in the pH and Carbon Dioxide Evolution Rate on the Measured Respiratory Quotient of Fermentations. Biotechnology and Bioengineering, 40, 1129-1138

[66] Schultz J.S. (1964) Cotton closure as an aeration barrier in shaken flask fermentations. Appl. Microbiol. 12 (4), 305-310

[67] Schumpe A., Quicker G. and Deckwer W. D. (1982) Gas solubilities in microbial culture media. Adv. Biochem. Eng. 24, 1-38

[68] Seletzky J et al. (2006) *Corynebacterium glutamicum* on lactatee under stress. Appl Mic robiol Biotechnol, (E-pub ahead of print)

[69] Shibai H., Ishizaki A., Mizuno H., and Hirose Y. (1973) Effects of oxygen and carbon dioxide on inosine fermentation (Studies on oxygen transfer in submerged fermentation. Part X.). Agric. Biol. Chem. 37, 91–97

[70] Sigma S. Mostafa and Xuejun Gu (2003) Strategies for improved dCO_2 removal in large-scale fed-batch cultures. Biotechnol. Prog. 19, 45-51

[71] Stansen C et al. (2005) Characterization of a *Corynebacterium glutamicum* lactatee utilization operon induced during temperature triggered glutamate production. Appl. Env. Microbio. l 71, 5920-8

[72] Stoeckmann C., Maier U., Anderlei T., Knocke C., Gellissen G. and Buechs J. (2003) The oxygen transfer rate as key parameter for the characterization of *Hansenula polymorpha* screening cultures J. Ind. Microbiol. Biotechnol. 30, 613-622

[73] Straskrabova V et al. (1980) Effect of Aeration and carbon dioxide on cell morphology of candida utilis. Appl. Env. Microbiol. 40(5), 855-861

[74] Sumino Y, Sonoi K, Doi M. (1993) Scale-up of purine nucleoside fermentation from a shaking flask to a stirred-tank fermentor. Appl. Microbiol. Biotechnol. 38(5), 581-585

[75] Tanaka H. (1991) New scale-up method based on the effect of ventilation on aerated fermentation systems. Ferment. Bioeng. 72(29), 204-209

[76] Van Suijdam J. C., Kossen N. W. F. and Joha A. C. (1978) Model for oxygen transfer in a shake flask. Biotechnol. Bioeng. 20, 1695-1709

[77] Wilke C. R., Di usional (1950) Properties of multi component gases. Chem. Eng. Progr. 2, 95-104

[78] Wittmann1 Christoph, Hyung Min Kim1, Gernot John and Elmar Heinzle1 (2003) Characterization and application of an optical sensor for quantification of dissolved O_2 in shake-flasks. Biotechnology Letters 25, 377–380.

[79] Yamada S., Wada M. and Chibata I. (1978) Oxygen transfer in shaken flask cultures and the conversion of sorbitol to sorbose by Acetobacter suboxydans. Ferment. Technol. 56 (1), 20-28

[80] Yoshio Hirose, Hiroshi Sonoda ,Kazumoto Kinoshita and Hiroshi Okada (1699) Studies on Oxygen transfer rate in submerged fermentations (Part IV. Determination of oxygen transfer rate and respiration rate in shaken cultures using oxygen analyzers). Agr. Biol. Chem. 30(1), 49 –58

Curriculum vitae

Born:	13.11.1965 Tehran
Nationality	Iran
Address of work:	„Department of Chem. Eng. faculty of Engineering University of Tehran", 16 Azar Street P.O.Box:11365-4563, Tehran – I.R.Iran
E-mail:	amoabedini@yahoo.com

Academic Achievement

1994 - 1996	**Master of Science (Engineering) in Chemical Engineering** at University of Tehran; Master Thesis: "Study of kinetic equation on bioleaching of pyretic Gold recovery in the mine of Mute by *Tiobassillus ferrooxidans*"
1990 - 1994	**Bachelor of Science** in Chemical Engineering at University of Tehran (***First Rank***)

Publication:

Amoabediny Gh. and Büchs J. (2006) Modelling and Advance Understanding of Unsteady State Gas Transfer in Shaking Bioreactors. **Biotechnology and Applied Biochemistry** Immediate Publication, doi:10.1042/BA20060120

Amoabediny Gh., Kremer A., Knoll A. J.and Büchs J. (2006) A new aeration strategy to scale up from shaken flasks to stirred tank bioreactors based on the effect of CO2 ventilation. (Poster Presentation), **European Symposium on Biochemical Engineering**, Salzburg, Austria

Amoabediny Gh. and Büchs J. (2006) A Novel and Easy Method for Quantification of CO2-Sensitivity of Microorganisms in Shaken Bioreactors (Poster Presentation), **DECHEMA-Jahrestagung der Biotechnologen** Wiesbaden, Germany

Bäumchen C., Knoll A., Bernward H., Seletzky J., Meier B., Dietrich C., **Amoabediny Gh**. And Buechs J. (2006) Effect of Increased Dissolved Carbon Dioxide Concentrations on Growth of *Corynebacterium glutamicum* on D-Glucose and L-Lactate, **Journal of Biotechnology** (submitted paper)

Amoabediny Gh. and Vatandoost Z. (2002) Nanobiotechnology a new conception in industry and life science Paper published to the **Congress of Nanotechnology** the next industrial revolution in Iran.

Amoabedin Gh., Tabatabaie yazdi. M. S, Mossavian. M.A and Shahverdi M. (2000) Study on equation on Kinetic in Pyrite by Bacterial leaching for Gold recovery Paper published to the fifth **national congress on Chem. Eng.** Shiraz, Iran.

Education and Practical activities:

2001	Preparation of the Manual for Set-up, start up and Experiments of the Unit Operation laboratory. Dep. of Chem. Eng. Faculty. of Eng. University of Tehran.
1993	Design of a fermentor for the production of citric acid from waste of cane sugar plants.
1969	Kinetics of Enzymatic reaction and microbial growth in the design of ideal and non-ideal bioreactors
1988	Selection Design and analyses of water and waste water treatment plants